The Effect of Rubber Fills on the Performance of Infrastructure

October 2024
Final Report

Project number TR202013
MoDOT Research Report number cmr 24-018

PREPARED BY:

Mohamed Elashram

Ahmed Gheni

Mohamed ElGawady

Missouri University of Science and Technology

PREPARED FOR:

Missouri Department of Transportation

Construction and Materials Division, Research Section

Technical Report Documentation Page

1. Report No. cmr 24-018	2. Government Accession No.	3. Recipient's Catalog No.
4. Title and Subtitle The Effect of Rubber Fills on the Performance of Infrastructure		5. Report Date September 2024 Published: October 2024
		6. Performing Organization Code
7. Author(s) Mohamed Elashram, https://orcid.org/0009-0004-9569-7775 Ahmed Gheni, Ph.D Mohamed ElGawady, Ph.D		8. Performing Organization Report No.
9. Performing Organization Name and Address Department of Civil, Architectural and Environmental Engineering Missouri University of Science and Technology 1401 N. Pine St. Rolla, MO 65409		10. Work Unit No. (TRAIS)
		11. Contract or Grant No. MoDOT project # TR202013
12. Sponsoring Agency Name and Address Missouri Department of Transportation (SPR-B) 1617 Missouri Blvd. Jefferson City, MO 65109		13. Type of Report and Period Covered Final Report (October 2019-September 2024)
		14. Sponsoring Agency Code

15. Supplementary Notes

Conducted in cooperation with the U.S. Department of Transportation, Federal Highway Administration. MoDOT research reports are available in the Innovation Library at https://www.modot.org/research-publications.

16. Abstract

One of the most environmentally friendly methods to recycle scrap tires is by shredding them into tire derived aggregate (TDA). TDA possesses desirable properties for various civil engineering applications and has been successfully used as fill material in numerous projects. To address the limitations of previous studies, 27 direct shear tests were conducted using a large-scale direct shear box (3 feet wide, 3 feet long, and 2 feet deep) on different TDA types mixed with soil. Additionally, 9 large-scale compressibility tests were conducted on the soil-TDA mixtures. TDA content was varied from 0 to 100% by weight in the soil mixtures. The direct shear tests were performed under confining pressures of 3.63, 7.25, and 10.88 psi. The results indicated that adding TDA to the soil significantly reduces the dry unit weight of the mixtures. When 25% TDA (Type A or Type B) was added to the soil, it provided the same shear resistance for the soil alone at all considered confining pressures. The compressibility test results showed that the inclusion of TDA increased the compressibility of the mixtures. It was observed that adding TDA to the soil contributed to a strain-hardening behavior in the mixtures. Also, adding 25% TDA reduced lateral earth pressure by 20% on average.

17. Key Words Scrap tires; Tire derived aggregate (TDA); Lightweight aggregates; Soil-TDA mixtures; Embankments; Retaining walls; Bridge abutments; Large-scale direct shear test; Compressibility; Lateral earth pressure; Recycling	18. Distribution Statement No restrictions. This document is available through the National Technical Information Service, Springfield, VA 22161.

19. Security Classification (of this report) Unclassified	20. Security Classification (of this page) Unclassified	21. No. of Pages 95	22. Price

Form DOT F 1700.7 (8-72) Reproduction of completed page authorized

The Effect of Rubber Fills on the Performance of Infrastructure

By

Mohamed Elashram
Ahmed Gheni, PhD
Mohamed ElGawady, PhD

Civil, Architectural and Environmental Engineering Department
Missouri University of Science and Technology

Prepared for
Missouri Department of Transportation (MoDOT)

September 2024

Final Report

cmr 24-018

Acknowledgments

The authors wish to express their gratitude to the numerous individuals and organizations that contributed to the success of this research project. A heartfelt thank you is extended to the Missouri Department of Transportation (MoDOT) for their financial support, vision, and commitment to innovative concepts, which pushed the boundaries of current practices. The project's success was largely due to MoDOT's support and encouragement.

Furthermore, the authors acknowledge Missouri S&T for their significant contributions to the research. The tireless efforts of the staff from the Department of Civil, Architectural, and Environmental Engineering, and the Center for Infrastructure Engineering Studies, were invaluable. Special thanks go to John Whitchurch for his extensive assistance with the various tests, and to Jason Cox for his valuable technical support during the experimental work. Appreciation is also extended to the many students who helped in assembling the shear box.

Disclaimer

The opinions, findings, and conclusions presented in this document are solely those of the investigators and do not necessarily reflect the views of the Missouri Department of Transportation, the U.S. Department of Transportation, or the Federal Highway Administration. Furthermore, this information does not constitute a standard or specification.
Two figures included in this report feature materials previously published in the literature. Every effort has been made to properly acknowledge and cite the original sources of these figures in accordance with copyright laws and MoDOT guidelines. Where applicable, written permission for reprinting copyrighted materials has been obtained. These figures are provided solely for illustrative purposes to enhance the understanding of the report’s content. The authors assume full responsibility for the use of these figures, and no responsibility rests on MoDOT for their inclusion.

Copyright

Table of contents

List of tables

List of figures

List of equations

List of abbreviations and acronyms

AASHTO	……	American Association of State Highway and Transportation Officials
ASTM	……	American Society for Testing and Materials
Calrecycle	……	California Department of Resources Recycling and Recovery
Cc	……	coefficient of gradation
Cu	……	coefficient of uniformity
DOT	……	Department of Transportation
DRRR	……	Disaster Risk Reduction Resource Manual
EPA	……	United States Environmental Protection Agency
FHWA	……	Federal Highway Administration
GEM	……	Geotechnical Engineering Manual
Gs	……	specific gravity
LL	……	liquid limit
MDNR	……	Missouri Department of Natural Resources
MD	……	Maryland Department of the Environment
ME	……	Manual for Engineering
MoDOT	……	Missouri Department of Transportation
PI	……	plasticity index
PL	……	plastic limit
String Pot	……	string potentiometer sensor
TDA	……	tire derived aggregate
TDF	……	tire derived fuel
USTMA	……	U.S. Tire Manufacturers Association

Executive summary

In 2021, the United States generated nearly 500 million scrap tires. Due to environmental considerations, landfilling scrap tires is no longer allowed in many countries, and stockpiling tires is not a viable option due to them becoming fire hazards and breeding grounds for mosquitoes and vermin. An environmentally friendly method to recycle scrap tires is to shred them into tire derived aggregate (TDA). One of the promising applications for TDA is its use in soil improvement.

Using TDA alone has issues with self-ignition and high compressibility. However, mixing TDA with soil shows great potential as a light filling material. Several studies have examined only the effect of TDA content smaller than 1 inch on the shear strength behavior and compressibility of soil, especially sandy soil. This report addresses a gap in the literature by presenting the results of large-scale shear and compressibility testing of soil classified as clayey gravel and sand soil mixed with different percentages and types of TDA.

In conclusion, incorporating tire derived aggregate (TDA) into soil significantly alters the geotechnical properties of the mixtures, with notable differences depending on the type and amount of TDA used. Adding 25% TDA decreases the dry unit weight by approximately 13% for soil-TDA Type A mixtures and 31% for soil-TDA Type B mixtures. Cohesion decreases slightly by 6% with TDA Type A, from 2.84 psi to 2.67 psi, while it increases by 15% with TDA Type B, from 2.84 psi to 3.27 psi. The angle of internal friction increases by 16%, from 14.38^{o} to 16.70^{o}, with TDA Type A, but decreases by 19.5%, from 14.38^{o} to 11.57^{o}, with TDA Type B.

Normalized lateral earth pressure at rest decreases by 14% with TDA Type A, from 79 to 68, and by 25% with TDA Type B, from 79 to 59, potentially leading to cost savings in retaining wall design. Shear resistance is slightly reduced by 12% with TDA Type A and by 2% with TDA Type B, while shear modulus increases significantly under higher confining pressures, by 30% with TDA Type A and 10% with TDA Type B. In terms of compressibility, mixtures with TDA Type B exhibit lower compressibility compared to those with TDA Type A, with axial strain increments of 3.00%, 7.30%, and 12.50% for 25%, 50%, and 100% TDA Type A, respectively, and 1.05%, 1.47%, and 5.47% for the corresponding percentages of TDA Type B.

These results suggest that the choice between TDA Type A and Type B should be guided by the specific requirements of the project, as each type offers distinct benefits in terms of strength, stability, and compressibility.

1. Chapter 1. Introduction

1.1. Background

Rapidly expanding populations are generating significant volumes of discarded tires annually. In the USA alone, the staggering accumulation of over 500 million scrap tires each year underscores the urgency of addressing this issue (Edinçliler et al., 2010; Gheni, A., et al., 2017). A massive portion of scrap tires is directed towards recycling and various end-uses.

Of particular interest are two market sectors: ground rubber and civil engineering applications. 1.41 million tons (77 million tires) are processed into ground rubber, which is used in rubberized asphalt applications, rubberized chip seal playground surfaces, and sports fields as discussed in many studies (Moustafa and ElGawady, 2013; Youssf, et al., 2013; Youssf, et al., 2014; Youssf, et al., 2015; Moustafa and ElGawady, 2015; Youssf, et al., 2016; Moustafa and ElGawady, 2016; Gheni, A., et al., 2017; Moustafa, et al., 2017; Gheni, A., et al., 2018; Pourhassan, et al., 2023).

This sector has displayed steady growth over the years. The civil engineering market sector has fluctuated over the last few years, including the construction of retaining walls, road embankments, and other infrastructure. One reason for this fluctuation is the lack of knowledge about the performance of rubber in infrastructure applications. An example of a stockpile of scrap tires is shown in Figure 1.1.

Figure 1.1 A stockpile of scrap tires
Modified from Missouri Department of Natural Resources (MDNR) website

1.2. Tire composition and structure

A tire comprises approximately 40 - 50% rubber, 20 - 30% carbon black and reinforcing materials, and 20% adhesive cord and steel wires (Rahman, 2004; Presti, 2013). Figure 1.2 shows a standard vehicle tire.

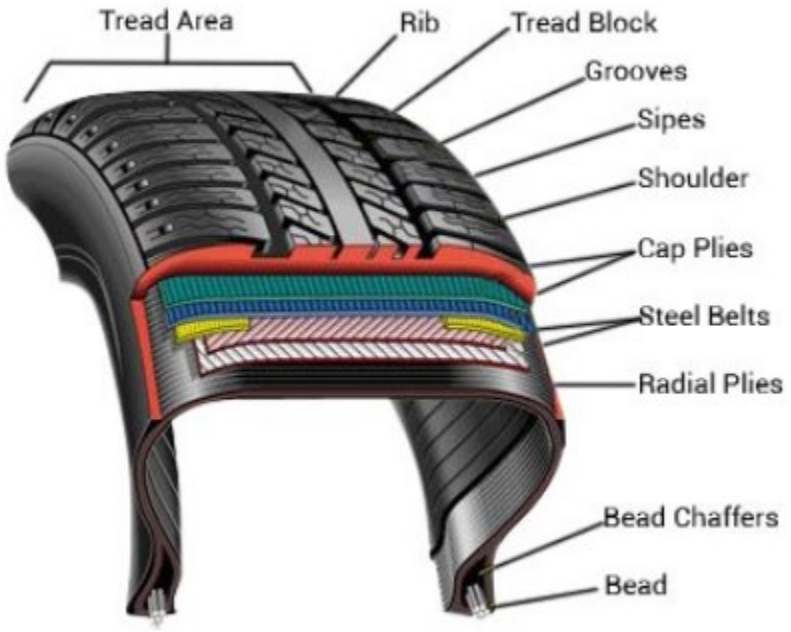

Figure 1.2 The components of a car tire
Modified from CARiD.com

1.3. Environmental issues caused by scrap tires

Recycling waste tires is imperative as they occupy considerable landfill space, and improper disposal can cause adverse environmental consequences. Stockpiled tires accumulate rainwater and organic matter, creating breeding grounds for insects such as mosquitoes, which pose health risks by transmitting diseases like encephalitis to humans.

Owing to their chemical composition, tires are highly combustible, with illegal scrap tire stockpiles presenting a heightened fire risk. Once ignited, tire fires present challenges for extinguishment, necessitating extensive efforts and subsequent cleanup operations, placing substantial economic burdens on local authorities. For instance, the Hagersville fire incident in southern Ontario, Canada, in February 1990 required significant resources, with 200 firefighters working for 17 days at a cost of nearly $1,000,000 for cleanup and environmental remediation efforts (Mawhinney, 1990a; Eldin and Piekarski, 1994).

Tire combustion produces copious amounts of toxic black smoke, contributing to air pollution, and releases substantial quantities of oil, which can seep into soil and groundwater aquifers. The

migration of these toxic contaminants via running water further exacerbates the environmental impact, potentially affecting ecosystems far beyond the fire site (Chamberlin and Gupta, 1986; Eldin and Piekarski, 1994; Ashish Singh et al., 2015; Senoro et al., 2016; Cecich et al., 2016; Gheni, Ahmed, et al., 2018; Liu, Xuesong, et al., 2018).

In response to the environmental issues associated with tires, the USA has initiated proactive measures to address tire recycling. These measures include imposing an environmental fee upon the purchase of new tires. The funds accrued through this levy are allocated towards diverting scrap tires from landfills and promoting sustainable recycling practices.

1.4. Shredded tire sizes

Some of the common sizes of rubber are as follows:

- **Shredded rubber**: Produced by mechanically cutting whole tires into larger pieces, shredded rubber provides excellent drainage and compaction properties. It is ideal for use in road sub-bases and embankments.
- **Crumb rubber**: Finely ground from scrap tires, crumb rubber offers a higher surface area-to-volume ratio. It is often used in asphalt modification and playground surfaces for enhanced flexibility and shock absorption.
- **Rubber chips and granules**: Intermediate in size between shredded rubber and crumb rubber, these forms combine the benefits of both types. They are versatile for various applications such as retaining wall backfill and drainage layers.

1.5. Tire derived aggregate (TDA)

TDA is a prominent product of shredded scrap tire that has the potential to utilize a large number of tires. The production of one ton of TDA typically necessitates recycling approximately 100 automobile tires as TDA has large particle sizes. Furthermore, TDA is characterized by its lightweight nature, excellent drainage capabilities, and high thermal resistivity. TDA has been used as fill material in embankments, retaining walls, bridge abutments, slope stabilization, and vibration mitigation. TDA has also been effectively employed as insulation to reduce frost penetration, thereby protecting infrastructure from potential damage caused by freezing temperatures. Furthermore, TDA serves a vital role as a drainage layer in road construction projects, facilitating efficient water management and contributing to the longevity and resilience of road surfaces (Humphrey, 2008).

Realizing the potential of TDA in civil engineering necessitates a thorough understanding of its properties. However, the commonly used soil characterization apparatus is ill-equipped to characterize TDA or TDA-soil mixtures due to the large particle size of TDA. Furthermore, the inclusion of steel wires within TDA presents an additional hurdle for laboratory testing procedures. Consequently, much of the TDA examined in the literature has small particle sizes and/or lacks the presence of steel wires

1.6. Specifications and guidelines for use of scrap tire in civil engineering

The main standard specification currently available for using scrap tires in various civil engineering applications is ASTM D6270. This standard provides guidelines for using processed scrap tire materials, primarily in the form of TDA. More key references addressing the guidelines and properties of TDA in various geotechnical applications are DRRR-2011-038, DRRR-2014-1489, DRRR-2016-1545, EPA530-R-10-010, FHWA/IN/JHRP-93/04, FHWA/IN/JTRP-2002/35, FHWA-RD-97-148, FHWA/TX-03/0-1808-1, GEM-20, and ME0012-11/MD04173.

2. Chapter 2. Literature review

The use of recycled rubber in infrastructure has evolved significantly over the past few decades. Initially driven by the need to find sustainable solutions for the disposal of scrap tires, researchers and engineers began exploring the potential of rubber materials in construction (Humphrey, 1999).

Early applications focused on using shredded tires in road construction and embankments. These studies recommended proper confinement and modified construction techniques to enhance performance, including improved shear capacity and damping against earthquake actions. Without proper confinement, higher deflections can be recorded when shredded tires are incorporated into the soil mix (Read and Thomas, 1991, Hoppe, 1994, Bosscher, et al., 1997, Gacke and Boyd, 1997, Salgado, and Siddiki, 2003, Haranatti, et al. 2003, Hoppe and Mullen, 2004, Edincliler, 2007, Tandon, V., et al., 2007, Edinçliler and Saygılı, 2010, Signes, et al., 2017, Chaiyaput, et al., 2022, Duda and Siwowski, 2022, Tandon, et al., 2023, Barman, et al., 2024, Kazemzadeh, et al., 2024, Qi, Y., et al., 2024).

2.1. Benefits of using shredded tires in geotechnical engineering applications

Over time, the engineering community has recognized the unique properties of rubber fills that make them suitable for a broader range of applications (Qamhia et al., 2024; Mahgoub, 2020; Mahgoub et al., 2020; Kliszczewicz and Kowalski, 2020; Alzabeebee et al., 2022; Duda and Siwowski, 2022; Rizvi et al., 2022; Zhang et al., 2023; Tutumluer and Qamhia, 2024). These studies have highlighted the promising potential of rubber fills, though with certain limitations. Factors such as rubber content, particle size, and soil gradation control the overall properties of mixtures, affecting unit weight, shear strength, and compressibility. The key findings from these studies are as follows:

a) Lightweight: Recycled tire materials are significantly lighter compared to traditional construction materials like soil and gravel. The inclusion of recycled rubber into soil mixtures results in a decrease in the unit weight of the resultant mixtures. Furthermore, smaller rubber particles can fill voids between larger soil particles, resulting in higher density and better compressibility. This weight reduction reduces the load on underlying structures, making them ideal for use in areas with poor soil conditions or where load reduction is crucial (Lee, et al., 2010, Akbarimehr and Aflaki, 2020, Akbarimehr, et al., 2021, Tasalloti, et al., 2021, Indraratna, et al., 2021, Singh, Goli, and Singh, 2023, Wu, et al.,2023).

b) Shear strength and friction: The interlocking nature of shredded rubber particles provides good shear strength, making rubber fills suitable for applications where stability is essential, such as in retaining walls and embankments. Furthermore, filling small voids within granular soil contributes to high friction at sand–rubber interfaces, delaying or inhibiting the relative motion and erosion of sand particles (Wu, et al., 2023).

c) Compressibility and resilience: The high compressibility and resilience of recycled tires allow them to absorb and dissipate energy. This characteristic is beneficial in applications requiring shock absorption, such as under playground surfaces and in seismic isolation. However, the

compressibility of granular soil-rubber mixtures increased with rubber content due to the high compressibility of rubber compared to soil grains. This impact can be mitigated by increasing confining and overburden pressures (Lee, et al., 2007, Valdes and Evans, 2008, Lee, et al., 2014).

d) Drainage and permeability: The porous nature of recycled tires ensures excellent drainage, which helps prevent water accumulation and reduces hydrostatic pressure. This property is particularly advantageous in landfill liners and drainage layers. The porosity of rubber-soil mixtures can increase from 0% in mixtures composed solely of soil to over 50% in uncompacted rubber. This variability in porosity is influenced by factors such as particle size distribution, the shape of soil and rubber particles, and their arrangement in a deformation test. These factors collectively impact the void ratio and overall porosity of the mixture. However, the porosity of granular soil-rubber mixtures decreased rapidly with increasing confining pressure and normal stress (Edil and Bosscher, 1994, Masad, et al., 1996, Mohajerani et al., 2020; Akbarimehr et al., 2021; Rouhanifar et al., 2021; Tasalloti et al., 2021; Cui and Zhang, 2022; Gao et al., 2022; Lu et al., 2022; Bernal and Barreto, 2023; Wu et al., 2023; Yang et al., 2023).

e) Economical: Rubber fills can be cost-effective, especially considering the long-term benefits of durability and reduced maintenance needs.

In summary, the use of shredded tires in highway construction offers engineering, environmental, and economic benefits under certain conditions.

2.2. Field implementation of TDA

In field implementation, researchers integrated TDA into full-scale projects, meticulously monitoring the short-term and long-term deformations and stresses experienced by the material. These real-world observations facilitated the deduction and back-calculation of TDA's mechanical properties under actual service conditions. Such in situ studies are invaluable as they provide insights into the performance of TDA within the complex interplay of environmental factors and loading conditions characteristic of practical applications.

The Michigan Department of Transportation (MDOT) recently demonstrated actual projects with structural backfill consisting of TDA and gravel to construct 20-foot tall geosynthetic reinforced soil (GRS) walls and a full-scale bridge (Park and Wahl, 2023, Qamhia, et al., 2024). The height of a GRS wall or bridge abutment using granular fill is generally limited to 15 feet for stability reasons. Unlike traditional backfill, the Michigan Minimum Structural Backfill (MMSB) sections needed to be exposed to extreme weather conditions during construction. The temperatures within the embankments reached 150°F due to the exothermic oxidation of the TDA, which may have significant effects on the likelihood and extent of any temperature-induced interfacial degradation. This work provided insights into improving the design of thermally resilient GRS walls and bridge abutments using TDA.

In California, TDA has been utilized extensively for road repairs and slope stabilization projects. For instance, it was used in the Dixon Landing Interchange Embankment and several landslide

repairs in Mendocino and Sonoma Counties. Similarly, TDA has been employed in various backfilling projects across the United States due to its advantageous properties.

2.3. Effect of rubber shape and size

Recycled tire rubber is available in several forms (section 1.4 in this report), each offering distinct characteristics suited for specific uses. Understanding the different sizes of recycled tires and their respective properties is crucial for selecting the appropriate material for specific engineering requirements and optimizing performance in infrastructure projects.

Shredded rubber has been utilized in soil embankments as lightweight fill in highway applications. The overall road performance was similar to gravel roads when the proposed soil was properly confined (Hoppe, 1994, Bosscher and Eldin, 1992, Hoppe and Mullen, 2004, Zutting and Naktode, 2020, Chowdhury and Kundu, 2021, Artoshi, et al., 2024, Al-Subari and Ekinci, 2024, Kazemzadeh, et al., 2024). Those studies revealed the following key findings:

a) California Bearing Ratio (CBR) values: Using shredded rubber content of 10%, 20%, and 30% resulted in reduced CBR values of 3.3%, 2.98%, and 2.3%, respectively, compared to 4.4% without tire shred content.

b) Shear stress: Direct shear tests revealed that increasing tire shred content significantly increased shear stress. For 10%, 20%, and 30% tire shred content, shear stresses were 82.25, 84.14, and 85.87 kPa, respectively.

c) Unconfined compression strength (UCS): Adding shredded rubber tires sized 10 × 20 mm increased UCS by 32% with 3% rubber content and by 13% with 1% rubber content, while longer rubber pieces decreased UCS. The same trend was noticed with small particle size of rubber where the maximum UCS was achieved with 45% improvement at 10% rubber and then started to decrease with higher ratios.

d) Stiffness and ductility: Results indicated that 2.5% shredded rubber improved rubberized cemented clay's strength, stiffness, and ductility index by around 12–15%. Increasing the aspect ratio of the tire shreds also increased the bearing capacity of the soil.

Crumb rubber was used in different soil applications affecting the maximum dry density, optimum moisture content, and several mechanical properties. Several studies revealed the following key findings (Prasad, et al., 2014, Juliana, et al. 2020, Saparudin, et al., 2022, Vaishnavi, et al. 2022, Abdullah, et al., 2023):

a) Unconfined compressive strength (UCS) values: The UCS value increased with the percentage of crumb rubber, with maximum values observed at 10% to 15% for soils with different clay content.

b) Shearing resistance: Compressible clays treated with 5% crumb rubber displayed a 260% increase in the angle of shearing resistance.

c) Lateral earth pressure: Sand–crumb rubber mixtures with an optimum crumb content of 20% provided maximum reduction in lateral earth pressure when used as backfill material behind retaining walls.

Rubber chips and granules have been investigated in several studies focusing on mixing them with soil. Several studies revealed the following key findings (Liu, et al., 2020, Yang, Z., et al., 2020, Akbarimehr, et al., 2021, Eslami and Materials, 2021, Tasalloti, et al., 2021, Balaban, et al., 2022, Elhakim, and Elkhouly, 2022, Jaramillo, et al., 2022, Abdullah, et al., 2023, Wu, et al., 2023, Pradeep, and Kumar, 2024):

a) Consistency and Uniformity: Rubber granules exhibit a more consistent size and shape compared to crumb rubber and shredded rubber. This uniformity enhances the predictability of their behavior when mixed with soil, leading to more reliable performance in embankment applications.

b) Improved Drainage: Rubber granules can create more effective and predictable drainage pathways within the embankment. This helps in managing water flow and minimizing erosion.

c) Enhanced Load Distribution: The uniform size and shape of rubber granules contribute to better load distribution within the soil matrix. This improves structural stability and the ability to bear heavier loads without significant deformation or settling.

d) Compaction and Stability: Rubber granules offer superior interlocking capabilities compared to the finer crumb rubber or irregularly shaped shredded rubber. This leads to improved compaction and increased stability of the embankment.

e) Ease of Handling: Rubber granules are generally easier to handle and apply during construction compared to crumb rubber and shredded rubber. Their uniformity reduces dust generation and allows for more even distribution within the embankment.

2.4. Effects of TDA on shear strength

2.4.1. Shear testing methods

Previous investigations have employed various experimental methodologies, including the direct shear test and the triaxial compression test, to evaluate the shear strength characteristics of soil mixtures. These testing methods have distinct advantages and limitations that influence their applicability and accuracy in geotechnical analysis.

The direct shear test, despite its inability to control pore water pressure along the shear surface, offers significant practical advantages due to its simplicity and ease of execution. In this method, failure is artificially constrained to occur along a predetermined horizontal plane, which may not align with the material's weakest plane. This constraint can lead to either overestimation or underestimation of the material's shear strength properties. Despite this limitation, the direct shear test remains highly popular among geotechnical engineers. Its straightforward setup, shorter preparation time, and less intensive equipment requirements contribute to its widespread use in preliminary site investigations and routine testing. Additionally, the versatility of the direct shear test in handling various soil and aggregate types underscores its utility in

geotechnical practice. Although it may not provide the same level of detail as the triaxial compression test, the direct shear test offers valuable insights, particularly in contexts where rapid assessment is essential or where the complexity and cost of triaxial testing are prohibitive.

The triaxial compression test is widely regarded for its ability to offer comprehensive control over confinement and saturation conditions during testing. This method allows failure to develop along a naturally occurring failure plane, thereby providing a more accurate representation of the material's behavior under stress conditions that simulate real-world scenarios. The ability to meticulously adjust and monitor confining and pore water pressures makes the triaxial compression test a preferred choice for detailed analysis of the mechanical properties of geotechnical materials.

2.4.2. Shear strength of soil-TDA mixtures

In recent years, numerous researchers have investigated the shear strength of TDA-soil mixtures. Among the analyzed variables, such as normal stresses, densities, and tire sizes, the most studied has been the confining pressure of the soil mixtures in the direct shear box apparatus. Generally, the shear strength of TDA is influenced by factors such as stress state, normal stress level, particle density, surface properties, temperature, and moisture content. Under unconsolidated undrained (UU) conditions, an increase in confining stress was found to decrease the friction angle and increase the cohesion of TDA. Additionally, the shear strength of TDA is lower under unsaturated conditions.

Large-scale direct shear tests have been conducted to study the effect of TDA particle size on shear properties. These tests were performed under normal stresses of 7.3, 14.3, and 28.5 psi using a constant shearing rate of 0.02 inches/min. Results showed that the angle of internal friction of TDA increased as the maximum particle size increased from 0.75 to 4.0 inches. However, the cohesion from interlocking among the TDA particles was not significantly affected by particle size. Furthermore, all Type A TDA samples exhibited contractive behavior, with smaller TDA aggregates being more compressible than larger ones (El Naggar et al., 2021). Their study revealed that a composition comprising 15% TDA by volume increased the angle of internal friction by 3° to 6.5° compared to sand alone and induced strain-hardening behavior.

Another study investigated the effect of shear box size on the shear strength properties of TDA, using five shear boxes with different sizes and aspect ratios. Results indicated that smaller shear box sizes could measure slightly higher friction angles, though no clear trend was observed for cohesion (Zahran, 2021).

The combined effects of relative density, temperature, and low normal stress level on shear strength for sand-TDA mixtures were also explored. Findings showed that the optimum relative density of sand-TDA mixtures increased with temperature, and shear strength increased with the relative density of TDA. Additionally, shear strength increased with normal stress level under constant relative density and temperature. Peak and residual shear strengths of TDA decreased by 35% and 50%, respectively, compared to conventional direct shear tests (Zahran and El

Naggar, 2020; Araujo et al., 2021; Zahran, 2021; El Naggar et al., 2022; Meziani and Mourad, 2022; Zhang et al., 2022; Yarahuaman et al., 2024).

Foose et al. (1996) conducted extensive large-scale direct shear tests on sand and tire shred mixtures, using specimens with a diameter of 279 mm and height of 314 mm. TDA sizes were divided into three groups: less than 50 mm, 50 to 100 mm, and 100 to 150 mm, mixed with sand at volumes of 10%, 20%, and 30%. Failure was defined at the peak or at a relative horizontal displacement of 9% if no peak was observed. Results demonstrated that tire shred content, unit weight of the sand matrix, and normal stress significantly influenced shear strength. Incorporating 30% by volume of tire shreds with a length of 150 mm increased the angle of internal friction to as much as 67°. Similar trends were observed by Tatlisoz et al. (1998) and Akbulut et al. (2007) when conducting extensive large-scale direct shear tests on sand, sandy silt, and clayey soil mixed with tire chips. However, further addition reduced shear strength due to segregation between soil and tire shred particles.

To determine friction angles and cohesion, Humphrey and Sandford (1993) conducted extensive direct shear box tests on tire shreds using a shear box with dimensions 305 mm × 305 mm × 228 mm. Shearing was conducted at a rate of 7.6 mm/min under confining pressures of 17, 34, and 68 kPa. Angles of internal friction varied from 19° to 25°, while cohesion intercepts ranged between 7.7 and 11.5 kPa.

The diverse experimental studies reviewed above illustrate the varying effects of TDA content, fiber orientation, and confining pressures on the shear strength properties of soil-TDA mixtures. These findings underscore the importance of selecting appropriate TDA proportions and testing methods to optimize the mechanical performance of geotechnical materials.

2.4.3. Triaxial compression test

Imtiaz Ahmed (1993) undertook a series of large-scale triaxial compression tests using specimens with a diameter of 152.4 mm to examine the shear strength behavior of tire chips and mixtures of tire chips with sand. Confining pressures were varied from 31.02 to 206.8 kPa. Ahmed evaluated shear strength at axial strains of 5%, 10%, 15%, and 20%, discovering that incorporating tire chips up to 38% by weight decreased the dry unit weight while simultaneously enhancing the shear strength of the mixture.

Masad et al. (1996) conducted triaxial compression tests with specimens having a diameter of 71.1 mm on tire shreds, sand, and their combinations, utilizing tire shreds with a maximum size of 4.75 mm. They observed that adding tire shreds to sand increased compressibility and decreased the density of the mixture. Moreover, the modulus of elasticity of the tire shred-sand blend was notably lower than that of sand alone. However, the resilient modulus of the mixture surpassed that of sand alone under higher confining pressures. The study also identified a strain-hardening behavior for pure tire chips, with angle of internal friction s of 6°, 11°, and 15° and cohesion values of 70, 71, and 82 kPa at axial strains of 10%, 15%, and 20%, respectively.

Wu et al. (1997) conducted small-scale triaxial compression tests with specimens having a diameter of 100 mm, employing a constant stress path method. They investigated five tire chip products with varying sizes and shapes, ranging from 2 to 38 mm long, including flat, granular, elongated, and powder forms. Confining pressures were within the range of 34.5 to 55 kPa. Their observations revealed that shear strength reached full mobilization at over 5% axial strain. The angle of internal friction s for tire chips ranged from 44° to 56°, with the highest angle recorded for flat tire chips measuring 38 mm long.

Lee et al. (1999) conducted extensive large-scale triaxial compression tests utilizing specimens with a diameter of 150 mm and a height of 300 mm. Their objective was to examine the shear strength behavior of tire chips when mixed with sand. The tests were conducted under consolidated drained conditions, applying confining pressures ranging from 28 to 193 kPa and a 1% axial strain loading rate per minute. The findings revealed a nearly linear relationship between deviatoric stress and axial strain up to 25%, with a similar trend observed for volumetric change versus strain.

Youwai and Bergado (2003) performed triaxial compression tests on sand-tire shred mixtures, utilizing specimens with a diameter of 100 mm and a height of 200 mm. The mixing ratios ranged from 0:100 to 100:0 by weight, with tire shreds up to 16 mm in size. The sand used had an optimum water content of 7.5%, while the tire shreds were dry. Tests were conducted under consolidated drained conditions with confining pressures of 50, 100, and 200 kPa. Failure was defined at 25% axial strain with a loading rate of 0.19 axial strain per minute. The study observed that mixtures containing more than 70% tire shreds exhibited significant deformation, showing dilation and compression characteristics.

Zornberg et al. (2004) conducted large-scale triaxial compression tests using specimens with a diameter of 153 mm and a height of 305 mm. They examined both pure tire shreds and sand-tire shred mixtures. The tire shreds had a maximum length of 102 mm and were blended with sand in various proportions ranging from 0 to 100% by weight. Tests were conducted under consolidated drained conditions with confining pressures ranging from 48.3 to 207 kPa and a loading rate of 0.5% axial strain per minute. Failure was identified at a peak or, in the absence of a peak, at 15% axial strain. Their findings revealed that tire shred content and aspect ratio were crucial in influencing the shear stress-strain behavior. An increase in aspect ratio improved shear strength and incorporating up to 35% tire shreds into sand increased shear strength, although higher contents reduced shear strength.

Rao and Dutta (2006) conducted small-scale triaxial compression tests with specimens measuring 100 mm in diameter and 200 mm in height on mixtures of sand and tire chips. The tire chips, available in sizes of 10 mm × 10 mm, 20 mm × 20 mm, and 20 mm × 10 mm, were blended with sand at concentrations ranging from 0 to 20% by weight. The tests were conducted under consolidated drained conditions with confining pressures ranging from 34.5 to 276 kPa. They discovered that increasing the tire chip content from 0 to 20% by weight resulted in a slight enhancement of the angle of internal friction from 38° to 40.1° and an increase in cohesion intercept from 0 to 18.4 kPa.

In summary, the studies conducted triaxial compression tests on mixtures of TDA and sand, varying TDA content, aspect ratio, and confining pressures. The findings indicated that incorporating up to 35% TDA into sand increased shear strength, with enhancements in angle of internal friction and cohesion intercept. However, beyond optimal contents, benefits diminished due to increased compressibility and segregation within the mixture.

2.5. Compressibility and long-term, one-dimensional compression tests

Wartman et al. (2007) conducted long-term, one-dimensional compression tests to determine the secondary compression index of tire-derived aggregate (TDA). Their findings revealed an average secondary compression index of 0.0065. The study further elucidated that secondary consolidation is primarily influenced by the height of the TDA layer rather than the applied loads or particle size. This suggests that the long-term settlement behavior of TDA relies more on the initial thickness of the material used rather than the specifics of the load applied or the dimensions of the TDA particles.

Field measurements conducted by Ahn et al. (2014) provided insights into the secondary compression index, or creep, of TDA derived from several embankment projects in the USA and Canada. Their analysis revealed that settlements occur during or shortly after construction, with TDA exhibiting a secondary compression index ranging from 0.004 to 0.0047. Remarkably, these values closely resemble those observed in stiff clay formations, highlighting the comparable behavior of TDA in terms of secondary consolidation. This similarity suggests that TDA can be a viable material in geotechnical applications, offering performance characteristics like those of more traditional materials like stiff clay.

Foriero and Ghafari (2020) conducted an experimental study to determine the elastic, plastic, and creep characteristics of TDA-sand mixtures. The experiment involved sand specimens with a set volume of TDA, which were confined laterally and subjected to a prolonged axial stress increase. The results demonstrated an initial primary creep phase that quickly transitioned to a secondary steady-state creep phase without reaching the tertiary phase. The extent of creep strain was significantly influenced by the TDA volume fraction. At a constant TDA volume fraction, the creep strain rate increased with the applied load. This trend was consistent across all tests, with the strain rate magnitude varying depending on the applied stress and TDA volume fraction.

In summary, the long-term, one-dimensional compression tests revealed an average secondary compression index of 0.0065, with secondary consolidation primarily influenced by the height of the TDA layer. Field measurements showed TDA's secondary compression index ranging from 0.004 to 0.0047, similar to stiff clay formations. While TDA and sand mixtures demonstrated primary creep transitioning to a secondary steady-state creep phase, with creep strain influenced by TDA volume fraction and applied load.

2.6. Dynamic performance of TDA

Full-scale shake table tests on retaining walls with TDA backfill to assess its dynamic performance was conducted by (Ahn and Cheng, 2014). Additionally, large-scale cyclic triaxial tests were

conducted by (Moussa and El Naggar, 2021) to explore TDA's dynamic properties, such as damping ratio and shear modulus reduction curves under varying confining pressures.

The findings indicated that TDA exerted lesser dynamic pressure on retaining walls compared to conventional backfill materials, resulting in greater displacement. TDA exhibited consistent damping properties, with a damping ratio ranging from 14% to 24%, showcasing its ability to efficiently absorb and dissipate energy during dynamic loading. TDA's remarkable behavior as a damping material positions it as a beneficial resource for geotechnical engineering projects requiring vibration mitigation and dynamic stability.

3. Chapter 3. Material characterization and properties

This chapter is divided into two sections. The first section evaluates the physical properties of the materials utilized in this study. Particle size analyses were conducted on the tire derived aggregate (TDA) and soils to ascertain these properties. Additionally, hydrometer analysis was performed on the soil to determine the size distribution of particles passing through the No. 200 sieve. Laboratory compaction tests, using standard Proctor energy, were conducted to identify the materials' optimal water content and dry unit weight. The Atterberg limit test was also administered to the soil to determine its plasticity index. The second section provides a detailed description of the preparation of the mixtures in various mixing ratios.

3.1. Materials used

3.1.1. Tire derived aggregate (TDA)

This study used Type A and Type B TDA to replace soil at varying percentages by weight. The TDA was sourced from Granuband-Macon, LLC, Macon, Missouri. Figure 3.1 and Figure 3.2 show examples of the TDA utilized in this research. Table 3.1 and Table 3.2 present the physical properties of the TDA samples used in the tests. In the tables, D10, D30, D50, and D60 represent the particle diameters at which 10%, 30%, 50%, and 60% of the sample by weight are finer, respectively. Additionally, Cu (coefficient of uniformity) is calculated as D60 / D10, and Cc (coefficient of curvature) is calculated as $(D30)^2$ / (D10 × D60).

The particle size distribution of the Type A TDA material, per AASHTO T27 (2023), is illustrated in Figure 3.3, showing a uniform distribution with particle sizes ranging from 0.187 to 0.75 inches and a uniformity coefficient of 1.61 (i.e., less than 4). Due to the flat and elongated nature of Type B TDA pieces, a conventional sieve analysis is not feasible (Foose et al., 1996; El Naggar et al., 2016). Instead, a histogram analysis was performed, on 100 randomly selected TDA pieces, to determine the particle size distribution. The dimensions of the selected pieces were measured in all directions using a ruler. Figure 3.4 presents the histogram of the Type B TDA sample. The histogram data was used to prepare a hypothetical sieve analysis of Type B TDA presented in Figure 3.5. The hypothetical sieve analysis was also used to determine D10 through D60 presented in Table 3.2.

Figure 3.1 The Type A TDA sample used in this study

Figure 3.2 The Type B TDA sample used in this study

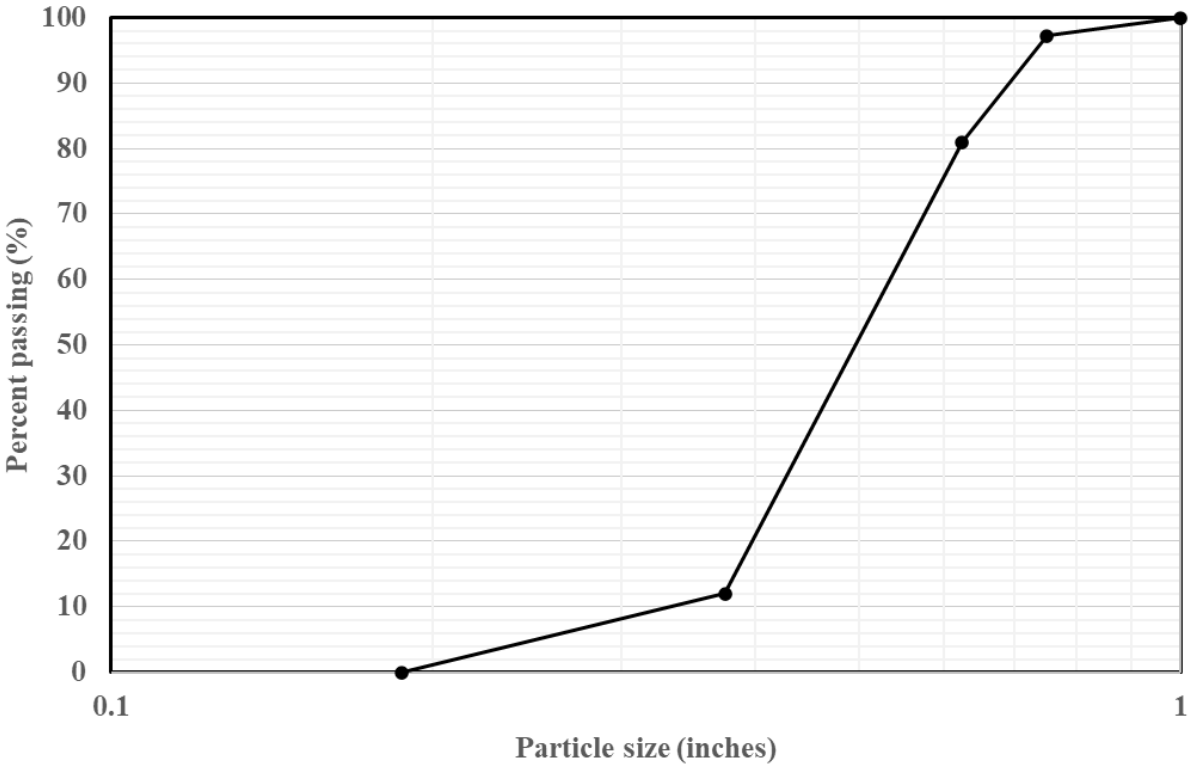

Figure 3.3 The particle size distribution of TDA Type A

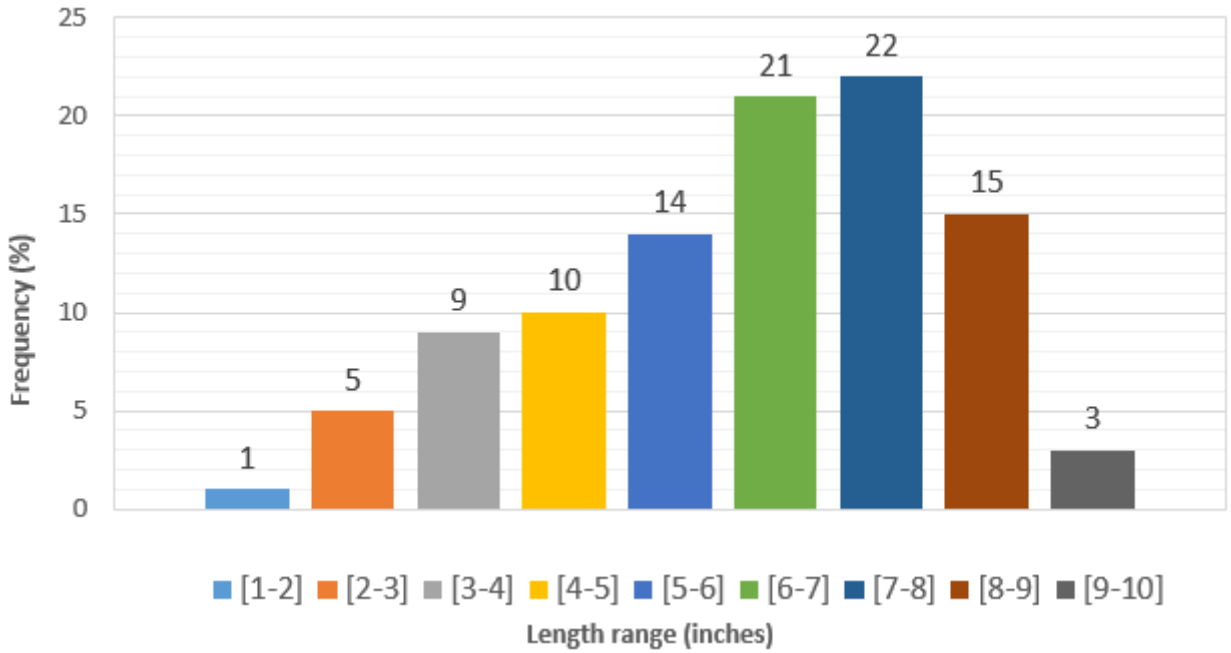

Figure 3.4 Histogram of the TDA Type B particles used in this study

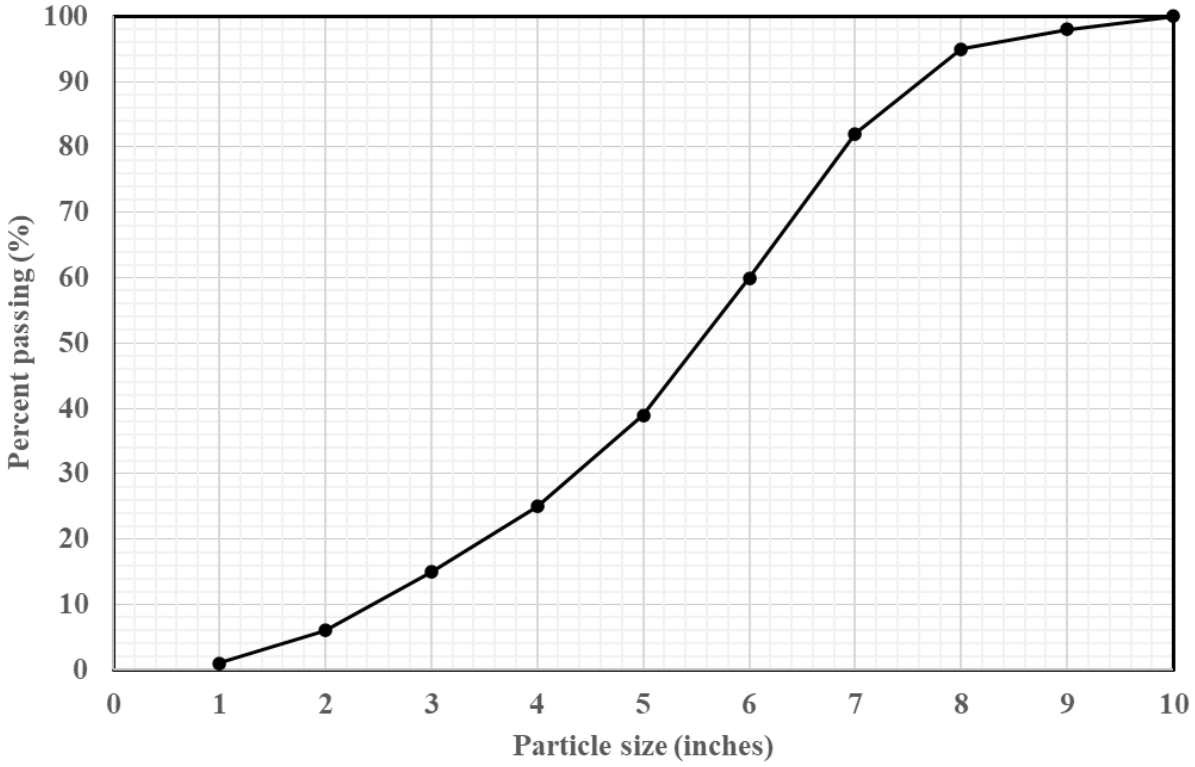

Figure 3.5 Hypothetical sieve analysis of TDA Type B

The dry unit weight (γ_{dry}) of the TDA samples was determined following ASTM D698 (2021). Due to the flexibility of the TDA particles, the compaction energy had a negligible effect on γ_{dry}. Therefore, 60% of the standard Proctor energy was applied to the specimen (Humphrey and Sandford, 1993). Additionally, since adding water does not alter γ_{dry} due to the hydrophobic properties of TDA, the compaction test was conducted on air-dried samples (Cecich et al., 2016; ASTM D6270, 2020).

Table 3.1 Physical properties of the TDA Type A

Characteristics	Value
Range of particles size (inches)	0.18 to 0.75
Range of particles thickness (inches)	0.28 to 0.50
D10 (inches)	0.37
D30 (inches)	0.47
D50 (inches)	0.55
D60 (inches)	0.59
Coefficient of uniformity (Cu)	1.61
Coefficient of gradation (Cc)	1.03
Dry unit weight, γ_{dry} (Ib/ ft3)	43
Absorption (%)	4.69
Specific gravity (Gs)	1.05

Table 3.2 Physical properties of the TDA Type B

Characteristics	Value
Average of particles size (inches)	4 to 9
Average of particles thickness (inches)	0.50
D10 (inches)	7.60
D30 (inches)	6.50
D50 (inches)	5.55
D60 (inches)	5
Coefficient of uniformity (Cu)	0.66
Coefficient of gradation (Cc)	1.11
Average aspect ratio	2.70
Dry unit weight, γ dry (Ib/ ft3)	31
Absorption (%)	2.26
Specific gravity (Gs)	1.29

3.1.2. Soil

The soil for this study was provided by the Missouri Department of Transportation (MoDOT). Figure 3.6 shows an example of the soil used in this study. This soil is classified per AASHTO M145 (2021) as silty or clayey gravel and sand. The soil exhibited a clayey-rock characteristic in its natural state, necessitating an initial drying at 230°F for 24 hours, followed by crushing into finer particles for use in the study.

Figure 3.7 displays the particle-size distribution of the clayey soil, which was determined in accordance with AASHTO T27 (2023). It is important to note that sieve analysis was conducted to determine the distribution of particles retained on the No. 200 sieve, while hydrometer analysis was used to determine the distribution of particles passing the No. 200 sieve. Additionally, the soil's dry unit weight and optimum water content were determined using the standard Proctor energy method per ASTM D698 (2021), as shown in Figure 3.8. To determine the plasticity index of the clayey soil, the Atterberg limit test was performed according to the standard methods outlined in AASHTO T89 (2022) and AASHTO T90 (2022). Table 3.3 presents the physical characteristics of the clayey soil.

Figure 3.6 Example of the soil used in this study

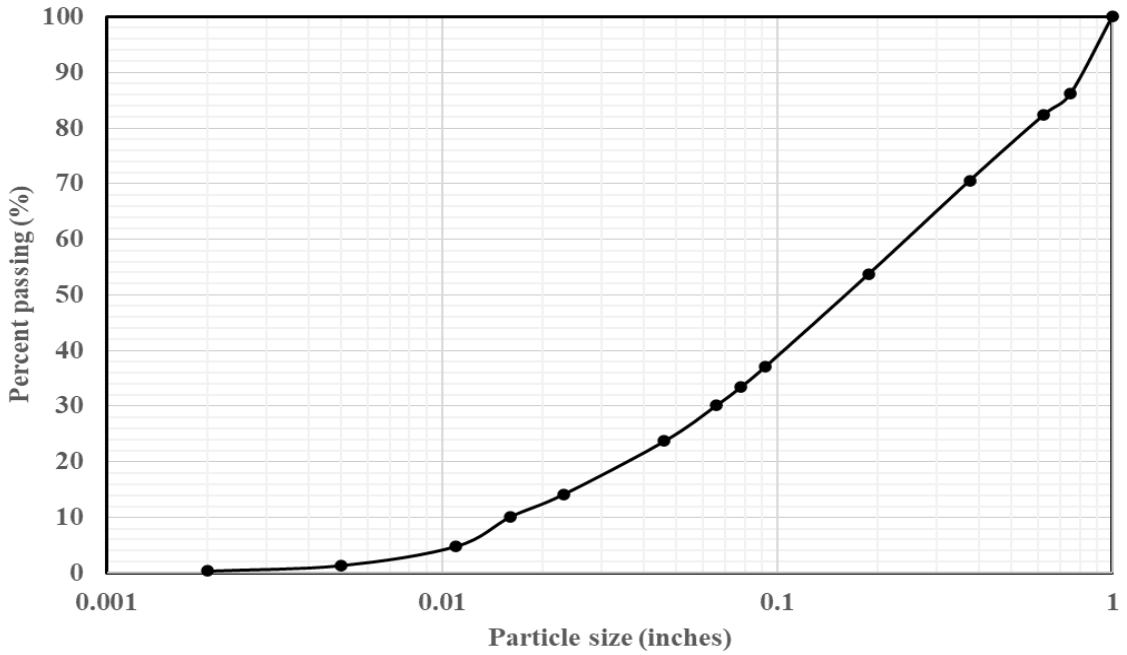

Figure 3.7 Particle-size distribution of the soil

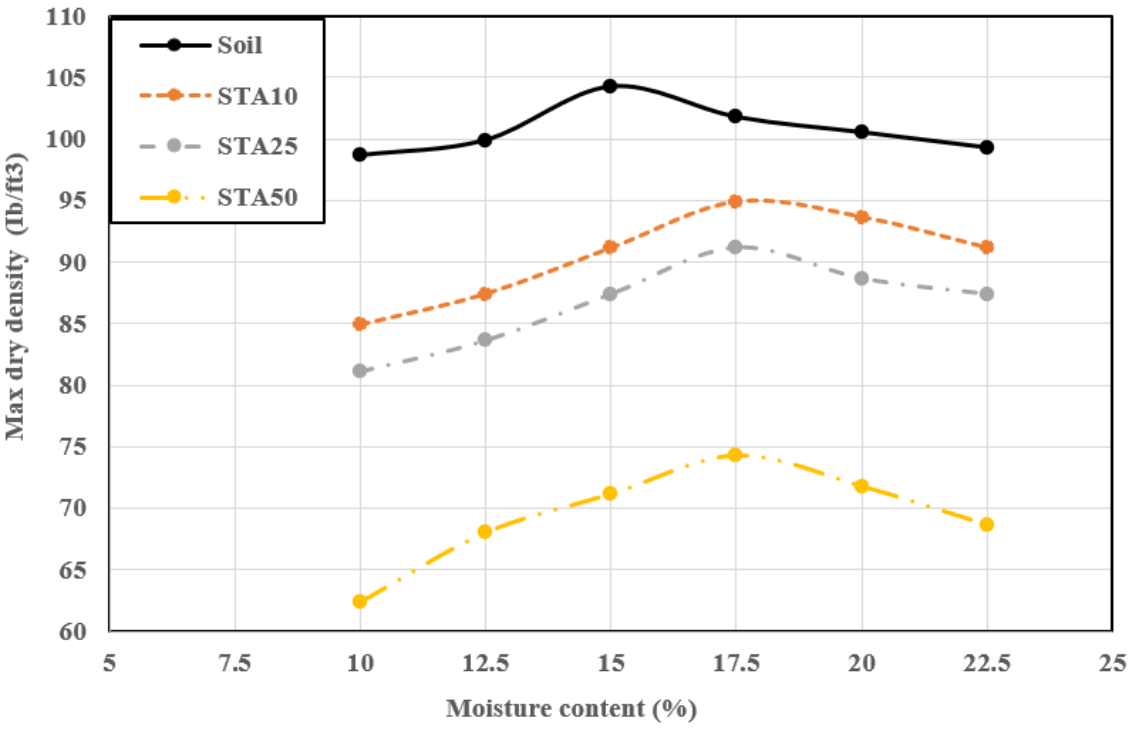

Figure 3.8 Max dry density versus optimum moisture content

Table 3.3 The physical characteristics of the soil used in this study

Characteristics	Value
D10 (inches)	0.01
D30 (inches)	0.07
D50 (inches)	0.15
D60 (inches)	0.23
Coefficient of uniformity (Cu)	13.95
Coefficient of gradation (Cc)	1.25
Dry density (loose) (Ib/ ft^3)	94.89
Optimum moisture density (compacted) (Ib/ ft^3)	104.25
Specific gravity (Gs)	2.38
Liquid limit (LL)	46
Plastic limit (PL)	19
Plasticity index (PI)	27

3.1.3. Preparation of the soil, TDA, and soil-TDA mixtures

This section outlines the process of preparing the soil and soil-TDA mixtures for the tests. Prior to mixing, soil samples were dried in an oven at 230°F for 24 hours and crushed if necessary. The TDA samples were air-dried at room temperature for 72 hours. After drying, precise quantities of soil, TDA, and water content were measured according to their respective mixing ratios and thoroughly mixed until a uniform consistency was achieved.

For the soil-TDA Type B mixtures, the same water content used for the soil-TDA Type A mixtures was applied. No additional water was added to the TDA itself, as the compaction water content for TDA particles is considered to be zero. Table 3.4 illustrates the weights of TDA, soil, and water for each mixture. The mixtures are labeled ST (soil-TDA), followed by letter A or B for TDA Type A or B, respectively. This is followed by the ratio of TDA to the total weight of the soil-TDA mixture. Special attention and continuous monitoring were employed during mixing to prevent any segregation in the mixtures. Thus, no segregation was observed between the soil and TDA particles during sample preparation and transfer into the shear box.

Table 3.4 Properties of the soil-TDA mixtures

Mixture	TDA/Soil	TDA (lb)	Soil (lb)	Water added (lb)	Unit Weight γ_{dry} (Ib/ft^3)
Soil	0	0	100	15	104.30
TDA (Type A)	1	100	0	0	43
TDA (Type B)	1	100	0	0	31
STA10	0.10	10	90	17.50	94.90
STA25	0.25	25	75	17.50	91.10
STA50	0.50	50	50	17.50	74.30
STB10	0.10	10	90	17.50	79.60
STB25	0.25	25	75	17.50	72.50
STB50	0.50	50	50	17.50	59.30

4. Chapter 4. Shear strength of TDA and soil-TDA mixtures

Due to the simplicity and accuracy of the direct shear test, it is preferred by most laboratories over more complex tests. However, TDA requires large-scale direct shear apparatus because of the consistently large size of its particles, and few facilities have this type of equipment. A shear device with larger dimensions and larger displacement capabilities can provide a better understanding of the shear strength of large TDA particles under a wide range of vertical overburden stresses. This study characterizes the shear strength of TDA-soil mixtures, specifically TDA Type A and TDA Type B mixed with soil at percentages ranging from 0% to 100%.

4.1. Experimental setup

The large-scale direct shear test equipment is shown in Figure 4.1 and Figure 4.2. The equipment consists of two boxes, each measuring 3 feet wide, 3 feet long, and 2 feet deep. Each box is constructed with four concrete metal formwork panels, while the bottom box includes an additional fifth bottom panel. Both boxes are laterally reinforced using four C 10x22 steel channels to withstand large vertical and horizontal loads.

The upper box is stationary and connected to an external steel frame using two 1x 2-inch steel angle link members. At the bottom of the upper box, there are twelve 2-inch diameter rollers, with six rollers on each side along the direction of movement (Figure 4.3 and Figure 4.4). The rollers support the weight of the upper box when placed on the lower box. After placing the upper box on the lower box, a gap of 0.25 inches remains between the two boxes. Therefore, during testing, the applied shear force is mainly resisted by the soil samples, with no friction between the edges of the two boxes. The lower box is the moving box; it is equipped with four wheels at its bottom, which move on a guide rail.

4.2. Loading and instrumentation

The vertical load is applied by a vertical hydraulic jack connected to a 1-inch-thick steel plate placed atop the soil sample to uniformly distribute the applied vertical load. Smooth plastic sheets line the inside of the four sides of each shear box to reduce friction between the soil and the inner sides, ensuring that the applied normal force is transferred to the soil. Each mixture was subjected to three vertical pressures: 3.63, 7.25, and 10.88 psi (25, 50, and 75 kPa). It is important to note that each pressure was a new test applied to a freshly prepared soil sample, ensuring accurate and independent results for each pressure level.

The bottom box is driven at a rate of 0.12 in./min by a horizontal hydraulic jack with a 7-inch stroke. This slow rate of applied displacement was selected to ensure that the load represented a static load.

The horizontal displacement of the bottom box was measured using a string potentiometer connected between the movable bottom box and the fixed steel frame. The applied horizontal force during the shear test was measured using a load cell installed between the hydraulic jack and the bottom box. The applied vertical load was measured using a load cell installed between the vertical jack and the top steel plate. A third load cell was placed inside the bottom box to

measure the weight of the mixtures. The string potentiometer and the two load cells were connected to a data acquisition system to automatically record the measured data.

Figure 4.1 Large-scale direct shear test device

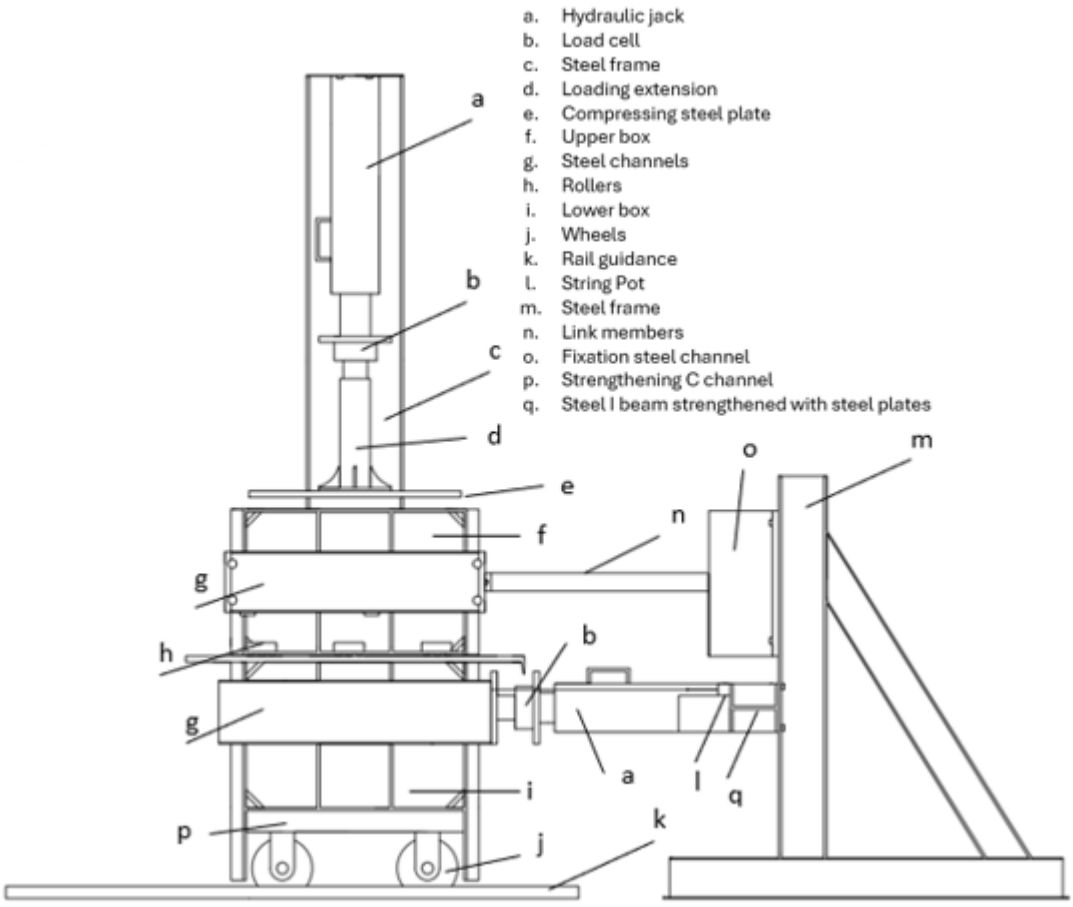

Figure 4.2 Two dimensional schematic diagram for the shear box

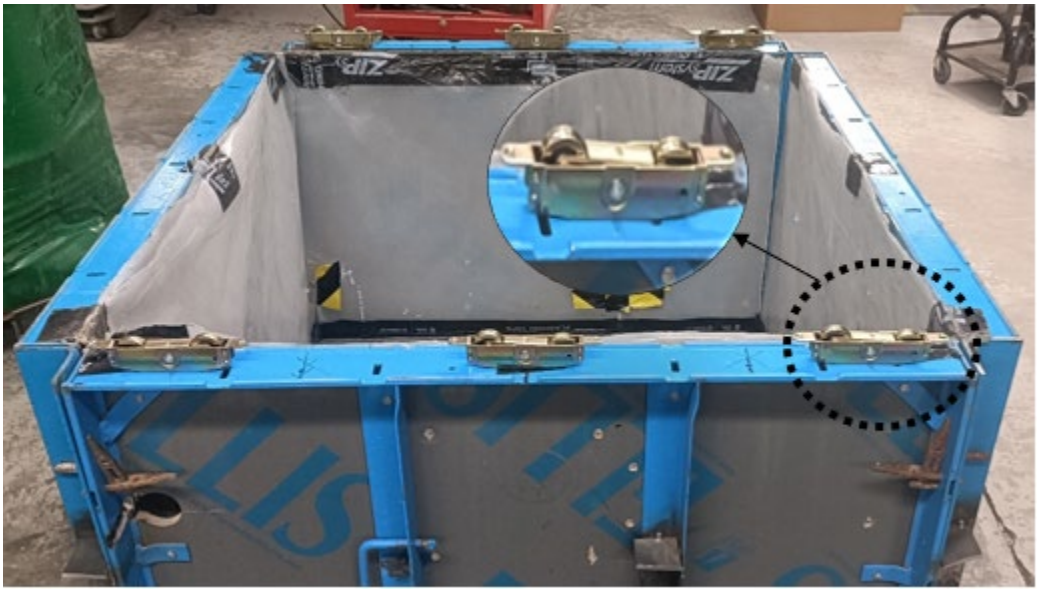

Figure 4.3 The upper shear box before installing the outstanding rollers

Figure 4.4 The upper shear box after installing the outstanding rollers

4.3. Test procedure

The lower box was filled with samples of soil, TDA, or TDA-soil mixtures in three layers (Figure 4.5). Each layer was compacted using the vertical hydraulic jack as static compaction (Figure 4.6) to reach the maximum dry density for each mixture: 104.25 lb/ft³ for soil, 43 lb/ft³ for TDA Type A, and 31 lb/ft³ for TDA Type B. The soil samples had an optimum water content of 15%, while the TDA samples were dry. For soil-TDA mixtures, the soil had an optimum water content of 17.50% (Figure 3.8).

The target densities were 94.89 lb/ft³ for STA10, 91.14 lb/ft³ for STA25, 74.29 lb/ft³ for STA50, 79.62 lb/ft³ for STB10, 72.51 lb/ft³ for STB25, and 59.34 lb/ft³ for STB50. Figure 4.7 shows the dry unit weight versus the TDA content for the soil-TDA mixtures for the different samples. It is important to note that during compaction, the shear plane defined by the shear box should not be located at the interface between two compacted layers, as this would result in lower and non-representative shear resistance. Therefore, during compaction, it was ensured that the shear plane was approximately in the middle of a compacted layer.

Once the samples were placed and compacted in the lower box, the upper box was aligned on top and filled with soil in the same manner (Figure 4.8). The top steel plate was then placed atop the sample, followed by the installation of the vertical load cell on the steel plate, which was then connected to the vertical hydraulic jack (Figure 4.9).

The design vertical load was applied using the hydraulic jack and maintained constant throughout the shear testing. The direct shear tests were conducted at three confining pressures: 3.63, 7.25, and 10.88 psi (25, 50, and 75 kPa). Subsequently, the lower box was displaced at a constant rate

of 0.12 in./min using the horizontal hydraulic jack. The horizontal resistance force, horizontal displacement of the lower shear box, and vertical force were recorded by the data acquisition system at a rate of approximately 2,000 readings per second. After each shear test, the samples were removed from the shear box, fully mixed again, and used for the next test as freshly prepared material.

Figure 4.5 Filling the bottom shear box with TDA Type A

Figure 4.6 Compacting the different samples before the test

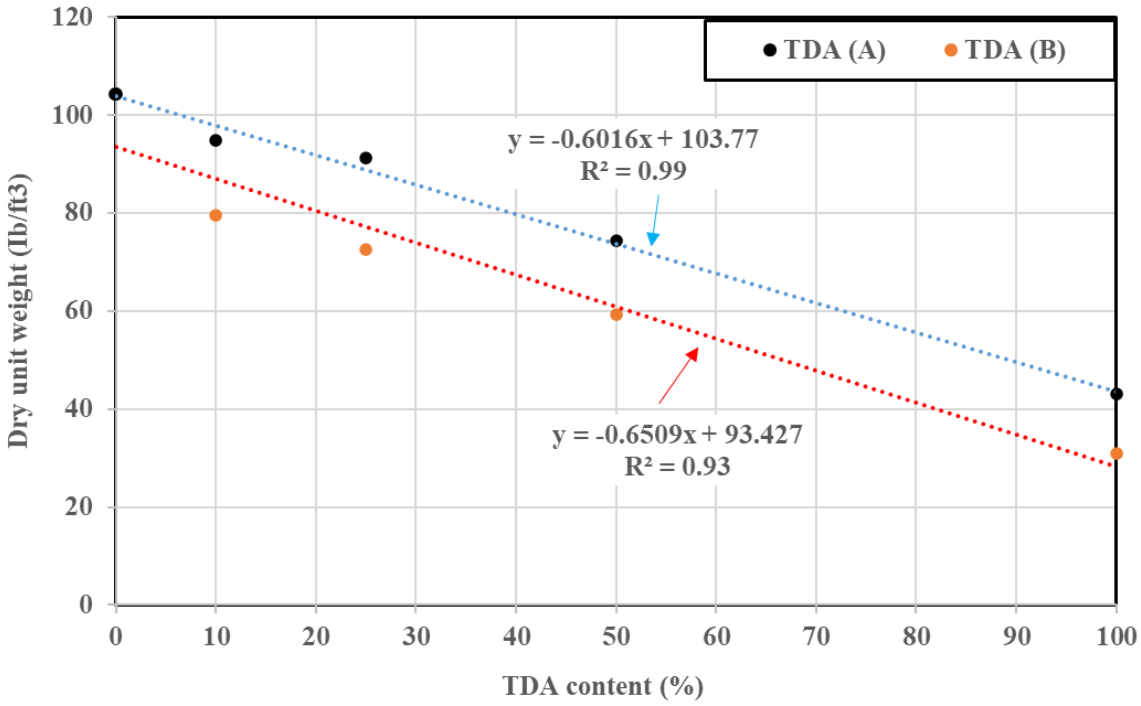

Figure 4.7 The dry unit weight versus the TDA content for the soil-TDA mixtures

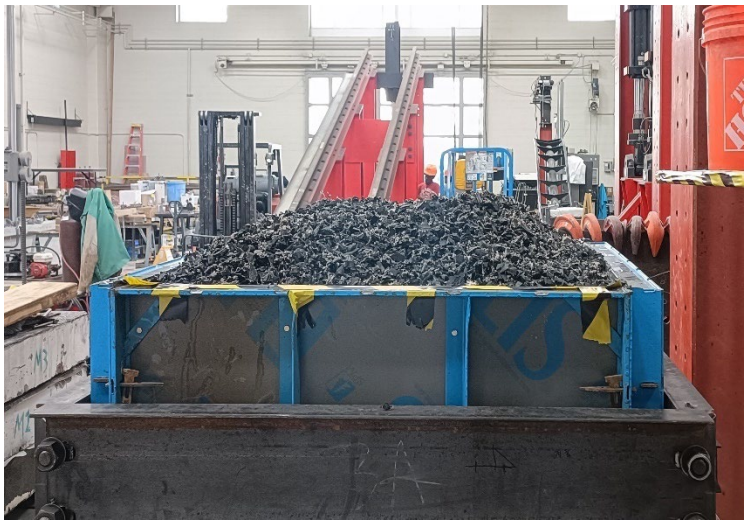

Figure 4.8 Filling the upper shear box with TDA Type A

Figure 4.9 Placing the upper box in its place preparing for the direct shear test

4.4. Results and discussion

The shear force versus displacement for all mixtures is shown in Figure 4.10 through Figure 4.18. As shown in the figures, all specimens displayed similar behavior with two distinct stages. In stage one, the specimens exhibited elastic response where the shear forces significantly increased with the applied displacement. This was followed by stage two, where stiffness softening occurred and the shear forces slightly increased with further displacement.

As expected, the applied normal force did not significantly affect the elastic shear stiffness. However, the peak shear force significantly increased with the applied normal force. Furthermore, softening for pure TDA samples started at relatively small shear forces compared to those of the pure soil or soil-TDA mixtures. Additionally, it is noteworthy that the variations in peak shear force among the different soil-TDA mixtures become less pronounced as the applied normal force increases. Furthermore, the peak shear force across soil-TDA Type B mixtures is generally higher than that of soil-TDA Type A mixtures at the same vertical loads.

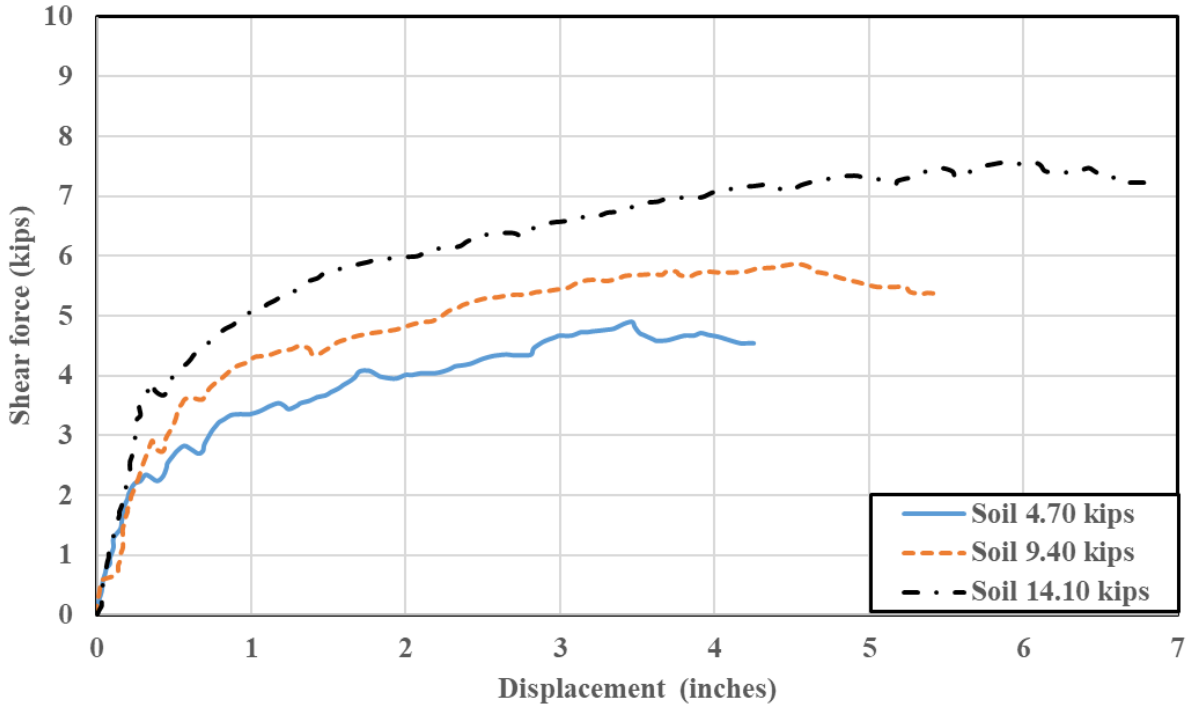

Figure 4.10 The shear force versus displacement for the soil

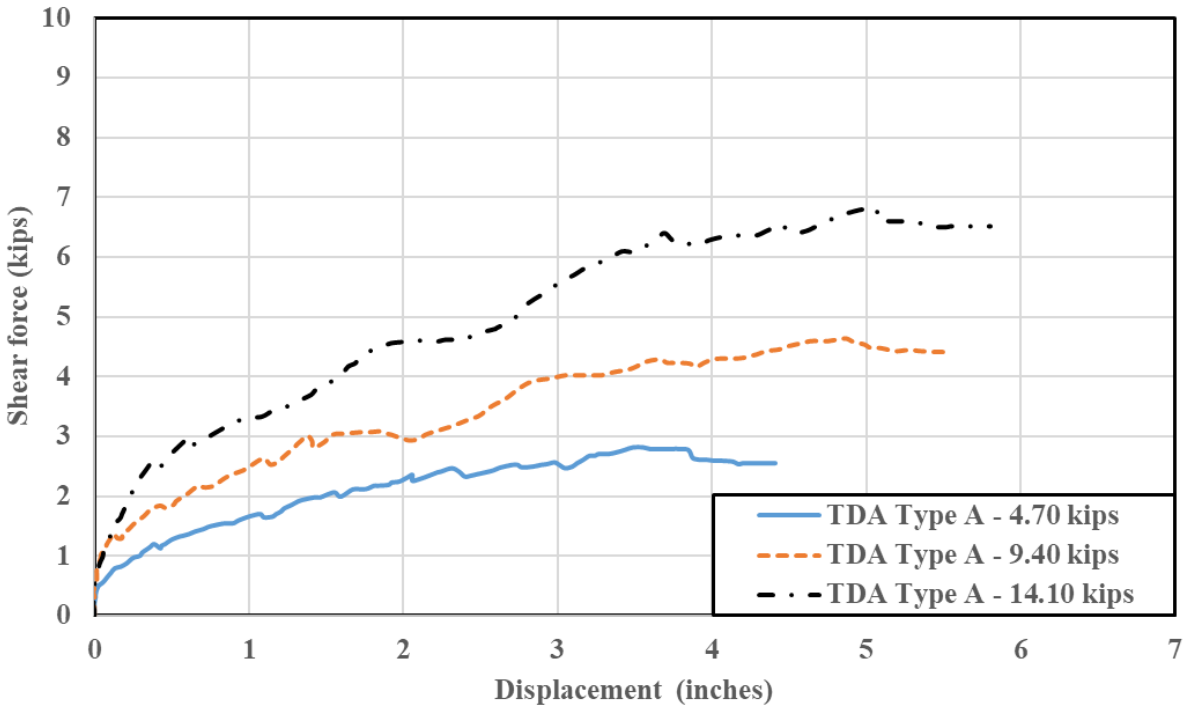

Figure 4.11 The shear force versus displacement for the TDA Type A

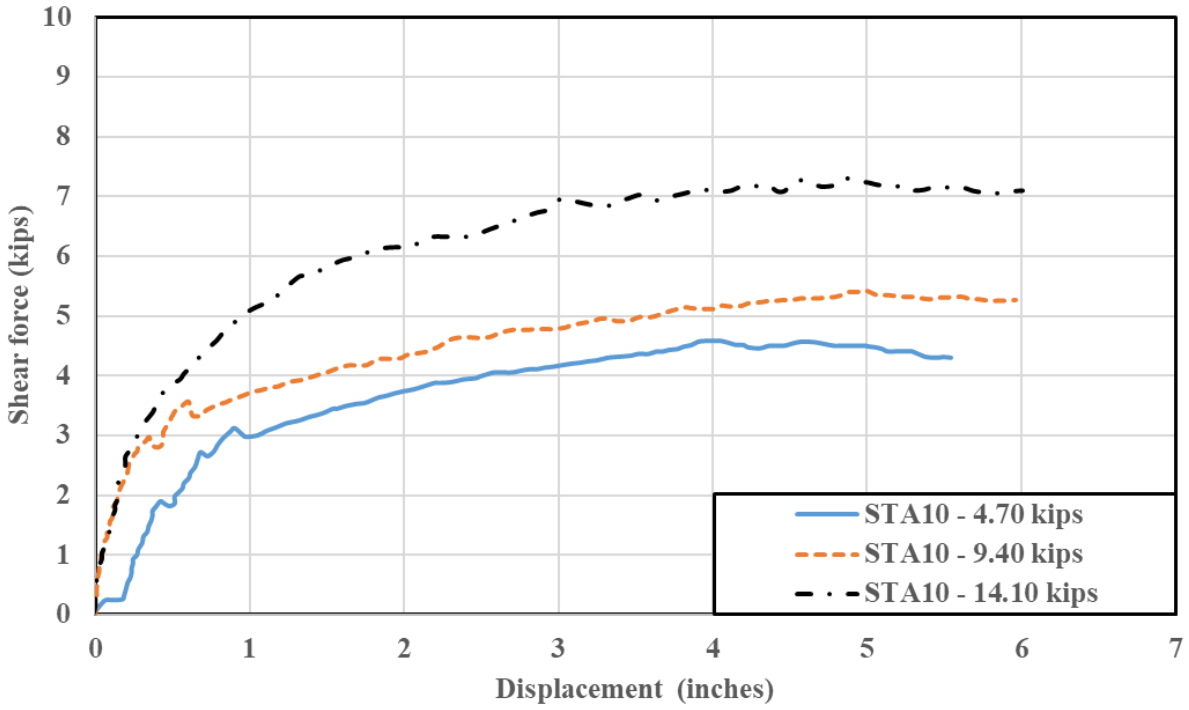

Figure 4.12 The shear force versus displacement for the soil mixed with 10 percent of TDA Type A

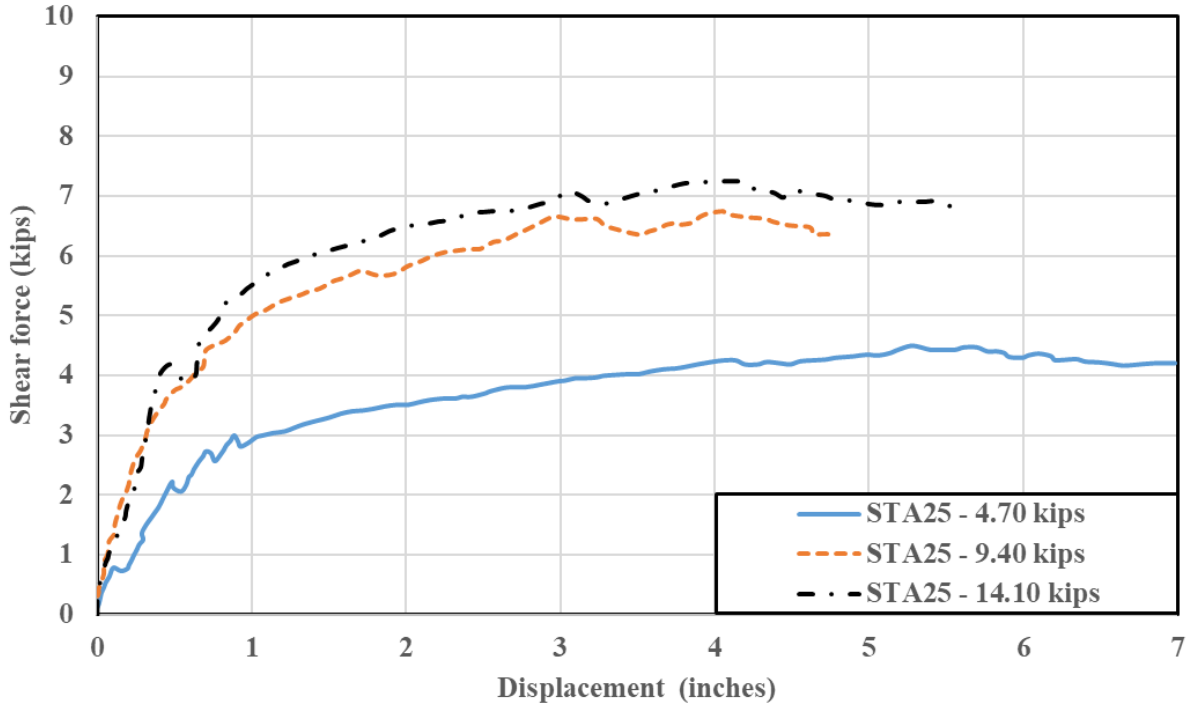

Figure 4.13 The shear force versus displacement for the soil mixed with 25 percent TDA Type A

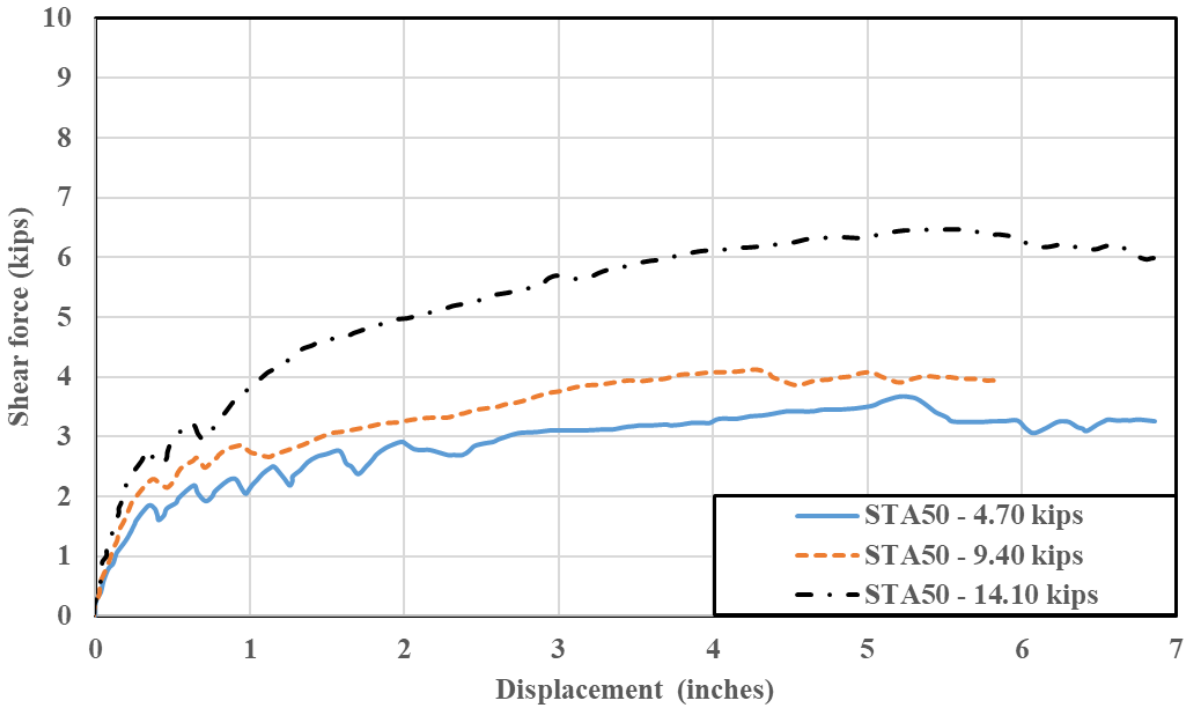

Figure 4.14 The shear force versus displacement for the soil mixed with 50 percent of TDA Type A

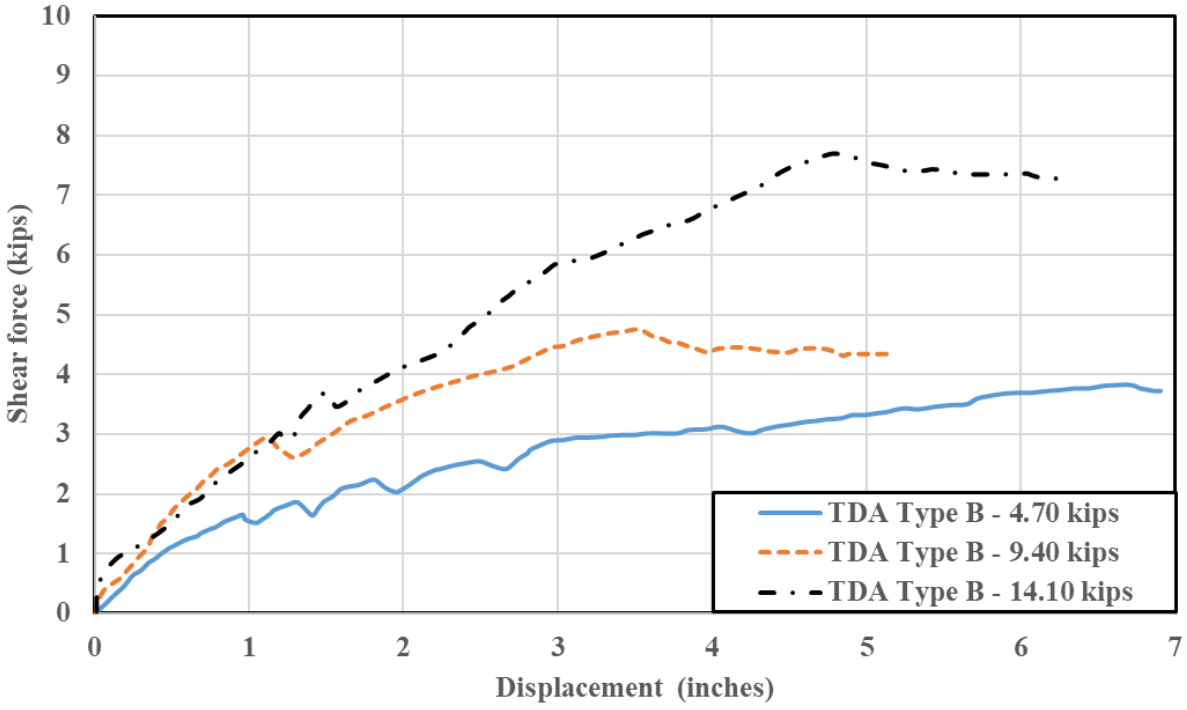

Figure 4.15 The shear force versus displacement for the TDA Type B

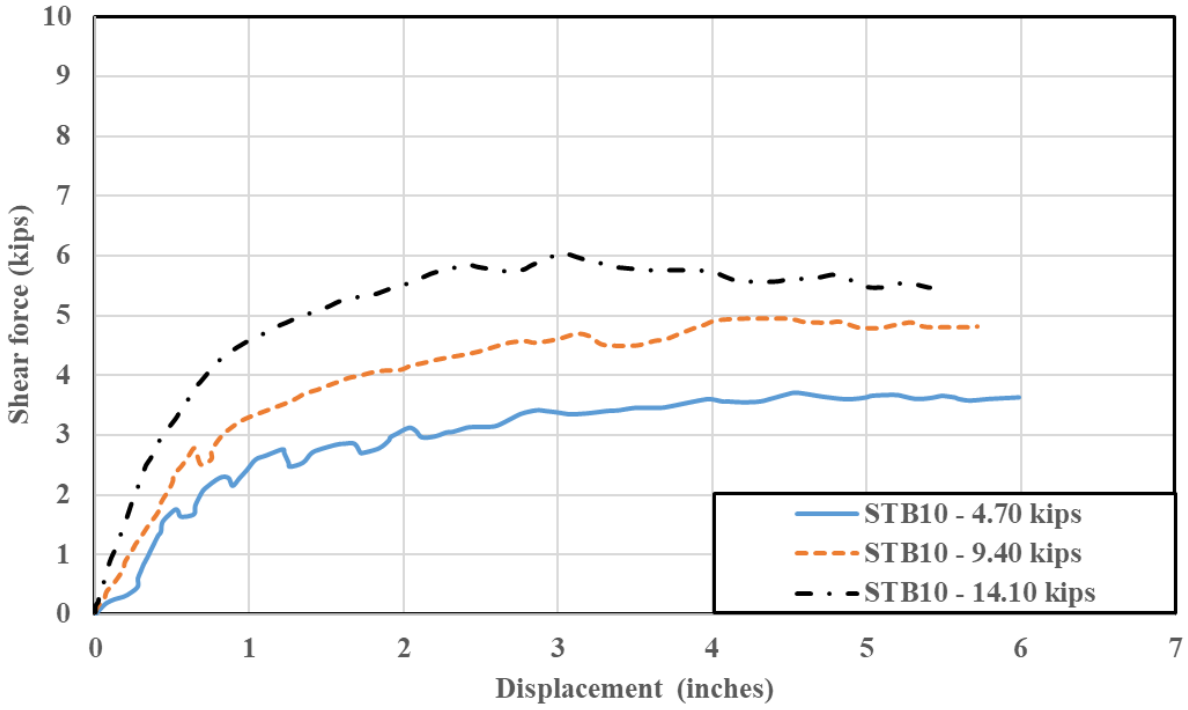

Figure 4.16 The shear force versus displacement for the soil mixed with 10 percent of TDA Type B

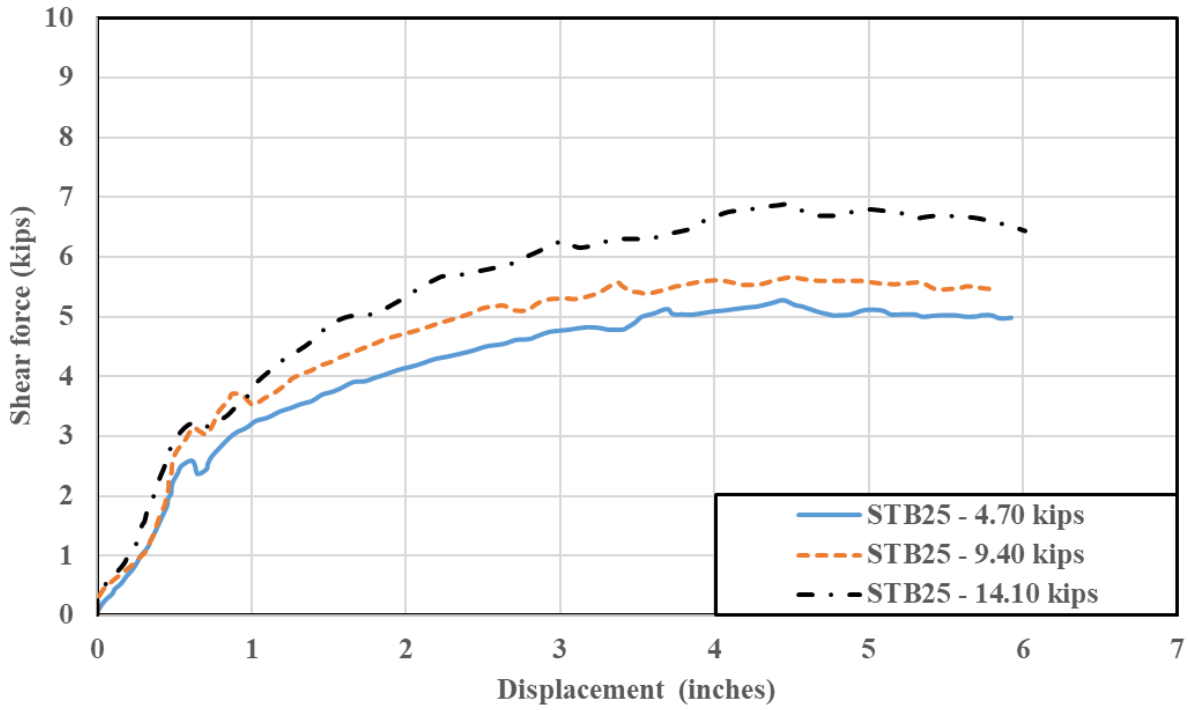

Figure 4.17 The shear force versus displacement for the soil mixed with 25 percent of TDA Type B

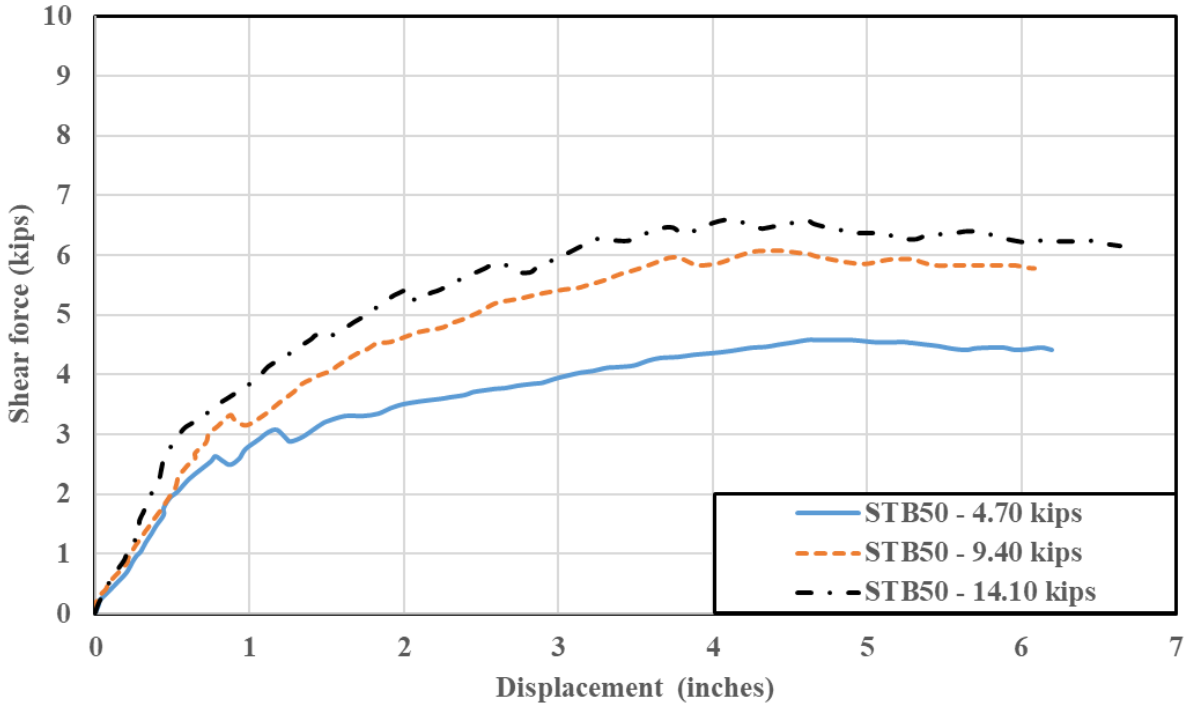

Figure 4.18 The shear force versus displacement for the soil mixed with 50 percent of TDA Type B

For each sample, the peak shear force under each normal load was used as the failure shear stress, and it was plotted versus the applied normal force in Figure 4.19 through Figure 4.27. The shear failure envelope yielded an average soil cohesion of 2.84 psi for pure soil, which dropped tenfold to approximately 0.24 psi for TDA Type A and 1.21 psi for TDA Type B. However, mixing soil with TDA significantly improved the soil cohesion compared to the pure TDA specimens, with cohesion ranging from 1.62 psi to 2.33 psi for soil-TDA Type A mixtures and 2.21 to 3.03 psi for soil-TDA Type B mixtures.

Table 4.1 summarizes the cohesion values for all specimens. Similarly, the shear failure envelope yielded an average soil angle of internal friction of 14.38° for pure soil, which doubled to approximately 27.10° for TDA Type A and 23.05° for TDA Type B. Mixing soil with TDA did not significantly affect the soil's angle of internal friction, with angles ranging from 11.17° to 16.70° for soil-TDA Type A mixtures and 10.55° to 12.59° for soil-TDA Type B mixtures. Table 4.2 summarizes the angle of internal friction s for all specimens.

Table 4.1 Summary of the cohesion values for all specimens

TDA content (%)	Cohesion - TDA Type A mixtures (psi)	Cohesion - TDA Type B mixtures (psi)
0	2.84	2.84
10	2.33	2.21
25	2.67	3.27
50	1.62	3.03
100	0.24	1.21

Table 4.2 Summary of the angle of internal friction

TDA content (%)	Angle of internal friction for TDA Type A mixtures (degrees)	Angle of internal friction for TDA Type B mixtures (degrees)
0	14.38	14.38
10	16.70	12.59
25	15.75	10.55
50	11.17	12.59
100	27.10	23.05

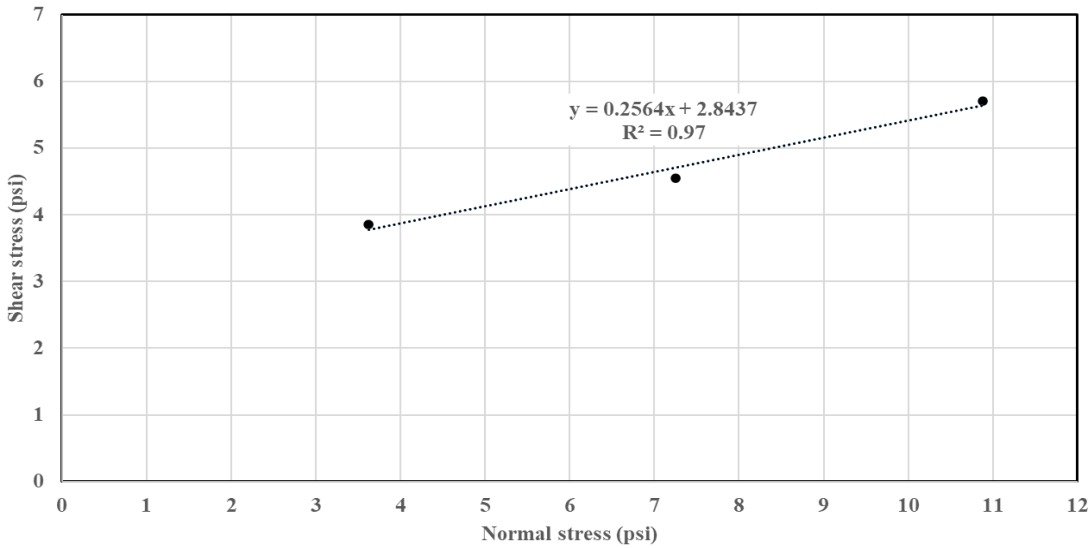

Figure 4.19 The shear failure envelope of the soil

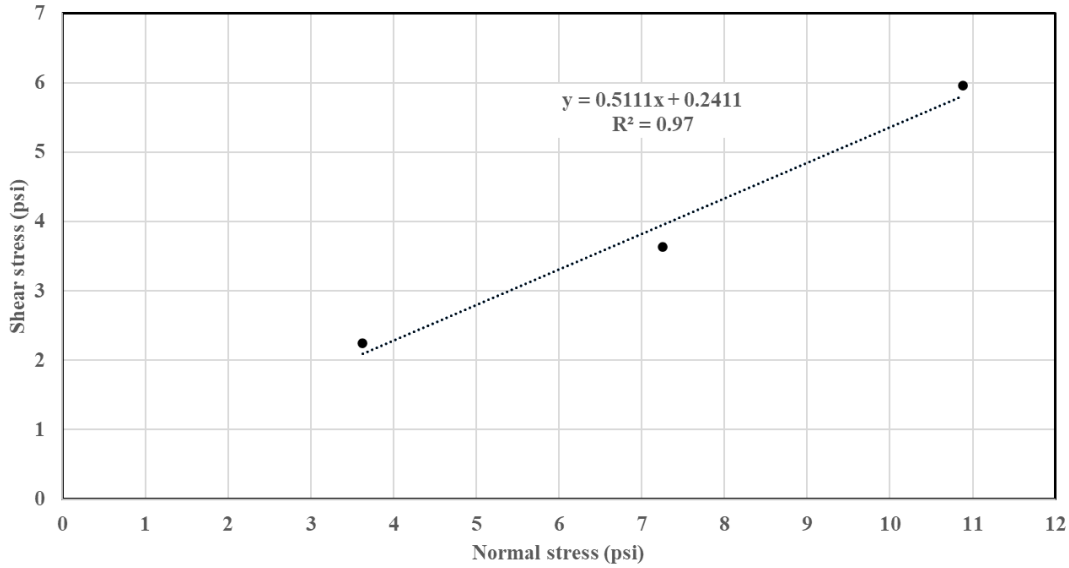

Figure 4.20 The shear failure envelope of the TDA Type A

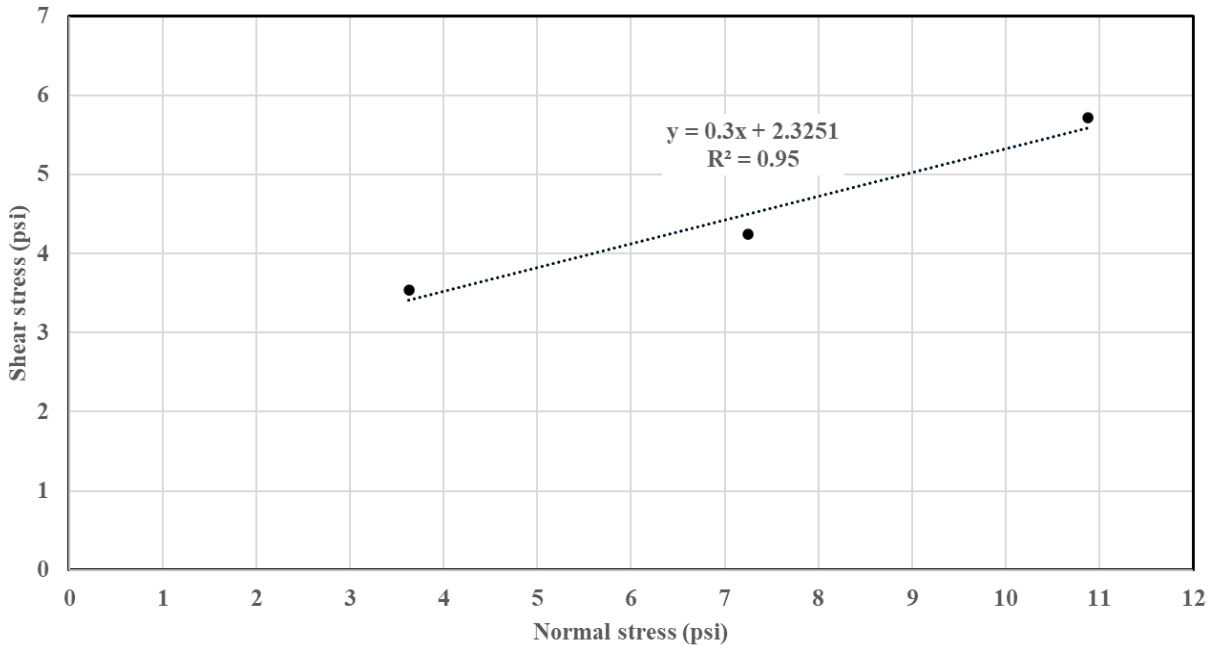

Figure 4.21 The shear failure envelope of the soil mixed with 10 percent of TDA Type A

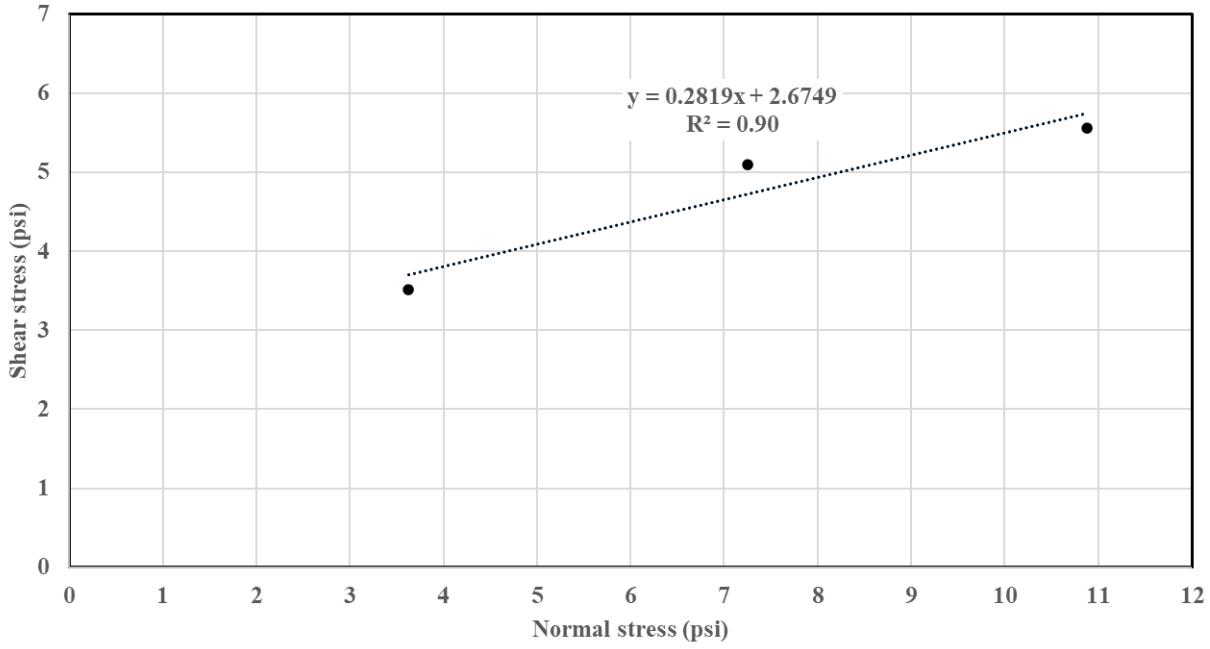

Figure 4.22 The shear failure envelope of the soil mixed with 25 percent of TDA Type A

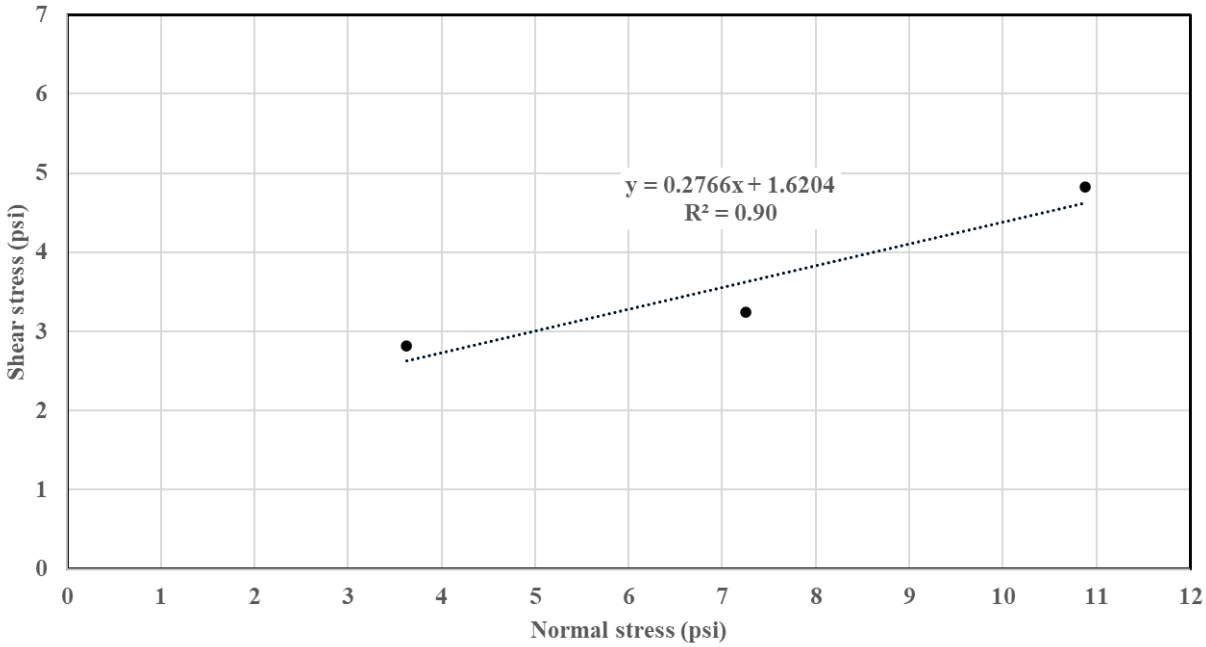

Figure 4.23 The shear failure envelope of the soil mixed with 50 percent of TDA Type A

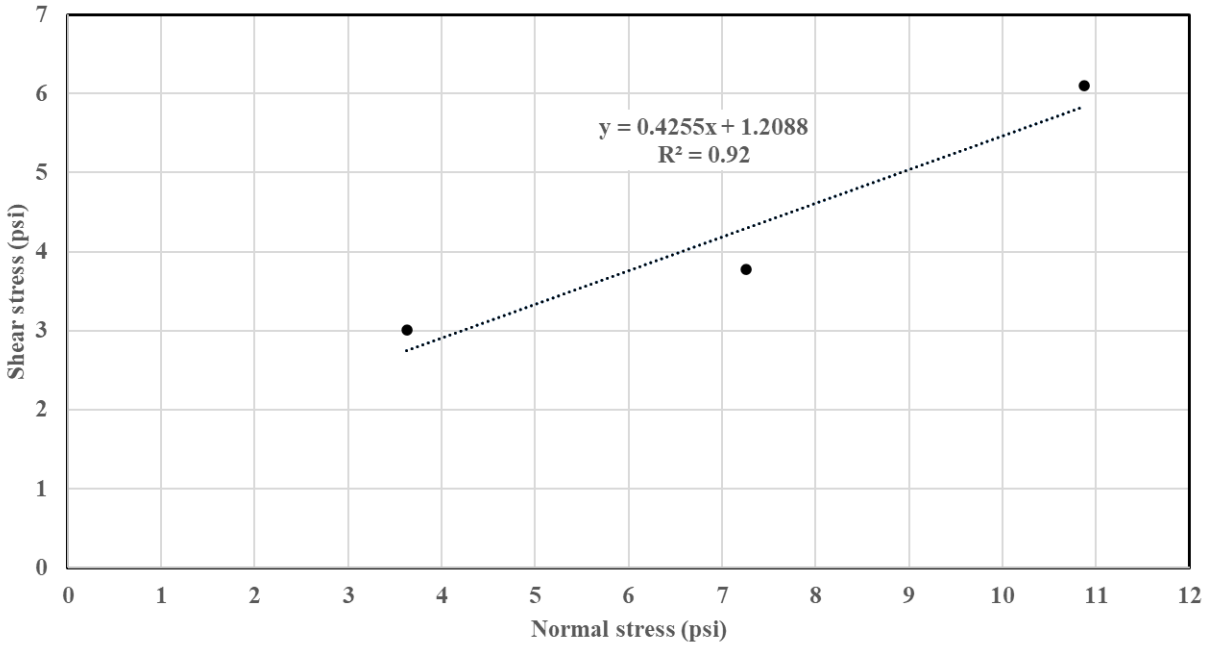

Figure 4.24 The shear failure envelope of the TDA Type B

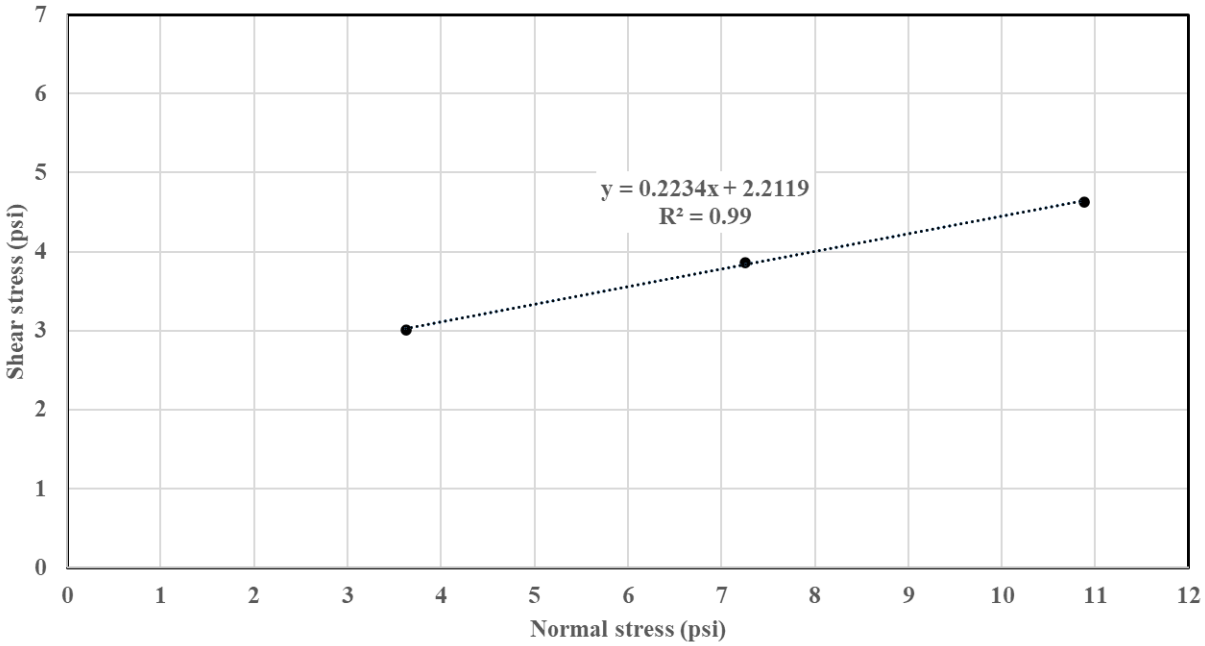

Figure 4.25 The shear failure envelope of the soil mixed with 10 percent of TDA Type B

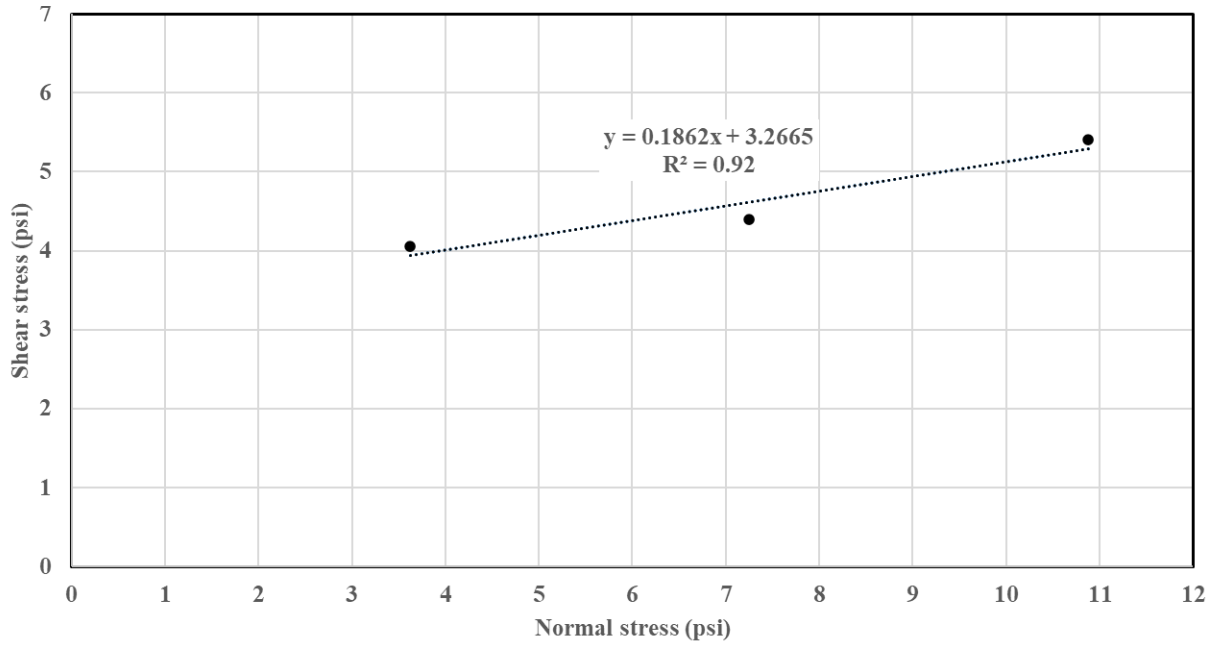

Figure 4.26 The shear failure envelope of the soil mixed with 25 percent of TDA Type B

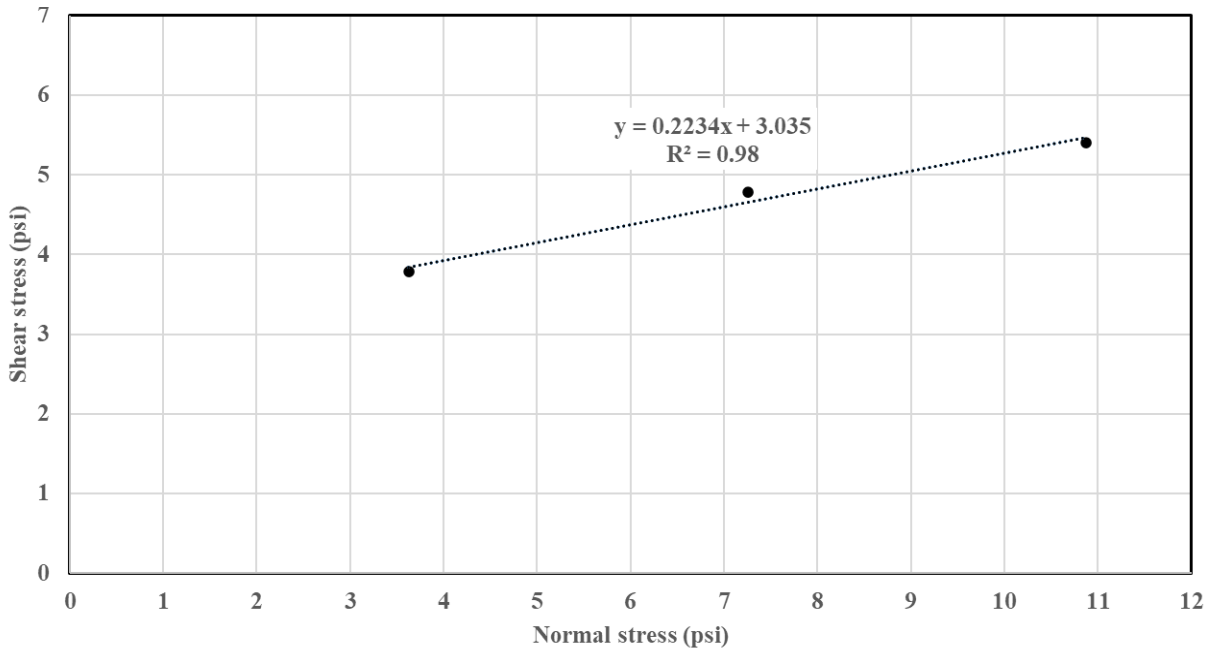

Figure 4.27 The shear failure envelope of the soil mixed with 50 percent of TDA Type B

4.5. Shear stress versus shear strain behavior of the soil-TDA mixtures

Figure 4.28 through Figure 4.33 present the shear stress versus shear strain for all mixtures under the evaluated confining pressures, revealing a peak shear stress indicative of the shear strength of the samples. The introduction of TDA Type A consistently reduced the shear resistance across all confining pressures. Specifically, at confining pressures of 3.63 and 7.25 psi, increasing the TDA Type A content up to 10% by weight did not significantly impact peak shear resistance, though a reduction was observed at 10.88 psi for the STA10 mixture. Increasing TDA Type A content up to 25% by weight did not significantly alter peak shear resistance at 3.63 and 10.88 psi, but a decrease was noted for the STA25 mixture at 7.25 psi. The addition of TDA Type A up to 100% by weight resulted in a gradual decrease in peak shear resistance at higher shear strains across all confining pressures.

In contrast, adding TDA Type B up to 10% by weight reduced the shear resistance at all confining pressures. However, the STB25 mixture exhibited increased peak shear resistance at higher shear strains under confining pressures of 3.63 and 7.25 psi. When the TDA Type B content was raised up to 50% by weight, the peak shear resistance remained largely unchanged at these pressures. Although increasing TDA Type B content up to 100% by weight decreased the peak shear resistance at 3.63 and 7.25 psi, it did not significantly affect peak shear resistance at 10.88 psi. These findings underscore the distinct impacts of TDA Type A and Type B on the shear resistance of soil-TDA mixtures under varying confining pressures. The data consistently show that increasing the confining pressure from 3.63 to 10.88 psi enhances shear resistance in mixtures containing the same amount of TDA, indicating that higher confining pressures contribute to improved shear strength in soil-TDA blends, regardless of TDA type and content.

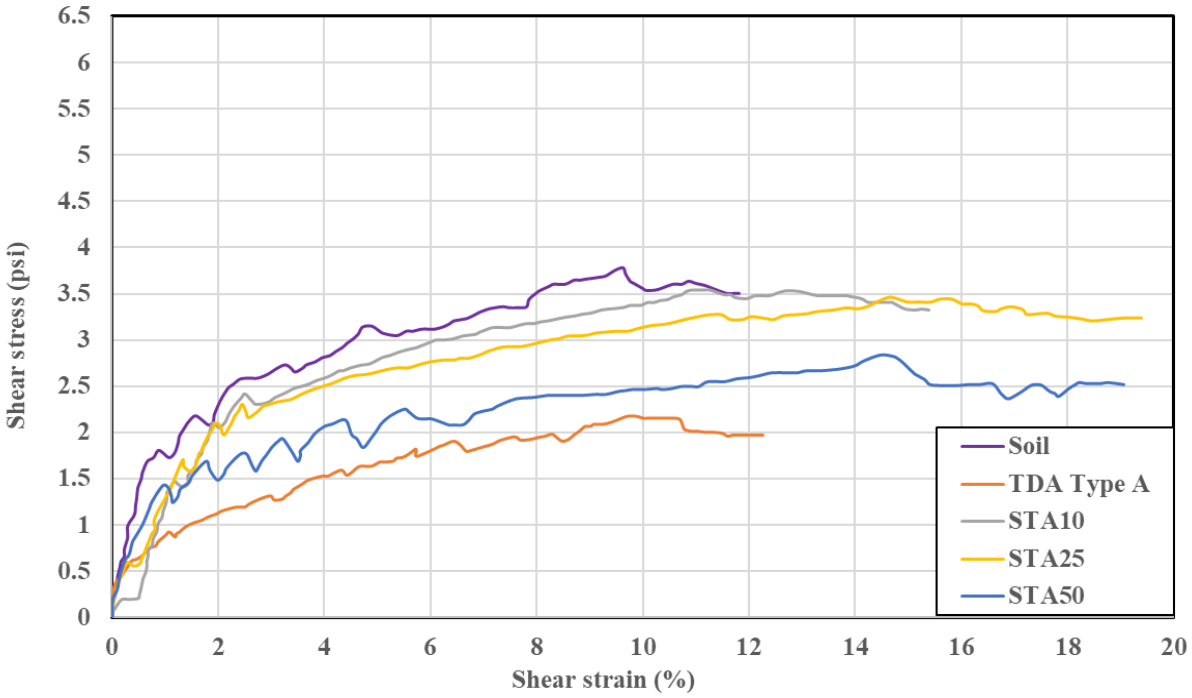

Figure 4.28 Shear stress versus shear strain for the soil-TDA Type A mixtures at confining pressures of 3.63 psi

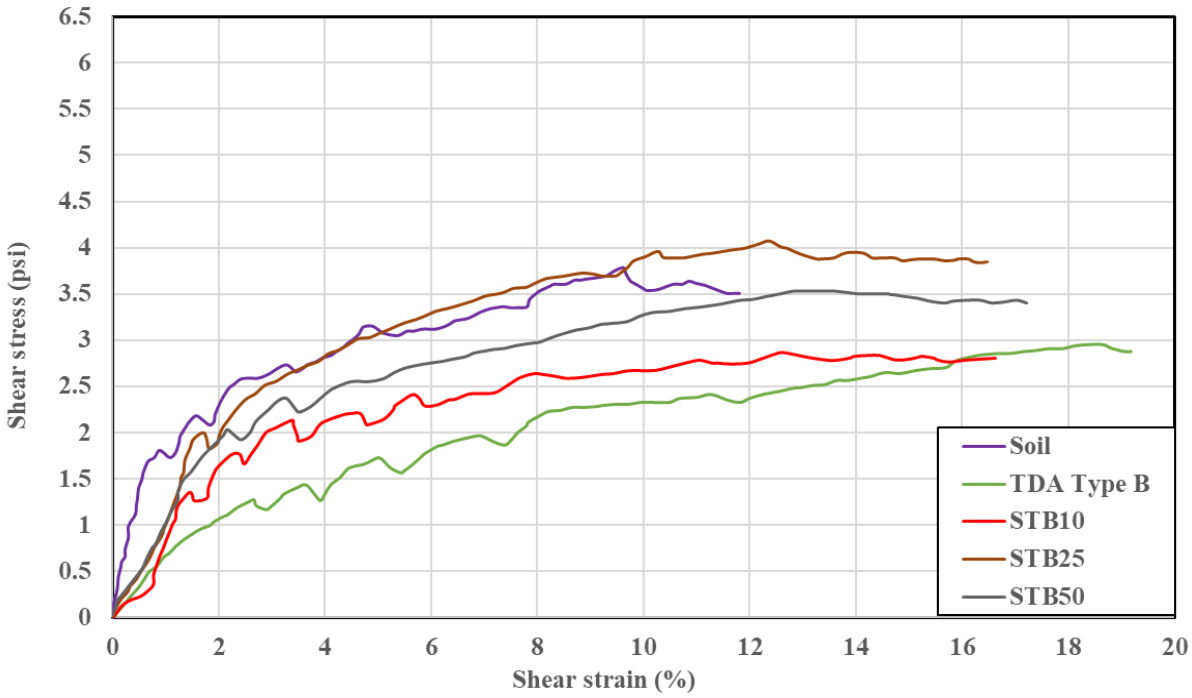

Figure 4.29 Shear stress versus shear strain for the soil-TDA Type B mixtures at confining pressures of 3.63 psi

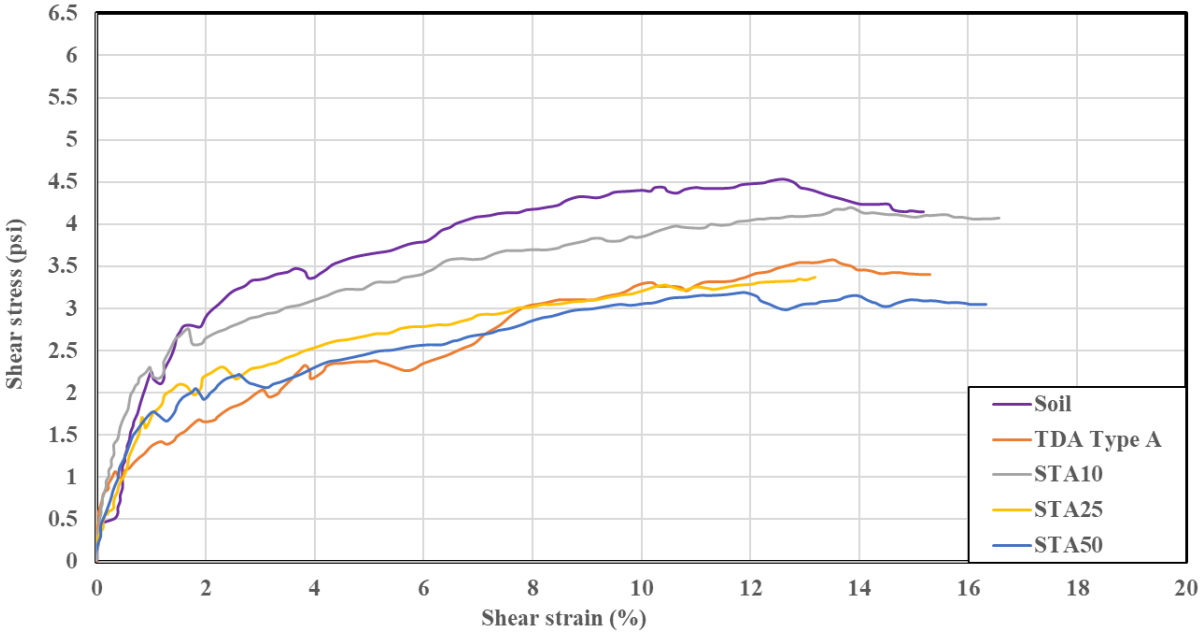

Figure 4.30 Shear stress versus shear strain for the soil-TDA Type A mixtures at confining pressures of 7.25 psi

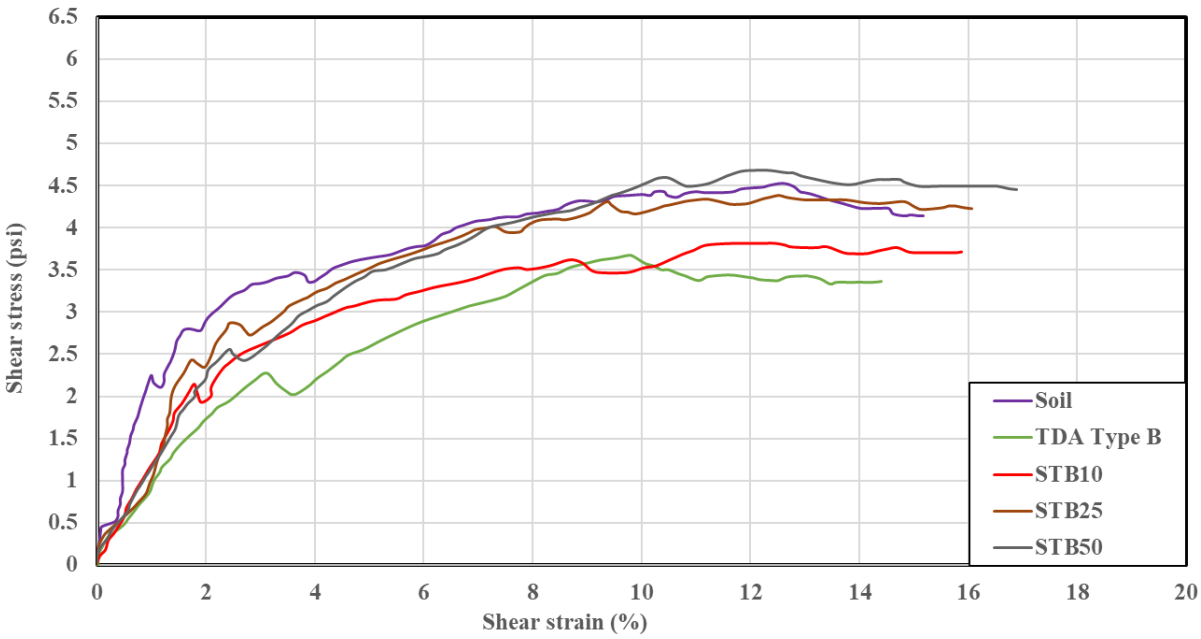

Figure 4.31 Shear stress versus shear strain for the soil-TDA Type B mixtures at confining pressures of 7.25 psi

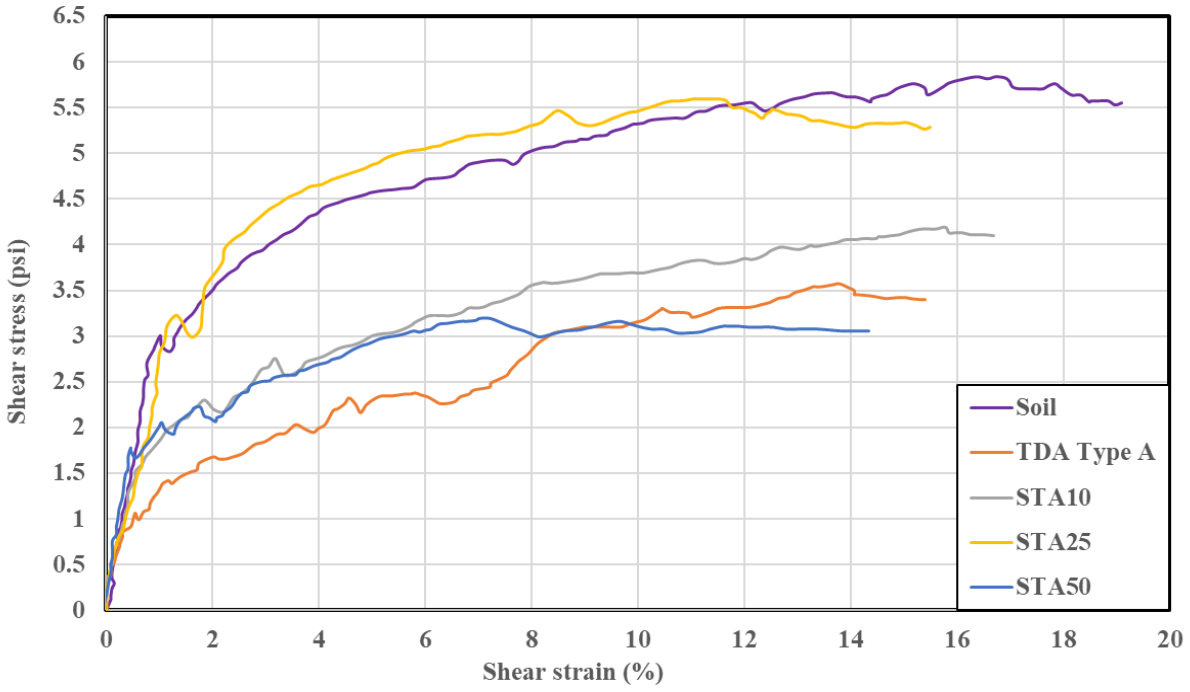

Figure 4.32 Shear stress versus shear strain for the soil-TDA Type A mixtures at confining pressures of 10.88 psi

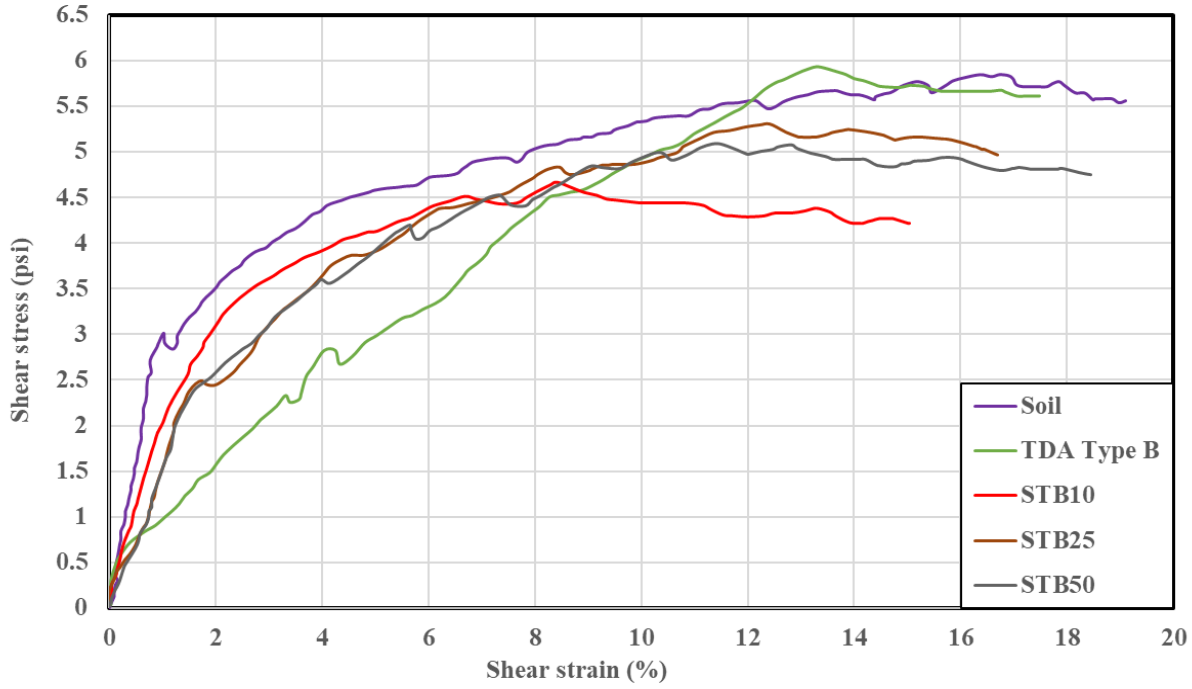

Figure 4.33 Shear stress versus shear strain for the soil-TDA Type B mixtures at confining pressures of 10.88 psi

4.6. Discussion of the shear strength parameters of the soil-TDA mixtures

4.6.1. Cohesion for the mixtures

Figure 4.34 and Figure 4.35 present the cohesion for each mixture and the cohesion of each mixture normalized by that of pure soil, respectively. Figure 4.35 also includes the normalized cohesion with a ±20% tolerance band. It was observed that, generally, the cohesion for mixtures including TDA Type B was higher than that for mixtures including TDA Type A. For STA25 and STA50, the cohesion reduced from 2.84 psi to an average of 2.15 psi, representing a decrease of 24.47%. For STB25 and STB50, the cohesion slightly increased from 2.84 psi to an average of 3.15 psi, representing an increase of 10.84%. However, at 100% TDA, both types displayed an average cohesion of 0.73 psi, representing a decrease of 74.30% compared to that of the reference soil specimens. Based on a ±20% threshold for acceptable cohesion changes, a maximum of 25% TDA Type A and 50% TDA Type B can be mixed with pure soil without significant changes in cohesion. Beyond this TDA threshold, substantial alterations in cohesion occur.

4.6.2. Angle of internal friction for the mixtures

Figure 4.36 and Figure 4.37 show the angle of internal friction for each mixture, and the angle of internal friction normalized by that of the pure soil sample. Figure 4.37 also includes the normalized angle of internal friction with a ±20% tolerance band. Generally, mixtures incorporating TDA Type A exhibited a higher angle of internal friction than those with TDA Type B. For STA10 and STA25, the angle of internal friction values slightly increased from 14.38^{o} to an average of 16.70^{o}, representing a 16% increase. In contrast, for STB10 and STB25, the angle of internal friction decreased from 14.38^{o} to an average of 11.57^{o}, reflecting a 19.50% reduction. However, at 100% TDA, both types displayed an average angle of internal friction of 25.30^{o}, representing a 75.94% increase compared to the reference soil specimens. Based on a 20% threshold for acceptable changes in the angle of internal friction, a maximum of 70% TDA Type A or TDA Type B can be mixed with pure soil without significant deviation from the acceptable friction angle values.

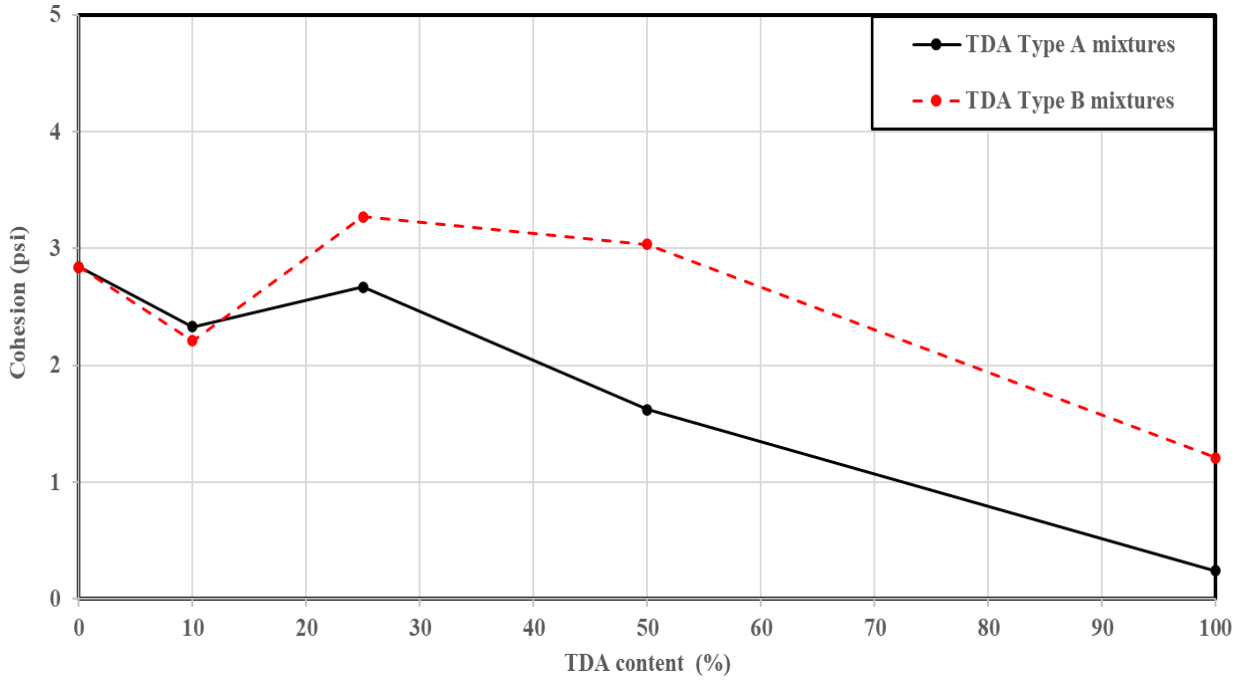

Figure 4.34 The cohesion of the soil-TDA mixtures

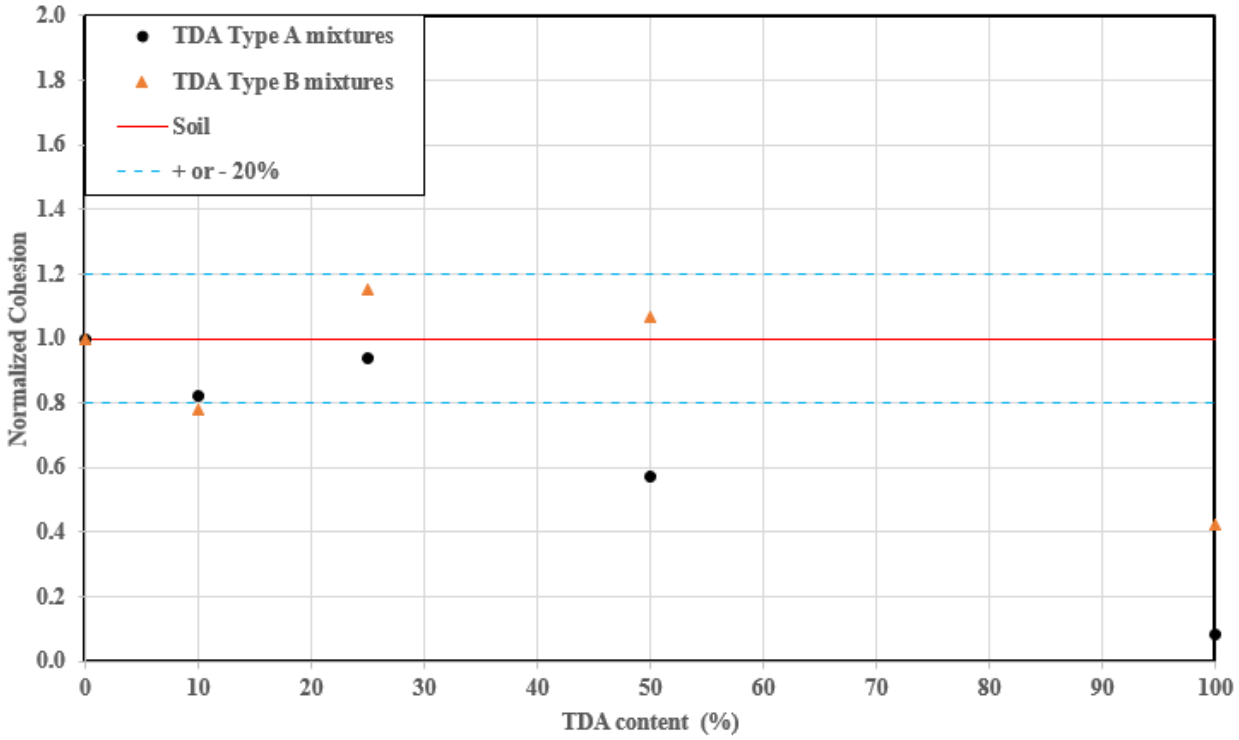

Figure 4.35 The normalized cohesion of each mixture

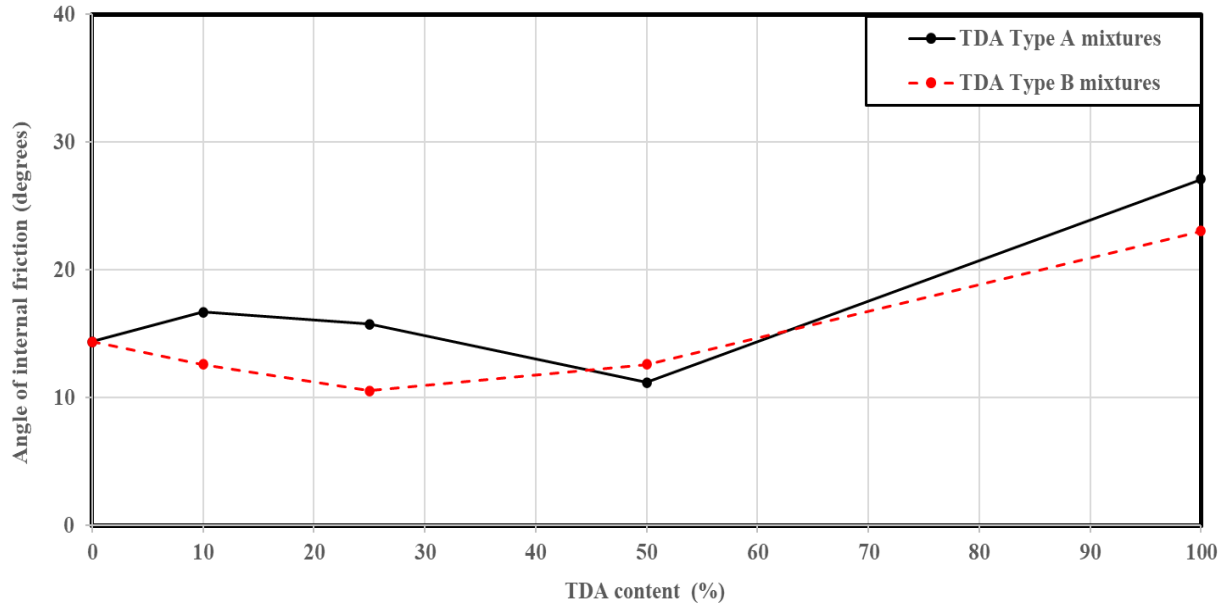

Figure 4.36 The angle of internal friction for the soil-TDA mixtures

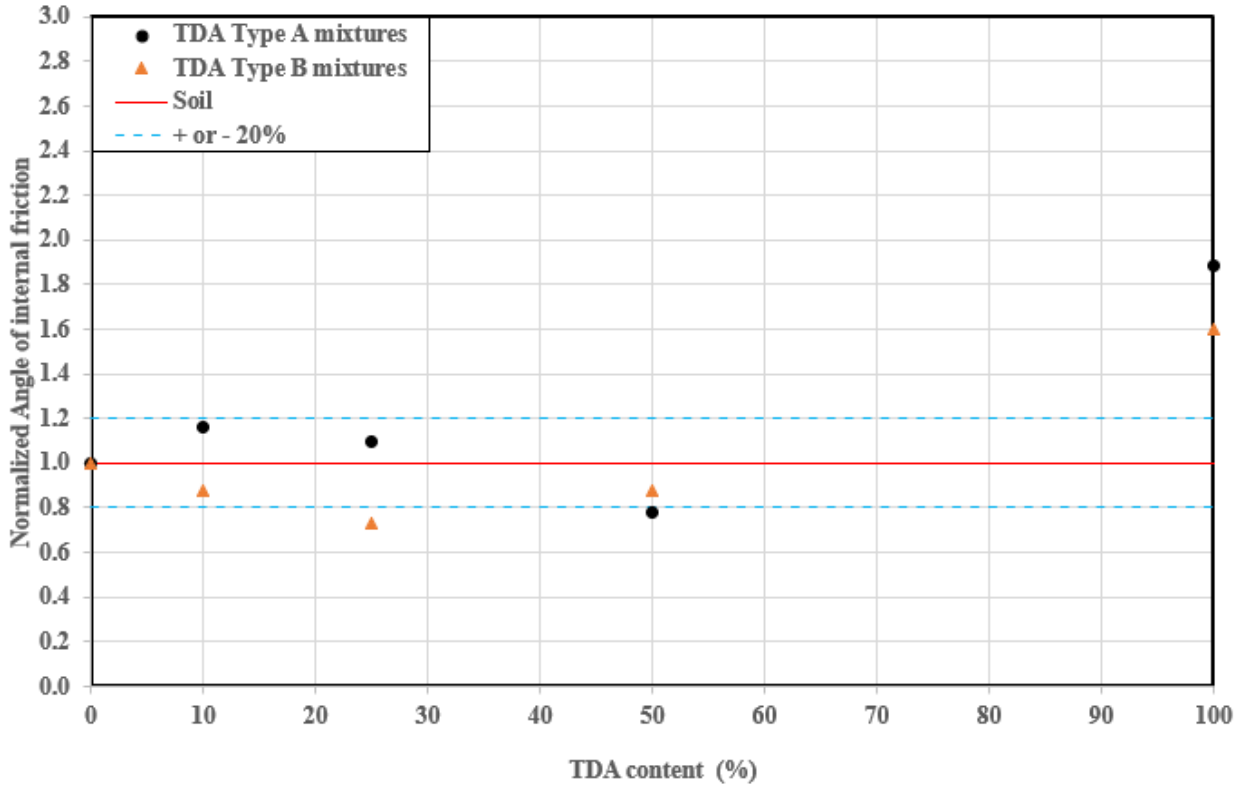

Figure 4.37 The normalized angle of internal friction of each mixture

4.6.3. Shear modulus for the mixtures

The shear modulus is a mechanical parameter used to analyze the behavior of materials during shearing. Equation 4-1 was used to calculate the shear modulus (Braja, 2014):

$$G = \tau / \varepsilon$$

Equation 4-1 Equation of the shear modulus

where G is the shear modulus, τ is the shear stress, and ε is the shear strain. Figure 4.38 and Figure 4.39 show the shear modulus plotted against the TDA Type A and Type B content, respectively, for the soil-TDA mixtures at confining pressures of 3.63, 7.25, and 10.88 psi. Adding up to 10% TDA Type A or B by weight to the soil significantly decreased the shear modulus at confining pressures of 3.63 and 7.25 psi. However, increasing the confining pressures to 10.88 psi significantly increased the shear modulus. Adding more than 25% up to 50% TDA Type A sharply reduced the shear modulus at all confining pressures, after which the values remained almost constant. In contrast, adding more than 25% up to 50% TDA Type B resulted in greater values at confining pressures of 7.25 and 10.88 psi, except a gradual reduction at a confining pressure of 3.63 psi.

It can be concluded that for the soil-TDA mixtures, the stiffness behavior of the mixtures is enhanced by increasing the confining pressures.

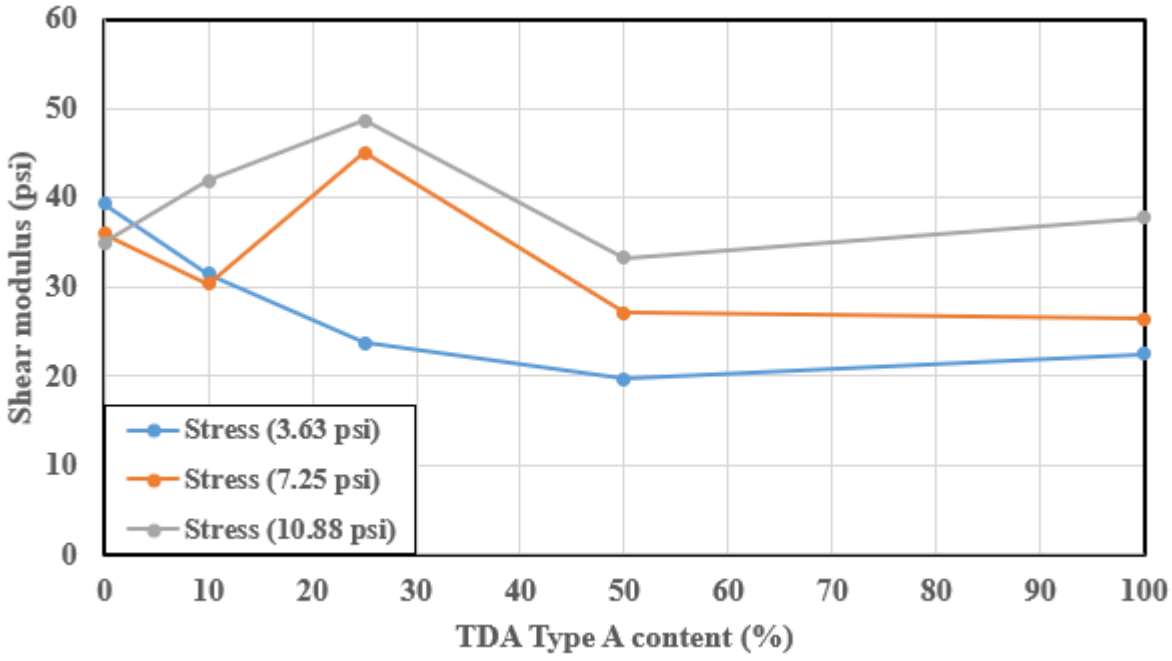

Figure 4.38 Shear modulus versus TDA content for the soil-TDA Type A mixtures

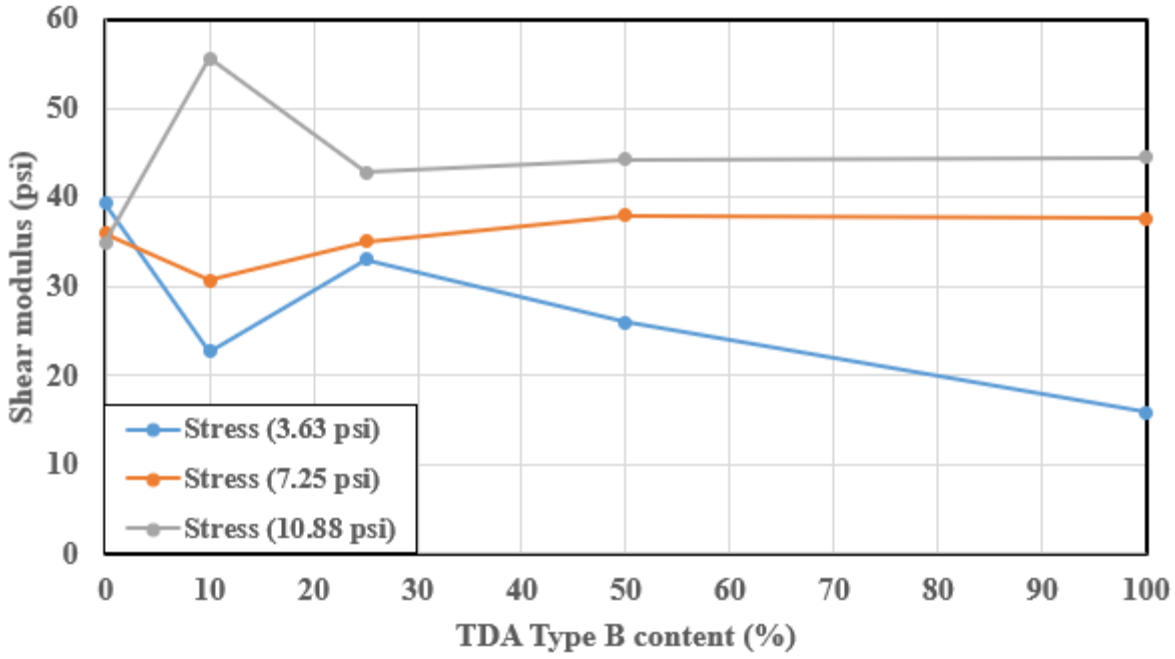

Figure 4.39 Shear modulus versus TDA content for the soil-TDA Type B mixtures

4.6.4. Normalized lateral earth pressure at rest for the mixtures

The normalized lateral earth pressure at rest is a crucial factor in the design of geotechnical applications, such as retaining walls. Two variables that affect the normalized lateral earth pressure are the angle of internal friction and the dry unit weight of the soil. Equation (2) was used to determine the normalized lateral earth pressure at rest (Braja, 2014):

$$\frac{p}{z} = (1-\sin\phi) \times \gamma_{dry}$$

Equation 4-2 Equation of the normalized lateral earth pressure at rest

where $\frac{p}{z}$ is the normalized lateral earth pressure at rest, z is the depth, ϕ is the angle of internal friction, and γ_{dry} is the dry unit weight of the soil. Figure 4.40 shows the normalized lateral earth pressure at rest plotted against the TDA content for soil-TDA mixtures. It can be observed that adding up to 10% TDA Type A and Type B by weight to the soils decreased the normalized lateral earth pressure at rest. However, increasing the TDA content from 10% to 25% stabilized the normalized lateral earth pressure at rest. With the further addition of TDA beyond 25% by weight, the normalized lateral earth pressure at rest continued to decrease for the soil-TDA mixtures.

Hence, it can be concluded that the addition of 25% TDA by weight to the soil results in a 20% reduction in the lateral earth pressure, which can lead to significant cost savings in geotechnical applications such as retaining wall design.

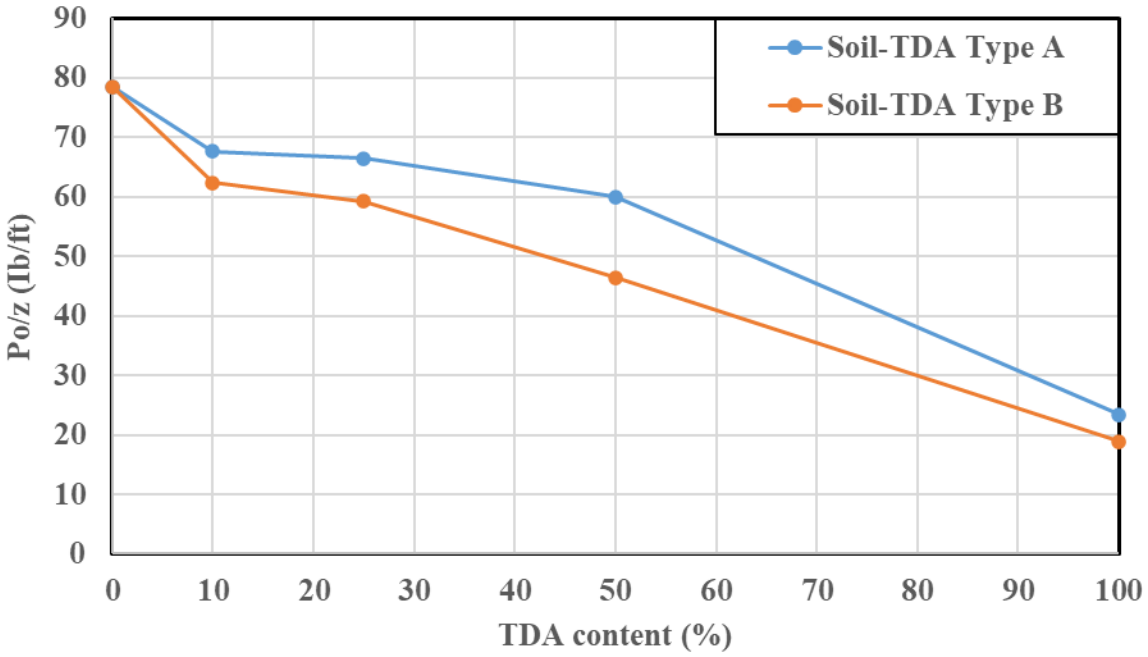

Figure 4.40 Normalized lateral earth pressure at rest versus TDA content for the soil-TDA mixtures

5. Chapter 5. Short-term compressibility tests

The compressibility of tire derived aggregate (TDA) is a critical parameter, as TDA demonstrates significantly higher compressibility than traditional mineral aggregates. In many applications, the design and performance criteria of TDA are primarily governed by its deformation characteristics rather than its strength properties (Edil and Bosscher 1994, Bosscher et al. 1997, Shalaby and Khan 2005, Wartman, J. et al., 2007, Meles et al. 2013, Sparkes, J. et al., 2019, Ghaaowd et al. 2017, and Yarahuaman and McCartney, 2023). This study investigated the compression behavior of TDA and TDA-soil mixtures using large-scale one-dimensional compression testing. Mixtures including pure soil, TDA Type A, TDA Type B, soil-TDA Type A, and soil-TDA Type B mixtures were prepared and tested. The testing procedure and results are presented in this chapter. It should be noted that due to the significant differences in the size of TDA Type A and Type B, two different test setups and specimen sizes were used for testing specimens incorporating Type A and Type B.

5.1. Apparatus and test procedure for mixtures incorporating TDA Type A

Five mixtures were used for this test, including pure soil, TDA Type A, STA10, STA25, and STA50. The design compacted densities for the mixtures are shown in Table 3.4. The container size should ideally be ten times larger than the particle size (ASTM 2011). Each specimen had a diameter of 11 inches and a length of 15 inches. The diameter of each cylinder was more than ten times larger than the largest TDA piece achieving the ASTM recommendation. Each specimen was placed inside a 0.50-inch-thick acrylic cylinder. The interior surfaces of the acrylic cylinder were lubricated with grease to reduce friction between the sample surface and the inner surface of the cylinder.

Compression tests were conducted using a HUMBOLDT MASTER-LOADER 5030 loading machine. Figure 5.1 shows the compressibility testing apparatus. The machine could apply pressure up to 26 psi. Loads were applied on top of each sample using a 1-inch thick, 10.90-inch diameter aluminum plate. The load was applied in a displacement control at a rate of 0.25 inches per minute. The applied load was measured using a load cell attached to the compression apparatus.

5.2. Apparatus and test procedure used for mixtures incorporating TDA Type B

Four mixtures were used for this test: TDA Type B, STB10, STB25, and STB50. The design compacted densities for the mixtures are shown in Table 3.4. Each specimen had a diameter of 24 inches and a length of 30 inches. A challenge with performing one-dimensional compression tests on Type B TDA is that ASTM 2011 (ASTM 2011) recommends the specimen diameter be at least ten times the maximum particle size. However, for Type B TDA, this would result in a sample diameter of at least 70 inches. Handling and testing such large samples is not practical. Therefore, it is more common in the literature to test Type B using samples with a diameter 3-4 times the maximum particle size (Meles et al. (2014) and Ghaaowd et al. (2017)). In this project, the cylinder diameter was designed to be four times the average size of the TDA pieces. Each specimen was placed inside a 0.50-inch-thick carbon fiber tube. The interior surfaces of the carbon fiber tubes were lubricated with grease to reduce friction between the sample surface and the inner surface

of the carbon fiber tube. It is important to note that, given the diameter of the test specimens and thickness of the carbon fiber, the confinement ratio and hence the confinement effects on the performance of the test specimens is insignificant and can be ignored.

Compression tests were conducted using an MTS 550 loading machine. Figure 5.2 illustrates the compressibility testing apparatus used in this section. Each specimen was subjected to vertical stress up to 26 psi, comparable to those applied to mixtures incorporating TDA Type A. Loads were applied on top of each sample using a 0.5-inch thick, 23.9-inch diameter steel plate to ensure uniform distribution of the applied loads. The load was applied in a displacement control at a rate of 0.25 inches per minute. The applied load was measured using a load cell attached to the compression apparatus.

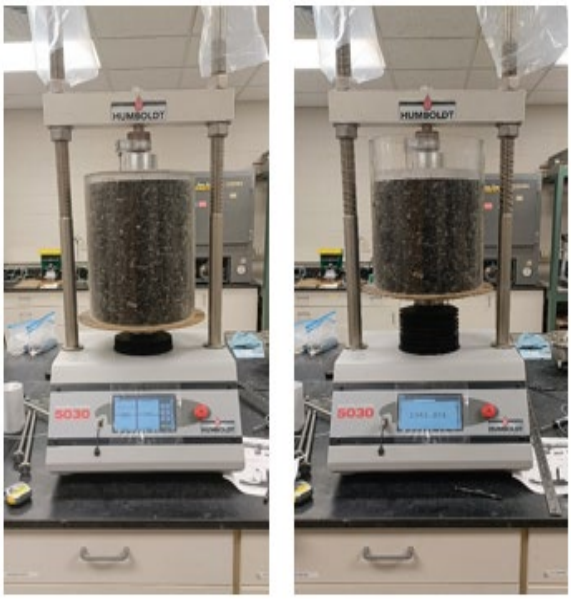

a b

Figure 5.1 Compressibility testing of a specimen incorporating TDA Type A: (a) before testing, and (b) during testing

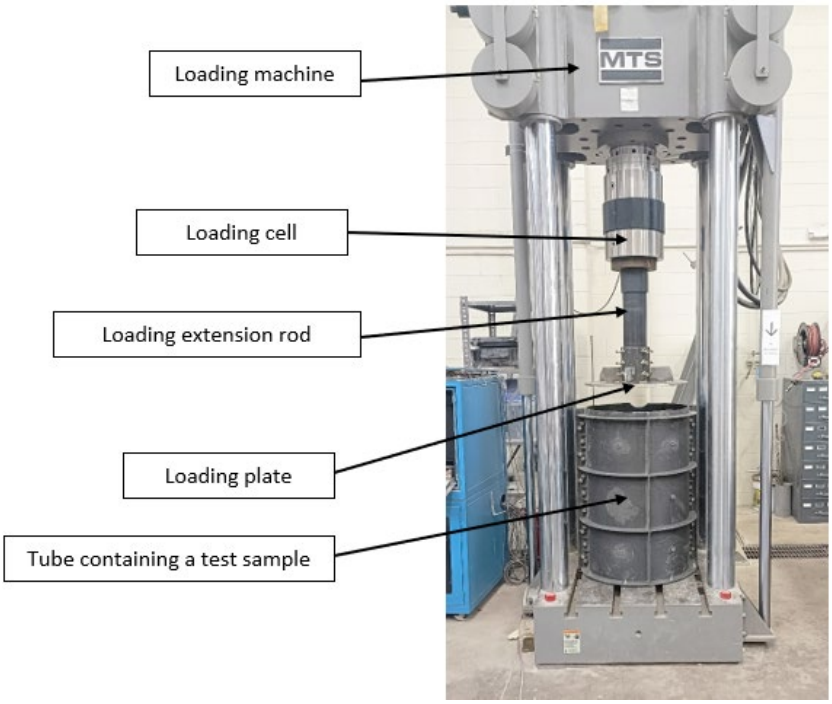

Figure 5.2 Compressibility testing of a specimen incorporating TDA Type B

5.3. Results and discussion

5.3.1. One-Dimensional compression

The applied vertical loads were measured using load cells and then divided by the cross-sectional areas of the test samples to determine the applied stresses. Displacements were recorded automatically using the linear variable displacement transducers (LVDTs) integrated into the testing machines.

The axial stress-strain curves for each sample are presented in Figure 5.3 and Figure 5.4 for TDA Type A mixtures and TDA Type B mixtures, respectively. The stress-strain relationship was nonlinear for the soil-TDA mixtures, with greater nonlinearity observed in the TDA Type A mixtures. Generally, for a given stress, increasing the percentage of TDA resulted in higher axial strain. Furthermore, for a given stress and the same percentage of TDA, using TDA Type B yielded smaller strains compared to TDA Type A.

For example, at a vertical stress of 7.25 psi (50 kPa), which is typical for various common geotechnical applications (Wartman et al., 2007), increasing the TDA Type A content from 0% to 10% increased the axial strain from 0.31% to 1.82%. Further increases in TDA content led to smaller increments in axial strain, reaching 3.00%, 7.30%, and 12.50% for 25%, 50%, and 100% TDA Type A, respectively.

Similarly, using TDA Type B showed the same trend but with smaller rates of increase. At a vertical stress of 7.25 psi (50 kPa), increasing the TDA Type B content from 0% to 10% increased the axial

strain from 0.43% to 0.63%. Further increases in TDA content led to smaller increments in axial strain, reaching 1.05%, 1.47%, and 5.47% for 25%, 50%, and 100% TDA Type B, respectively.

The smaller strains observed in the mixtures incorporating TDA Type B can be attributed to the rearrangement of TDA particles with varying lengths and angles, which further restricts the mixture from expanding back to its original state. Additionally, the presence of steel wires in TDA Type B enhances the interlocking action, thereby preventing expansion.

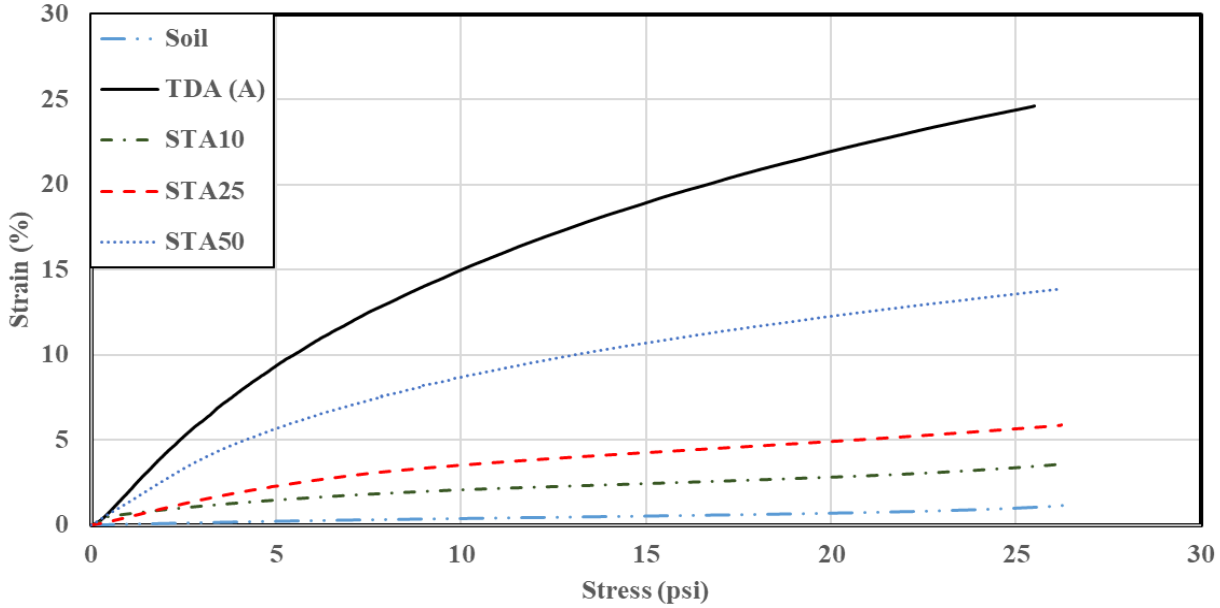

Figure 5.3 Stress-strain for soil mixtures incorporating TDA Type A

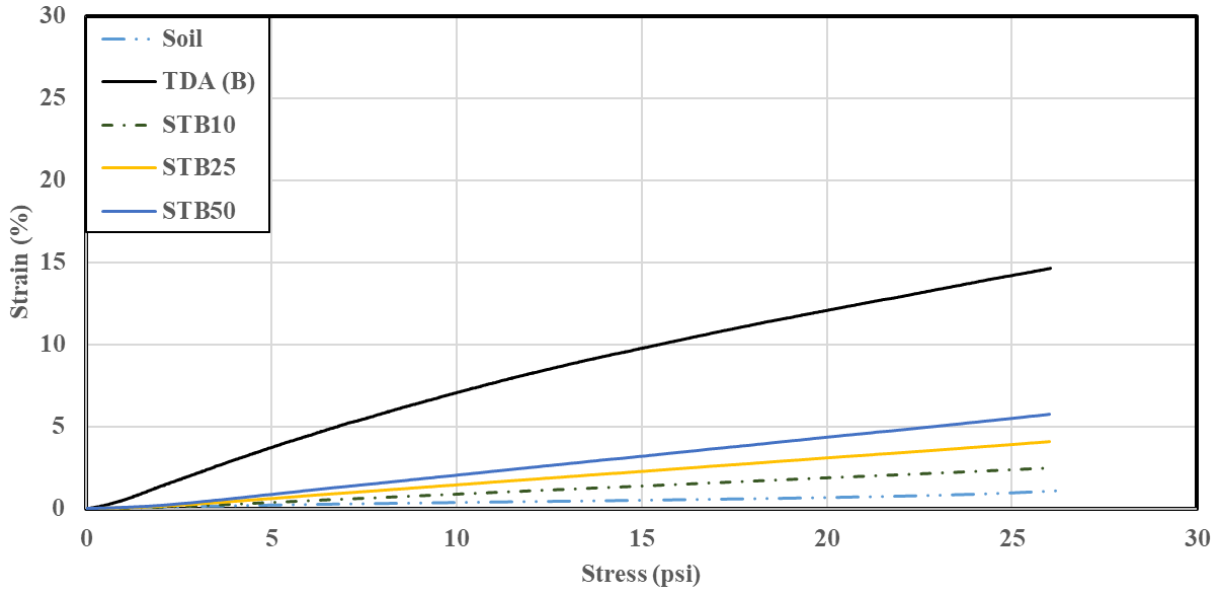

Figure 5.4 Stress-strain for soil mixtures incorporating TDA Type B

5.3.2. Unit weight change

Deformation in soil primarily arises from the expulsion of water from the voids, reorientation of soil particles, and minimal deformation of the soil particles themselves (Yi et al., 2015). Conversely, TDA, being a highly elastic material, deforms due to three main factors: (1) reorientation of TDA particles, which is generally irrecoverable upon unloading; (2) compression of TDA particles, which, unlike conventional soils, is typically recoverable upon unloading; and (3) bending of TDA particles, which significantly contributes to the overall compression of TDA when loaded (Meles et al., 2013).

This section presents the increase in unit weight of various TDA-soil mixtures after compression. Following compression, the height of each specimen is reduced, and the new volume is calculated. The bulk density is then determined by dividing the weight of the specimen by the new volume. In Figure 5.5 and Figure 5.6, the ratio between the bulk unit weight at a given stress and the mixture optimum unit weight is plotted against the applied stress for the different TDA-soil mixtures used in the tests.

For TDA Type A mixtures, samples with TDA content ranging from 50% to 100% exhibited a rapid unit weight increase, up to 15.50% and 31% at a 26-psi vertical stress, respectively. However, samples with TDA content ranging from 10% to 25% exhibited a steady increase in unit weight, up to 3% and 5%, respectively.

For TDA Type B mixtures, samples with TDA content percentages of 10%, 25%, and 50% exhibited a steady increase in unit weight, up to 2.50%, 4.25%, and 6% at a 26-psi vertical stress, respectively. However, the sample with 100% TDA exhibited a rapid unit weight increase, up to 17.15% at a 26-psi vertical stress.

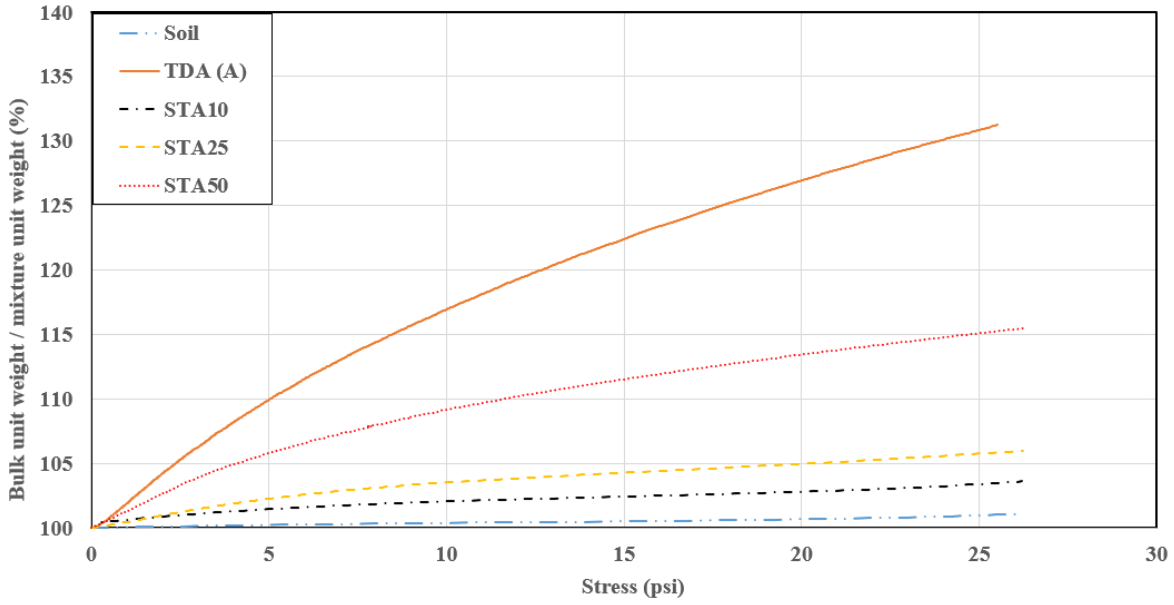

Figure 5.5 The ratio between the bulk unit weight and the mixture unit weight against the applied stress for the soil-TDA Type A mixtures

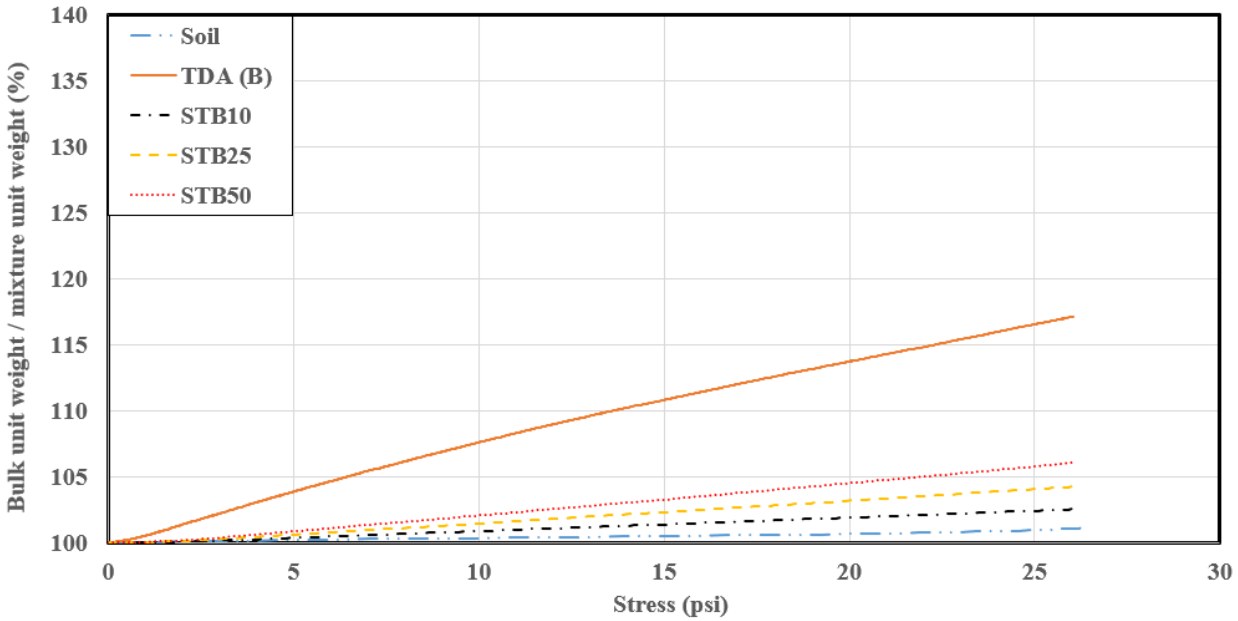

Figure 5.6 The ratio between the bulk unit weight and the mixture unit weight against the applied stress for the soil-TDA Type B mixtures

6. Chapter 6. Findings, conclusions, and recommendations

This report presents the results of investigating the performance of soil classified as clayey gravel and sand soil mixed with tire derived aggregate (TDA) Type A and Type B. Different percentages of TDA (0%, 10%, 25%, 50%, and 100% by weight) were used to replace the soil in various soil mixtures. Each mixture was compacted to an optimum dry density. The shear parameters and compressibility of the different mixtures were investigated.

6.1. Findings

The following findings can be drawn from this study:

- **Dry unit weight**: Incorporating TDA into soil linearly decreases the dry unit weight of the mixtures. For example, adding 25% TDA reduces the dry unit weight by approximately 13% for soil-TDA Type A mixtures and by 31% for soil-TDA Type B mixtures.
- **Cohesion**: For any given percentage of TDA, mixtures incorporating TDA Type A consistently exhibited lower cohesion compared to those with TDA Type B. The addition of up to 25% TDA, regardless of type, did not significantly affect the cohesion of the soil mixture. Incorporating 25% TDA Type A resulted in a slight decrease in cohesion, from 2.84 psi to 2.67 psi, indicating a 6% reduction. In contrast, adding 25% TDA Type B increased cohesion from 2.84 psi to 3.27 psi, reflecting a 15% improvement. Beyond the 25% threshold, cohesion gradually declined with increasing TDA content. At 100% TDA content, Type A reduced apparent cohesion by approximately 91.5%, while Type B caused a 57.4% reduction.
- **Angle of internal friction**: In general, mixtures incorporating TDA Type A exhibited a higher friction angle compared to those with TDA Type B. The angle of internal friction increased by 16%, from 14.38^{o} to 16.70^{o}, with the addition of 25% TDA Type A. In contrast, adding 25% TDA Type B resulted in a 19.5% decrease, reducing the friction angle from 14.38^{o} to 11.57^{o}. However, at 100% TDA content, both types demonstrated an average angle of internal friction of 25.30^{o}, which represents a 75.94% increase compared to the reference soil specimens.
- **Shear Modulus**: The shear modulus increased for all mixtures as confining pressure increased. However, the behavior of mixtures incorporating TDA Type A differed from those incorporating TDA Type B. For mixtures containing more than 50% TDA Type A, the shear modulus remained constant at approximately 70% of that of the soil mixtures. In mixtures with less than 50% TDA Type A and under low confinement pressure, the shear modulus gradually decreased. Under higher confinement pressures, above 7.25 psi, the shear modulus for mixtures with 25% TDA Type A exceeded that of the soil by approximately 17%. For mixtures incorporating TDA Type B, the shear modulus exhibited a linear decrease with increasing TDA content beyond 25% under low confinement pressure, reaching approximately 45% of that of the soil mixture. Under higher pressures, however, the shear modulus remained relatively constant, with no significant reduction compared to the soil mixtures. For mixtures incorporating 10% TDA Type B, the shear

modulus was 65% under a low pressure of 7.25 psi but increased by 38% under a higher pressure of 10.88 psi.

- **Normalized lateral earth pressure at rest:** As TDA content increases, mixtures with TDA Type A display higher normalized lateral earth pressure compared to those with TDA Type B. However, the normalized lateral earth pressure decreases linearly for both types as TDA content increases. With the introduction of 10% TDA, a noticeable drop in normalized earth pressure is observed for both types. As TDA content exceeds 50%, the lateral earth pressure continues to decline. Specifically, the normalized lateral earth pressure at rest decreases by 14%, from 79 lb/ft to 68 lb/ft, with 25% TDA Type A, and by 25%, from 79 lb/ft to 59 lb/ft, with 25% TDA Type B. These reductions can potentially lead to substantial cost savings in retaining wall design.
- **Compressibility:** Mixtures containing TDA Type B exhibit lower compressibility than those with TDA Type A. As TDA content increases, axial strain increments are observed. For TDA Type A, axial strains reach 3.00%, 7.30%, and 12.50% for 25%, 50%, and 100% TDA, respectively. In contrast, TDA Type B exhibits smaller increments of 1.05%, 1.47%, and 5.47% for the same percentages.

6.2. Conclusions and recommendations

Based on the findings of this study, it is recommended to incorporate 25% TDA into soil for geotechnical applications, particularly in the design of retaining walls and bridge abutments. The inclusion of TDA provides mechanical properties comparable to conventional soil while significantly reducing the normalized lateral earth pressure at rest, which can lead to substantial cost savings. Additionally, TDA Type B enhances cohesion and shear resistance while maintaining lower compressibility, making it an efficient and viable alternative to traditional backfill materials.

In summary, incorporating 25% TDA can reduce the mixture weight by up to 31%, and decrease normalized lateral earth pressure by approximately 20%. However, it should be noted that for both TDA types, compressibility increases significantly, depending on the applied pressure and type of TDA reaching strains up to 7.3% for Type A and 1.47% for Type B. Despite this, adopting TDA in such geotechnical projects can optimize both economic and engineering performance, providing cost-effective and efficient solutions.

7. References

1. AASHTO M145 2021. Standard Specification for Classification of Soils and Soil-Aggregate Mixtures for Highway Construction Purposes. Single American Association of State Highway and Transportation Officials, Washington DC.
2. AASHTO T 89 2022. Standard Method of Test for Determining the Liquid Limit of Soils. American Association of State Highway and Transportation Officials, Washington DC.
3. AASHTO T 90 2022. Standard Method of Test for Determining the Plastic Limit and Plasticity Index of Soils. American Association of State Highway and Transportation Officials, Washington DC.
4. AASHTO T27 2023. Standard Method of Test for Sieve Analysis of Fine and Coarse Aggregates. American Association of State Highway and Transportation Officials, Washington DC.
5. Abdullah, W., et al. 2023. “Evaluation of Sand–Tire Crumb Mixtures as Lightweight Fill Materials.” Geotechnical Testing Journal, Vol. 18, No.3, pp. 208-221.
6. Ahmed, I. 1993. “Laboratory Study on Properties of Rubber-Soils.” Publication FHWA/IN/JHRP-93/04. Joint Highway Research Project. Indiana Department of Transportation and Purdue University, West Lafayette, Indiana. https://doi.org/10.5703/1288284314210.
7. Ahn, I.S. and Cheng, L. 2014. “Tire-derived Aggregate for Retaining Wall Backfill Under Earthquake Loading.” Construction and Building Materials, 57, pp. 105-116. https://doi.org/10.1016/j.conbuildmat.2014.01.091.
8. Akbarimehr, D., Eslami, A. and Aflaki, E.J. 2020. “Geotechnical Behaviour of Clay Soil Mixed with Rubber Waste.” Journal of Cleaner Production, 271, p. 122632.
9. Akbarimehr, D., et al. 2021. “Investigating the Effect of Waste Rubber in Granular Form on Strength Behavior of Tehran Clay.” Arabian Journal of Geosciences, 14, pp. 1-12.
10. Akbulut, S., Arasan, S. and Kalkan, E. 2007. “Modification of Clayey Soils Using Scrap Tire Rubber and Synthetic Fibers.” Applied Clay Science, Vol. 38, No. 1-2, pp. 23-32. https://doi.org/10.1016/j.clay.2007.02.001.
11. Al-Subari, L. and Ekinci, A.J. 2024. “Evaluation of Mechanical and Microstructural Properties of Waste Tire Improved Cemented Clay.” Journal of Natural Fibers, Vol. 21, No. 1, p. 2349750.
12. Alzabeebee, S., Alshibany, S.M. and Keawsawasvong, S.J. 2022. “Influence of Using Tire-Derived Aggregate on the Structural Performance of Buried Concrete Pipe Under Embankment Load.” Geosciences, Vol. 2, No. 4, pp. 989-1002.
13. Araujo, G.L.S., et al. 2021. “Shear Behavior of Mixtures Involving Tropical Soils and Tire Shreds.” Journal of Cleaner Production, 276, p. 122061.

14. Artoshi, I.M.K., et al. 2024. “Efficiency and Durability Assessment of Soil Stabilization Using Waste Tire Shreds.” International Journal of Geotechnical Engineering, Vol. 14, No. 1, pp. 13012-13016.

15. ASTM D2435-04 2011. Standard Test Methods for One-dimensional Consolidation Properties of Soils Using Incremental Loading. West Conshohocken, PA: ASTM.

16. ASTM D6270 2020. Standard Practice for Use of Scrap Tires in Civil Engineering Applications. Annual Book of ASTM Standards, pp. 1-21. https://doi.org/10.1520/D6270-17.

17. ASTM D698-12 2021. Standard Test Methods for Laboratory Compaction Characteristics of Soil Using Standard Effort. West Conshohocken, PA: ASTM.

18. Badila, C.A. 2021. “Evaluating the Performance of Tire derived Aggregate (TDA) vs Natural Aggregate in Septic Systems.”

19. Balaban, E., et al. 2022. “Influence of Tire Crumbs on Mechanical Properties of Sand-Fine Soil Mixtures.” Geotechnical Testing Journal, Vol. 17, No. 1, pp. 64-79.

20. Barman, R., et al. 2024. “Composite Sand-Crumb Rubber and Geofoam Wave Barrier for Train Vibration.” Geosynthetics International, Vol. 42, No. 4, pp. 2321-2343.

21. Bernal-Sanchez, J., Leak, J. and Barreto, D.J. 2023. “Rubber-Soil Mixtures: Use of Grading Entropy Theory to Evaluate Stiffness and Liquefaction Susceptibility.” Bulletin of Earthquake Engineering, Vol. 21, No. 8, pp. 3777-3796.

22. Bosscher, P.J., Edil, T.B. and Eldin, N.N. 1992. “Construction and Performance of a Shredded Waste Tire Test Embankment.” Transportation Research Record, 1345.

23. Bosscher, P.J., Edil, T.B. and Kuraoka, S. 1997. “Design of Highway Embankments Using Tire Chips.” Journal of Geotechnical and Geoenvironmental Engineering, Vol. 123, No. 4, pp. 295-304.

24. Braja, M. 2014. Advanced Soil Mechanics, 5th ed. Boca Raton, FL, USA: CRC Press, Taylor & Francis.

25. CARID. 2020. “The Hidden Secrets of Tires.” https://www.carid.com/articles/the-hiddensecrets-of-tires.html.

26. Cecich, V., Gonzales, L., Hoisaeter, A., Williams, J. and Reddy, K. 2016. “Use of Shredded Tires as Lightweight Backfill Material for Retaining Structures.” Waste Management & Research, 14, pp. 433-451.

27. Chaiyaput, S., et al. 2022. “Natural Para Rubber in Road Embankment Stabilization.” Journal of Natural Fibers, Vol. 12, No. 3, p. 1394.

28. Chamberlin, W.P. and Gupta, P.K. 1986. Use of Scrap Automobile Tire Rubber in Highway Construction. REPORT FHWA/NY/SR-86/85. New York State Department of Transportation, New York.

29. Chowdhury, S. and Kundu, S. 2021. “Improvement of Soil Subgrade with Shredded Rubber Tire Waste.” In Indian Geotechnical Conference. Springer.

30. Cui, S.Q., Zhou, C. and Zhang, J.H. 2022. “Experimental Investigations on the State-Dependent Thermal Conductivity of Sand-Rubber Mixtures.” Journal of Materials in Civil Engineering, Vol. 34, No. 3, p. 04021492.

31. Duda, A. and Siwowski, T.W. 2022. “Stability and Settlement Analysis of a Lightweight Embankment Filled With Waste Tyre Bales Over Soft Ground.” The International Journal of Geotechnical Engineering, Vol. 9, No. 4, pp. 467-491.

32. Edil, T.B. and Bosscher, P.J. 1994. “Engineering Properties of Tire Chips and Soil Mixtures.” Geotechnical Testing Journal, Vol. 17, No. 4, pp. 453-464. https://doi.org/10.1520/gtj10306j.

33. Edincliler, A. 2007. “Using Waste Tire-Soil Mixtures tor Embankment Construction.” In Scrap Tire Derived Geomaterials-Opportunities and Challenges. CRC Press, pp. 337-346.

34. Edinçliler, A., Baykal, G. and Saygili, A. 2010. “Influence of Different Processing Techniques on the Mechanical Properties of Used Tires in Embankment Construction.” Waste Management, Vol. 30, No. 6, pp. 1073-1080.

35. El Naggar, H., Ashari, M. and Mahgoub, A.J. 2022. “Development of an Empirical Hyperbolic Material Model for TDA Utilizing Large-Scale Triaxial Testing.” International Journal of Geotechnical Engineering, Vol. 16, No. 2, pp. 133-142.

36. El Naggar, H., Soleimani, P. and Fakhroo, A. 2016. “Strength and Stiffness Properties of Green Lightweight Fill Mixtures.” Geotechnical and Geological Engineering, Vol. 34, No. 3, pp. 867-876. https://doi.org/10.1007/s10706-016-0010-1.

37. El Naggar, H., Zahran, K. and Moussa, A.J.G. 2021. “Effect of the Particle Size on the TDA Shear Strength and Stiffness Parameters in Large-Scale Direct Shear Tests.” Geosciences, Vol. 1, No. 1, pp. 1-17.

38. Eldin, N.N. and Piekarski, J.A. 1994. “Scrap Tires: Management and Economics.” Journal of Environmental Engineering, Vol. 119, No. 6, pp. 1217-1232. https://doi.org/10.1061/(ASCE)0733-9372(1993)119:6(1217).

39. Elhakim, A.F., Mohammed, M.J. and Elkhouly, M.A. 2022. “Improvement of Expansive Soil Using Granulated Scrap Tires.” Innovative Infrastructure Solutions, Vol. 7, pp. 1-11.

40. Eslami, A., Akbarimehr, D.J.C. and Materials, B. 2021. “Failure Analysis of Clay Soil-Rubber Waste Mixture as a Sustainable Construction Material.” Construction and Building Materials, 310, p. 125274.

41. Foose, G.J., Benson, C.H. and Bosscher, P.J. 1996. “Sand Reinforced with Shredded Waste Tires.” Journal of Geotechnical Engineering, Vol. 122, No. 9, pp. 760-767.

42. Foriero, A. and Ghafari, N. 2020. “Laboratory Creep Parameter Determination of Sand–TDA Mixtures with Subsequent FEM Validation.” Indian Geotechnical Journal, Vol. 50, pp. 710-725. https://doi.org/10.1007/s40098-019-00407-0.

43. Gacke, S., Lee, M. and Boyd, N.J. 1997. “Field Performance and Mitigation of Shredded Tire Embankment.” Transportation Research Record, Vol. 1577, No. 1, pp. 81-89.

44. Gao, M., et al. 2022. “Study on the Strength Mechanism of Red Clay Improved by Waste Tire Rubber Powder.” Geotechnical Testing Journal, Vol. 17, p. e01416.

45. Ghaaowd, I., McCartney, J. S., Thielmann, S., Sanders, M., and Fox, P. J. (2017). “Shearing behavior of tire derived aggregate with large particle sizes. I: Internal and concrete interface direct shear behavior.” ASCE *Journal of Geotechnical and Geoenvironmental Engineering*. 143(10), 04017078.

46. Ghaffari, J.J.A. 2021. “Triaxial Determination of Shear Strength of Tire Chips-Sand-Geotextile Mixtures.” Arabian Journal of Civil Engineering, Vol. 5, No. 1, pp. 95-114.

47. Gheni, A., Abdelkarim, O., Liu, X., Abdulazeez, M., Lusher, S., Liu, K., ElGawady, M., Shi, H. and Wang, J. 2017. “Mechanical and Environmental Performance of Eco-friendly Chip Seal with Recycled Crumb Rubber.” Journal of Cleaner Production.

48. Gheni, A., Liu, X., ElGawady, M.A., Shi, H. and Wang, J. 2018. “Leaching Assessment of Eco-Friendly Rubberized Chip Seal Pavement.” Transportation Research Record, Vol. 2672, No. 52, pp. 67-77.

49. Gheni, A.A., Abdelkarim, O.I., Abdulazeez, M.M. and ElGawady, M.A. 2017. “Texture and Design of Green Chip Seal Using Recycled Crumb Rubber Aggregate.” Journal of Cleaner Production, Vol. 166, pp. 1084-1101.

50. Gheni, A.A., ElGawady, M.A. and Myers, J.J. 2017. “Mechanical Characterization of Concrete Masonry Units Manufactured with Crumb Rubber Aggregate.” ACI Materials Journal, 114, No. 1.

51. Gheni, A.A., Lusher, S.M. and ElGawady, M.A. 2018. “Retention Behavior of Crumb Rubber as an Aggregate in Innovative Chip Seal Surfacing.” Journal of Cleaner Production, Vol. 197, pp. 1124-1136.

52. Haranatti, J.S., et al. 2023. “Stabilization of Expansive Soil by Using Shredded Tyre Chips as An Admixture.” In AIP Conference Proceedings. AIP Publishing.

53. Hoppe, E.J. 1994. Field Study of a Shredded-Tire Embankment. Virginia Transportation Research Council (VTRC).

54. Hoppe, E.J. and Mullen, W.G. 2004. Field Study of a Shredded-Tire Embankment in Virginia. Virginia Transportation Research Council (VTRC).

55. Humphrey, D.N. 1999. “Civil Engineering Applications of Tire Shreds.” In Proceedings of the Tire Industry Conference.

56. Humphrey, D.N. 2008. “Tire Derived Aggregate as Lightweight Fill for Embankments and Retaining Walls.” In Proceedings of the International Workshop on Scrap Tire Derived Geomaterials - Opportunities and Challenges, IW-TDGM 2007, pp. 59-81. Taylor & Francis Group.

57. Humphrey, D.N. and Sandford, T.C. 1993. “Tire Chips as Lightweight Subgrade Fill and Retaining Wall Backfill.” Symposium on Recovery and Effective Reuse of Discarded Materials and By-Products for Construction of Highway Facilities, no. 207, pp. 20.

58. Indraratna, B., et al. 2021. “Use of Recycled Rubber Inclusions with Granular Waste for Enhanced Track Performance.” Geomechanics for Energy and the Environment, Vol. 6, p. 100093.

59. Jaramillo, N.A.D., et al. 2022. “Mechanical Behavior of Clayey Soil Reinforced with Recycled Tire Rubber using Chips and Fibers.” Geosynthetics International, Vol. 40, No. 6, pp. 3365-3378.

60. Juliana, I., et al. 2020. “Effectiveness of Crumb Rubber for Subgrade Soil Stabilization.” In IOP Conference Series: Materials Science and Engineering. IOP Publishing.

61. Kazemzadeh, M., et al. 2024. “Influence of Tire-Shred Aspect Ratio on Performance of Mechanically Stabilized Retaining Walls.” Geosynthetics International, Vol. 49, No. 4, pp. 4597-4619.

62. Kliszczewicz, B. and Kowalska, M. 2020. “Numerical Study of the Use of Tyre-Derived-Aggregate (TDA) as the Backfill above Flexible PVC Pipeline.” In IOP Conference Series: Materials Science and Engineering. IOP Publishing.

63. Lee, C., et al. 2010. “Characteristics of Rubber-Sand Particle Mixtures According to Size Ratio.” Geotechnical and Geological Engineering, Vol. 22, No. 4, pp. 323-331.

64. Lee, C., et al. 2014. “Behavior of Sand–Rubber Particle Mixtures: Experimental Observations and Numerical Simulations.” Geomechanics for Energy and the Environment, Vol. 38, No. 16, pp. 1651-1663.

65. Lee, J.H., Salgado, R., Bernal, A. and Lovell, C.W. 1999. “Shredded Tires and Rubber-Sand as Lightweight Backfill.” Journal of Geotechnical and Geoenvironmental Engineering, Vol. 125, No. 2, pp. 132-141.

66. Lee, J.S., Dodds, J. and Santamarina, J.C. 2007. “Behavior of Rigid-Soft Particle Mixtures.” Journal of Materials in Civil Engineering, Vol. 19, No. 2, pp. 179-184.

67. Liu, L., et al. 2020. “Evaluation of Engineering Properties and Environmental Effect of Recycled Waste Tire-Sand/Soil in Geotechnical Engineering: A Compressive Review.” Construction and Building Materials, Vol. 126, p. 109831.

68. Liu, X., Wang, J., Gheni, A. and ElGawady, M.A. 2018. “Reduced Zinc Leaching from Scrap Tire During Pavement Applications.” Waste Management, Vol. 81, pp. 53-60.

69. Lu, Y., et al. 2022. “Mechanical Behaviour and Permeability of Expansive Soils Mixed With Scrap Tire Rubbers Subjected to Freeze-Thaw Cycles.” Construction and Building Materials, Vol. 199, p. 103580.

70. Mahgoub, A. 2020. Innovative Applications of Tire Derived Aggregate (TDA) for Buried Pipes and Culverts.

71. Mahgoub, A. and El Naggar, H.J. 2020. “Coupled TDA–Geocell Stress-Bridging System for Buried Corrugated Metal Pipes.” Journal of Geotechnical Engineering, Vol. 146, No. 7, p. 04020052.

72. Masad, E., Taha, R., Ho, C. and Papagiannakis, T. 1996. “Engineering Properties of Tire/Soil Mixtures as a Lightweight Fill Material.” Geotechnical Testing Journal, Vol. 19, No. 3, pp. 297-304.

73. Mawhinney, J.R. 1990. “The Hagersville Tire Fire February 12 to 28, 1990.” National Research Council of Canada (NRC). https://doi.org/10.4224/20378062.

74. Mccartney, J.S., Ghaaowd, I., Fox, P.J., Sanders, M.J., Thielmann, S.S. and Sander, A.C. 2017. “Shearing Behavior of Tire-Derived Aggregate with Large Particle Size. II: Cyclic Simple Shear.” Journal of Geotechnical and Geoenvironmental Engineering, Vol. 143, No. 10, p. 04017079. doi:10.1061/(ASCE)GT.1943-5606.0001781.

75. MDNR. “Scrap Tire Cleanup and Disposal Reimbursement.” https://dnr.mo.gov/waste-recycling/reduce-reuse-recycle/what-to-do-with-specific/scrap-tires.

76. Meles, D., Bayat, A. and Chan, D. 2013. “One-dimensional Compression Model for Tire-derived Aggregate Using Large-scale Testing Apparatus.” International Journal of Geotechnical Engineering, Vol. 8, No. 2, pp. 197-204. doi:10.1179/1939787913Y.0000000019.

77. Meles, D., Bayat, A., and Chan, D. (2014). “One-dimensional compression model for tire derived aggregate using large-scale testing apparatus.” *International Journal of Geotechnical Engineering*, 8:2, 197-204.

78. Meziani, F., Amar, K. and Mourad, Y. 2022. “Effect of the Addition of Aggregates Derived from Used Tires on the Mechanical Behavior of Clay.” In Advanced Engineering Forum. Trans Tech Publications.

79. Mohajerani, A., et al. 2020. “Recycling Waste Rubber Tires in Construction Materials and Associated Environmental Considerations: A Review.” Journal of Environmental Management, Vol. 155, p. 104679.

80. Moussa, A. and El Naggar, H. 2021. “Dynamic Characterization of Tire Derived Aggregates.” Journal of Materials in Civil Engineering, ASCE, Vol. 33, No. 2, doi:10.1061/(ASCE)MT.1943-5533.0003583.

81. Moustafa, A. and ElGawady, M. 2013. “Dynamic Properties of High Strength Rubberized Concrete.”

82. Moustafa, A. and ElGawady, M.A. 2015. “Mechanical Properties of High Strength Concrete with Scrap Tire Rubber.” Construction and Building Materials, Vol. 93, pp. 249-256.

83. Moustafa, A. and ElGawady, M.A. 2016. “Strain Rate Effect on Properties of Rubberized Concrete Confined with Glass Fiber–Reinforced Polymers.” Journal of Composites for Construction, Vol. 20, No. 5, p. 04016014.

84. Moustafa, A., Gheni, A. and ElGawady, M.A. 2017. “Shaking-Table Testing of High Energy–Dissipating Rubberized Concrete Columns.” Journal of Bridge Engineering, Vol. 22, No. 8, p. 04017042.

85. Mujibur Rahman. 2004. Characterisation of Dry Process Crumb Rubber Modified Asphalt Mixtures: A Thesis Submitted to the University of Nottingham. University of Nottingham. Nottingham.

86. Park, J.K., DeNooyer, I.G. and Wahl, J.H.J.S. 2023. “State of Knowledge on the Effects of Tire-Derived Aggregate (TDA) Used in Civil Engineering Projects on the Surrounding Aquatic Environment.” Sustainability, Vol. 15, No. 20, p. 15141.

87. Pourhassan, A., Gheni, A.A. and ElGawady, M.A. 2023. “Raveling Performance of Conventional and Rubberized Chip Seal Under Field And Laboratory Traffic Loading.” Construction and Building Materials, Vol. 370, p. 130674.

88. Pradeep, N.M. and Kumar, S.J.T.G. 2024. “Cyclic Performance of Geosynthetic-Encased Granular Pile with Tire Chips and Aggregates Mixture in Soft Soil–A Model Study.” Geotextiles and Geomembranes, Vol. 45, p. 101222.

89. Prasad, A.S., et al. 2014. “Study on Effect of Crumb Rubber on Behavior of Soil.” International Journal of Engineering Research and Technology, Vol. 4, No. 3, pp. 579-584.

90. Presti, D.L. 2013. “Recycled Tire Rubber Modified Bitumens for Road Asphalt Mixtures: A Literature Review.” Construction and Building Materials, Vol. 49, pp. 863-881. https://doi.org/10.1016/j.conbuildmat.2013.09.007.

91. Qamhia, I.I., et al. 2024. “Lightweight and Alternative Backfills for Highway Applications: State-of-the-Art Practice in the USA.” Transportation Research Record, Vol. 2678, No. 5, pp. 677-688.

92. Qi, Y., et al. 2024. “Sustainable Solutions for Railway Using Recycled Rubber.” Journal of Cleaner Production, Vol. 46, p. 101256.

93. Rao, G.V. and Dutta, R.K. 2006. “Compressibility and Strength Behaviour of Sand-Tyre Chip Mixtures.” Geotechnical and Geological Engineering, Vol. 24, pp. 711-724.

94. Read, J., Dodson, T. and Thomas, J. 1991. Experimental Project: Use of Shredded Tires for Lightweight Fill. Oregon Dept. of Transportation, Highway Division.

95. Rizvi, S.M.F., et al. 2022. “Evaluation of Open and Filled (TDA And RSM) Trenches Efficacy on Vibration Screening Caused by Transient Loads.” Soil Dynamics and Earthquake Engineering, Vol. 35, p. 100770.

96. Rouhanifar, S., et al. 2021. “Strength And Deformation Behaviour of Sand-Rubber Mixture.” Construction and Building Materials, Vol. 15, No. 9, pp. 1078-1092.

97. Salgado, R., Yoon, S. and Siddiki, N.Z. 2003. “Construction of Tire Shreds Test Embankment.” Purdue University.

98. Saparudin, N.A., et al. 2022. “Improvement of Problematic Soil Using Crumb Rubber Tyre.” International Journal of Geotechnical Engineering, Vol. 23, No. 2, pp. 72-84.

99. Senoro, D.B., et al. 2016. “Modeling of the Residue Transport of Lambda Cyhalothrin, Cypermethrin, Malathion and Endosulfan in Three Different Environmental

Compartments in the Philippines." Sustainable Environment Research, Vol. 26, No. 4, pp. 168-176. https://doi.org/10.1016/j.serj.2016.04.010.

100. Shalaby, A. and Khan, R.A. 2005. "Design of Unsurfaced Roads Constructed with Large-Size Shredded Rubber Tires: A Case Study." Resources, Conservation and Recycling, Vol. 44, No. 4, pp. 318-332.
101. Shettar, M.P., Ofegaa, G., and Gobana, A.B. 2020. "Soil Reinforcement with Waste Tire Chips."
102. Signes, C.H., et al. 2017. "An Experimental Study of a New Soil-Rubber Mix for Railway Embankment."
103. Singh, A., Spak, S.N., Stone, E.A., Downard, J., Bullard, R.L., Pooley, M., Kostle, P.A., et al. 2015. "Uncontrolled Combustion of Shredded Tires in a Landfill - Part 2: Population Exposure, Public Health Response, and an Air Quality Index for Urban Fires." Atmospheric Environment, Vol. 104, pp. 273-283.
104. Singh, P., Goli, V.S.N.S., and Singh, D.N. 2023. "Current Practices and the Way Forward in Waste Rubber Utilization for Infrastructural and Geoenvironmental Engineering Applications." Environmental Technology Reviews, Vol. 12, No. 1, p. 2252164.
105. Soltani, A., et al. 2022. "Stabilization of a Highly Expansive Soil Using Waste-Tire-Derived Aggregates and Lime Treatment." Journal of Environmental Management, Vol. 16, p. e01133.
106. Sparkes, J., El Naggar, H., and Valsangkar, A. 2019. "Compressibility and Shear Strength Properties of Tire-Derived Aggregate Mixed with Lightweight Aggregate." Journal of Pipeline Systems Engineering and Practice, ASCE, 1, p. 10. doi:10.1061/28ASCE29PS.1949-1204.0000354.
107. Tandon, K., et al. 2023. "Numerical Evaluation of Tire Chips–Filled Trench Barriers for Effective Vibration Isolation." Geosynthetics International, Vol. 42, No. 1, pp. 325-344.
108. Tandon, V., et al. 2007. "Performance Monitoring of Embankments Containing Tire Chips: Case Study." Journal of Geotechnical and Geoenvironmental Engineering, Vol. 21, No. 3, pp. 207-214.
109. Tasalloti, A., et al. 2021. "Physical and Mechanical Properties of Granulated Rubber Mixed With Granular Soils—A Literature Review." Applied Sciences, Vol. 13, No. 8, p. 4309.
110. Tatlisoz, N., Edil, T.B., and Benson, C.H. 1998. "Interaction between Reinforcing Geosynthetics and Soil-Tire Chip Mixtures." Journal of Geotechnical and Geoenvironmental Engineering, Vol. 124, No. 11, pp. 1109-1119. https://doi.org/10.1061/(ASCE)1090-0241(1998)124:11(1109).
111. Tutumluer, E. and Qamhia, I.I. 2024. Alternative Backfills for Highway Applications: State of the Practice. United States Department of Transportation, Federal Highway Administration.

112. Vaishnavi, V.S., et al. 2022. “Improvement of Low Compressible Clays Using Crumb Rubber.” Indian Geotechnical Conference. Springer.

113. Valdes, J.R. and Evans, T.M.J.C.G.J. 2008. “Sand–Rubber Mixtures: Experiments and Numerical Simulations.” Canadian Geotechnical Journal, Vol. 45, No. 4, pp. 588-595.

114. Wartman, J., Natale, M.F., & Strenk, P.M. 2007. “Immediate and Time-Dependent Compression of Tire Derived Aggregate.” Journal of Geotechnical and Geoenvironmental Engineering, Vol. 133, No. 3, pp. 245-256. https://doi.org/10.1061/(ASCE)1090-0241(2007)133:3(245).

115. Wolfe, S.L., Humphrey, D.N., and Wetzel, E.A. 2004. “Development of Tire Shred Underlayment to Reduce Groundborne Vibration from LRT Track.” GeoTrans, ASCE, pp. 750-759.

116. Wu, M., et al. 2023. “Micromechanics of Granulated Rubber–Soil Mixtures as a Cost-Effective Substitute for Geotechnical Fillings.” Geosynthetics International, Vol. 30, No. 13, pp. 2701-2717.

117. Wu, W.Y., Benda, C.C., and Cauley, R.F. 1997. “Triaxial Determination of Shear Strength of Tire Chips.” Journal of Geotechnical and Geoenvironmental Engineering, Vol. 123, No. 5, pp. 479-482.

118. Xiao, M., Bowen, J., Graham, M., and Larralde, J. 2012. “Comparison of Seismic Responses of Geosynthetically Reinforced Walls with Tire-Derived Aggregates and Granular Backfills.” Journal of Geotechnical and Geoenvironmental Engineering.

119. Yang, Z., et al. 2020. “Advances in Properties of Rubber Reinforced Soil.” Advances in Civil Engineering, No. 1, p. 6629757.

120. Yang, Z., et al. 2023. “Investigation of Rubber Content and Size on Dynamic Properties of Expansive Soil–Rubber.” International Journal of Geomechanics, Vol. 31, No. 3, pp. 269-282.

121. Yarahuaman, A.A. and McCartney, J.S. 2024. “Full-Scale Seismic Response Test on a Shallow Foundation Embedded in Tire-Derived Aggregate for Geotechnical Seismic Isolation.” Soil Dynamics and Earthquake Engineering, Vol. 177, p. 108417.

122. Yarahuaman, Axel, McCartney, John S. 2023. "Large-Scale Testing of the Static One-Dimensional Compression Response of Tire-Derived Aggregate." Geo-Congress 2023.

123. Youssf, O., ElGawady, M.A., and Mills, J.E. 2015, August. “Experimental Investigation of Crumb Rubber Concrete Columns Under Seismic Loading.” Structures, Vol. 3, pp. 13-27. Elsevier.

124. Youssf, O., ElGawady, M.A., and Mills, J.E. 2016. “Static Cyclic Behaviour of FRP-confined Crumb Rubber Concrete Columns.” Engineering Structures, Vol. 113, pp. 371-387.

125. Youssf, O., ElGawady, M.A., Mills, J.E., and Ma, X. 2013. “Analytical Modeling of the Main Characteristics of Crumb Rubber Concrete.”

126. Youssf, O., ElGawady, M.A., Mills, J.E., and Ma, X. 2014. “An Experimental Investigation of Crumb Rubber Concrete Confined by Fibre Reinforced Polymer Tubes.” Construction and Building Materials, Vol. 53, pp. 522-532.

127. Youwai, Sompote, and Bergado, Dennes. 2003. “Strength and Deformation Characteristics of Shredded Rubber Tire-Sand Mixtures.” Canadian Geotechnical Journal, Vol. 40, pp. 254–264.

128. Zahran, K. 2021. Experimental Investigation for the Particle and Sample Size Effect on the Shear Strength Parameters of Tire Derived Aggregate (TDA).

129. Zahran, K. and Naggar, H.E. 2020. “Effect of Sample Size on TDA Shear Strength Parameters in Direct Shear Tests.” Transportation Research Record, Vol. 2674, No. 9, pp. 1110-1119.

130. Zhang, H., et al. 2022. “An Investigation of the Pullout Behaviors of Tire Strips Embedded in Tire-Derived Aggregate Reinforced Sand.” Geotextiles and Geomembranes, Vol. 29, No. 24, pp. 35599-35614.

131. Zhang, H., Liu, Z., Wang, J., Sun, J., Yue, H., Yuan, X. and Song, X., 2023. A study of the bearing characteristics of slopes reinforced with waste tire strips based on TDA composite soil. *Environment, Development and Sustainability*, pp.1-27.

132. Zornberg, Jorge G., Cabral, Alexandre R. and Viratjandr, Chardphoom. 2004. “Behaviour of Tire Shred–Sand Mixtures.” Canadian Geotechnical Journal, Vol. 41, pp. 227–241. https://doi.org/10.1139/t03-086.

133. Zutting, D.V., and Naktode, P.J. 2020. “Soil Stabilization by Using Scrap Tire Rubber.” International Journal of Engineering Research and Applications, Vol. 9.

A- Appendix A: Material preparation procedures

Figure A.1 The soil used in this study (provided by MoDOT)

Figure A.2 Preparing the soil before putting it inside the oven to get it fully dry

Figure A.3 Putting the soil inside the oven

Figure A.4 Crushing the soil inside the mixer

Figure A.5 Sieve analysis of the soil

Figure A.6 Mixing the soil with water to determine the optimum water content and the max dry density

Figure A.7 Proctor test for the soil to determine the optimum water content and the max dry density

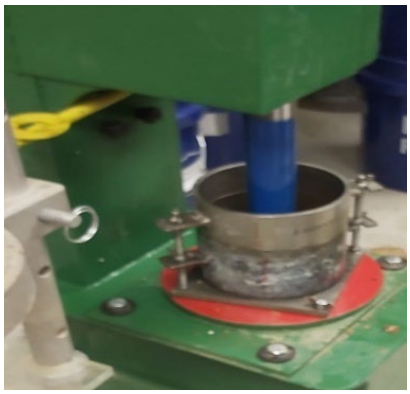

Figure A.8 Compaction of the soil sample in three layers

Figure A.9 Extracting the soil sample from the mold

Figure A.10 Mixing the soil with TDA Type A to determine the optimum water content and the max dry density

Figure A.11 Compaction of the soil-TDA sample in three layers

Figure A.12 Extracting the soil-TDA sample from the mold

Figure A.13 Determining the weights for the different samples

Figure A.14 Mixing the soil to get the Atterberg limits

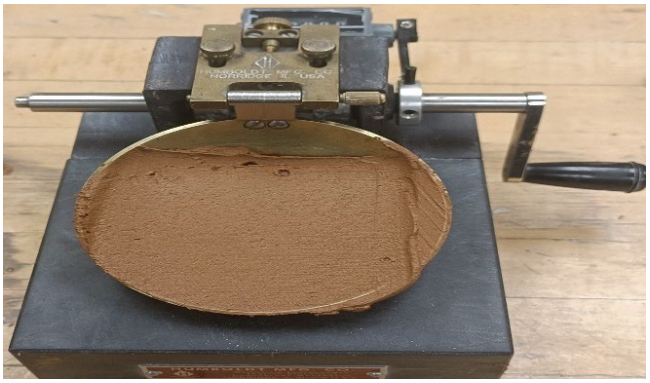

Figure A.15 Determining the liquid limit for the soil

Figure A.16 Determining the plastic limit for the soil

Figure A.17 Recording the weights to get the Atterberg limits

Figure A.18 Determining the specific gravity for the TDA

B- Appendix B: Direct shear test preparation procedures

Figure B.1 Preparing the formwork for the upper box

Figure B.2 Preparing the compaction plate used to compact the samples inside the shear box before testing

Figure B.3 Filling the shear box with TDA Type A

Figure B.4 Attaching the string pot to measure the horizontal displacement before the direct shear test

Figure B.5 Getting the test ready before running the direct shear test

Figure B.6 Running the direct shear test

Figure B.7 The TDA Type A after shearing

Figure B.8 The soil after shearing

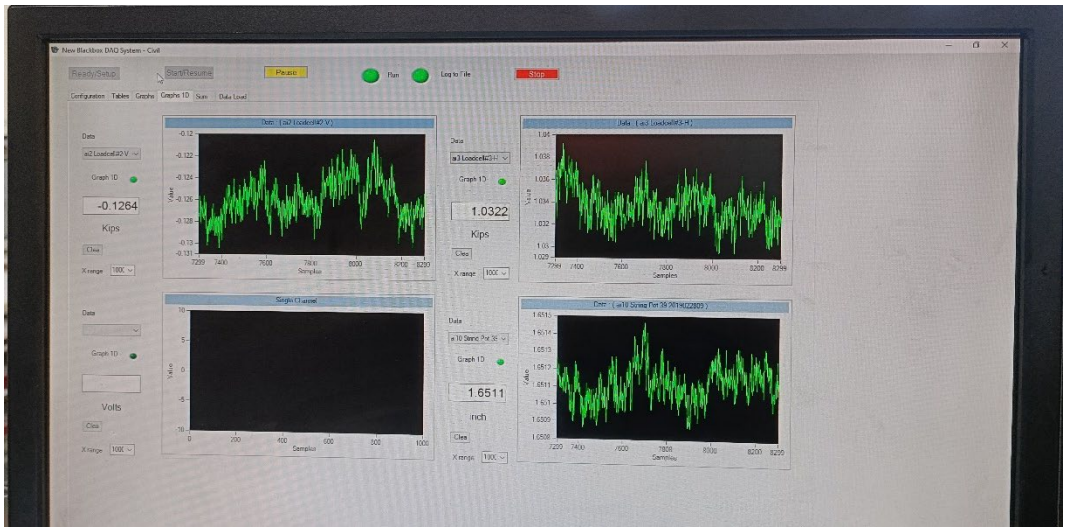

Figure B.9 The data of the direct shear test were recorded by an automatic data acquisition system

Figure B.10 Getting the soil outside the upper box

Figure B.11 Getting the soil outside the lower box

C- Appendix C: Compressibility test with soil-TDA Type A mixtures preparation procedures

Figure C.1 Preparing the compaction plate for the compressibility test with soil-TDA Type A mixtures

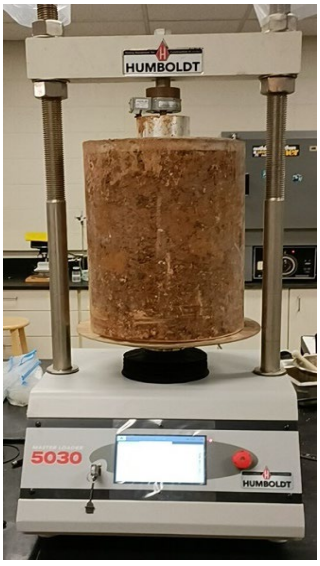

Figure C.2 Soil compressibility test

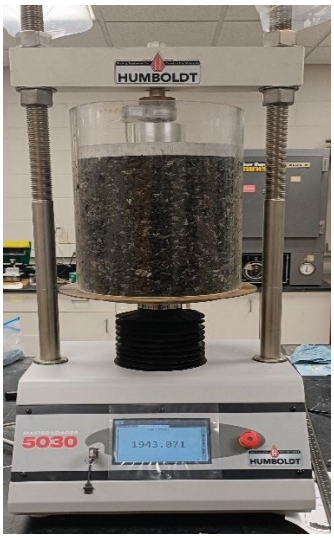

Figure C.3 TDA Type A compressibility test

Figure C.4 Soil-TDA Type A compressibility test

D- Appendix D: Compressibility test with soil-TDA Type B mixtures preparation procedures

Figure D.1 Running the compressibility test with soil-TDA Type B mixtures

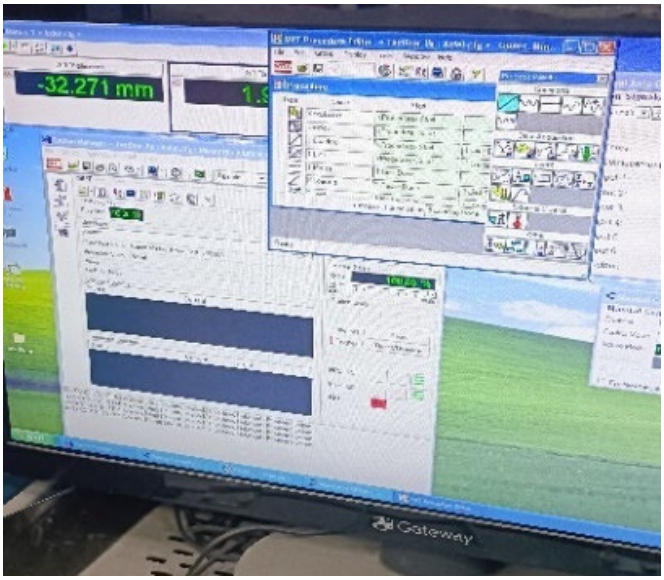

Figure D.2 The data of the compressibility test with soil-TDA Type B mixtures were recorded by an automatic data acquisition system